Noninvasive Electrical Neuroimaging of the Human Brain during Mobile Tasks including Walking and Running

by

Joseph T. Gwin

A dissertation submitted in partial fulfillment
of the requirements for the degree of
Doctor of Philosophy
(Kinesiology and Mechanical Engineering)
in The University of Michigan
2012

Doctoral Committee:

Professor Daniel P. Ferris, Co-Chair
Associate Professor Brent Gillespie, Co-Chair
Professor Noel C. Perkins
Associate Professor Rachael D. Seidler

Acknowledgements

First and foremost, I thank my advisor, Daniel Ferris, for his guidance and support. His contributions to this dissertation are too long to list. In addition, I thank all of my colleagues in the Human Neuromechanics Laboratory for their help.

None of this research would have been possible without the Swartz Center for Computational Neuroscience at the University of California, San Diego. I would especially like to thank Scott Makeig and Klaus Gramann for their direct involvement in much of this research. I also thank Jason Palmer for our fruitful discussions regarding the third chapter of this dissertation. Finally, I thank the entire team at the Swartz Center for welcoming me into their lab (twice) for research rotations.

I am also very grateful to Brent Gillespie for welcoming me into his laboratory and for his genuine interest in and enthusiasm for my research.

I thank my committee for their support, as well as for their openness towards interdisciplinary research and the Individual Interdepartmental Degree Program.

The following sources of financial support are gratefully acknowledged: grants from the Office of Naval Research (N000140811215), the Army Research Laboratory (W911NF-09-1-0139 & W911NF-10-2-0022), and the Rackham School of Graduate Studies at The University of Michigan; a gift from The Swartz Foundation (Old Field, NY); and a National Defense Science and Engineering Graduate Fellowship (32 CFR 168a).

Table of Contents

List of Figures

List of Tables

Abstract

Noninvasive brain imaging during mobile activities could have far reaching scientific, clinical, and technological benefits. Electroencephalography (EEG) is the only mobile noninvasive sensing modality with sufficient temporal resolution to record brain activity on the time scale of natural motor behavior. In the past, EEG has been limited to stationary settings to prevent contamination by electromyographic and movement artifacts. I overcame this limitation by using Independent Component Analysis (ICA) to parse electrocortical processes from artifact contaminated EEG.

Chapters 2 through 4 of this dissertation demonstrate the feasibility of measuring electrocortical activity during human locomotion. In Chapter 2, subjects performed a visual target discrimination and response task while standing, walking, and running. Cognitive event-related cortical potentials during walking and running were nearly identical to those during standing. Chapter 3 provided the first intra-stride measurements of brain activity during walking. Electrocortical sources in the anterior cingulate, posterior parietal, and sensorimotor cortex exhibited significant intra-stride changes in spectral power. A substantive scientific contribution of this study is the observation that synchronous neural firing in the anterior cingulate and posterior parietal cortex, not just the sensorimotor cortex, is modulated within the stride cycle during repetitive, steady-state locomotion. A 264-channel electrode array was used in

Chapters 2 and 3. By systematically reducing the number of channels used, Chapter 4 demonstrated that 35 channels were sufficient to record the most dominate electrocortical sources.

In Chapters 5 and 6, I studied healthy subjects performing isometric and isotonic lower-limb muscle contractions while seated to better understand the relationship between electrocortical dynamics and lower limb muscle activity. Isometric contractions elicited motor cortex event related desynchronization at joint torque onset and offset, while isotonic contractions elicited sustained cortical desynchronization throughout the movement. There was significant coherence between contralateral motor cortex signals and lower-limb electromyographic signals. The frequency of this coherence shifted from the beta-range for isometric contractions to the gamma-range for isotonic contractions.

This dissertation demonstrated that EEG-based brain imaging in dynamic environments is possible and expanded our understanding of cortical involvement in voluntary lower limb movement. It also provided direction for future developments of clinical neuro-monitoring, neuro-assessment, and neuro-rehabilitation technologies.

Chapter 1: Introduction

To a large extent the field of neuroscience is driven by studies using animal models and studies using human subjects in stationary (seated or prone) positions. There are noninvasive approaches for assessing human brain function in dynamic environments. These technologies either provide an indirect assessment of brain function (e.g., transcranial magnetic stimulation (TMS)) or they measure slow cortical hemodynamics that cannot assess brain dynamics on the time scale of natural motor behavior (e.g., near-infrared spectroscopy (NIRS)). Therefore, the primary goals of this dissertation were to assess the feasibility of mobile noninvasive electrical neuroimaging of the human brain and begin to explore cortical involvement in dynamic motor behaviors using this imaging approach.

Noninvasive electrical neuroimaging could be a powerful tool with far reaching scientific, clinical, and technological benefits (Makeig et al., 2009). Neuroscientists exploring the theory that cognitive processes are deeply rooted in the body's interactions with the world (i.e., embodied cognition) could study brain dynamics during whole body interactions within natural environments (Borghi and Cimatti, 2010; Chiel and Beer, 1997; Wilson, 2002) and studies of human motor control would no longer be limited to studies of constrained movements. In addition, recording electrocortical dynamics during locomotion would provide a better understanding of how human

cortex is involved in controlling locomotion. It is generally accepted that humans use a multifaceted locomotion control strategy, including descending, peripheral, and central inputs (Dietz, 2003; Dietz and Duysens, 2000; Drew et al., 2004; Nielsen, 2003; Yang and Gorassini, 2006). However, no existing neuroimaging techniques allow for direct assessment of cortical involvement in locomotion with sufficient time resolution to study intra-stride brain dynamics.

There are also several possible clinical and technological applications of mobile non-invasive neuroimaging. The ability to quantify brain activation during gait could help clinicians diagnose subsets of patients with similar symptoms (Alexander et al., 2009; Boyd et al., 2007), choose a rehabilitation strategy with the best chance of success, and track brain plasticity during an intervention to gauge the success of a therapy or drug (Boyd et al., 2007; Mielke and Szelies, 2003; Weiller, 1998; Yang and Gorassini, 2006). In addition, mobile non-invasive neuroimaging could form the foundation for brain computer interfaces (BCIs) that operate in dynamic environments. These devices could be used to monitor the cognitive status of a civilian or military operator in a high-risk, fatigue prone situation, and they could be used for brain based control of electromechanical motor augmentation devices. Using features of brain activity to control devices that compensate for impaired neuromuscular control during gait rehabilitation may increase the relearning rate by encouraging active neurological participation from patients and producing more normal sensory afferents that induce central nervous system plasticity (Daly and Wolpaw, 2008). In addition, neural control of a prosthetic limb or powered orthosis could restore functional mobility to amputees and

patients with paralysis (Hatsopoulos and Donoghue, 2009; Kim et al., 2009; Leuthardt et al., 2009; Millan et al., 2008; Scherberger, 2009).

There are several techniques that have been used to assess cortical neural activity in mobile environments, such as during walking. Each of these techniques has limitations. Studies using NIRS have shown increases in oxygenated hemoglobin broadly distributed in the frontal, premotor, and supplementary motor cortex during walking (Harada et al., 2009; Miyai et al., 2001; Suzuki et al., 2008; Suzuki et al., 2004) but the cortical hemodynamic response is too slow to reflect intra-stride changes in neuronal activity. Studies using TMS have demonstrated that corticospinal excitability is modulated during the human gait cycle (Capaday et al., 1999; Petersen et al., 2001; Schubert et al., 1997) but TMS is an external perturbation to ongoing brain dynamics so its use in the context of BCI is limited. Control signals for noninvasive BCI have been derived from functional magnetic resonance imaging (Weiskopf et al., 2004) and magneto-encephalography (Georgopoulos et al., 2005) but these imaging techniques are not mobile and require subjects to remain in a seated or prone posture with limited body movement.

Invasive electrophysiological recordings (i.e., sub-dermal, subdural, and intra-cortical electrodes) provide high temporal and spatial resolution measures of electrocortical activity. Fitzsimmons et al. (2009) demonstrated that a series of decoders could accurately predict lower-limb muscle activations and kinematics from neuronal firing rates recorded using intra-cortical electrode arrays in rhesus monkeys that were trained to walk bipedally. Intra-cortical electrode arrays require surgically implanted

sensors, which have inherent infection and complication risks; they are typically only implanted to record signals from targeted regions of the cortex; and they have a lifespan on the order of a few months before cortical scar tissue develops and signal quality degrades (Leach et al., 2010; Schwartz, 2004). In humans, electrocorticography (recordings from subdural electrodes on the surface of the cortex) has been used to show that spectral properties of electrocortical processes correlate with upper-limb kinematics (Hatsopoulos and Donoghue, 2009; Kim et al., 2009; Leuthardt et al., 2009; Millan et al., 2008; Scherberger, 2009). Subdural electrodes are less invasive and have greater long-term stability (Chao et al., 2010) than intra-cortical electrodes, but still require surgical implantation with inherent costs and risk of complications.

Electroencephalography (EEG) is the only noninvasive brain imaging modality that uses sensors that are light enough to wear during locomotion and have sufficient temporal resolution to record brain activity on the time scale of natural motor behavior. In the past, the use of EEG has been limited to stationary settings to prevent contamination by electromyographic and movement artifacts. I have overcome this limitation by using Independent Component Analysis (ICA) to parse underlying electrocortical processes from artifact contaminated EEG. ICA is a blind source separation technique that parses independent signals from correlated time-series data. The use of ICA for analysis of EEG is based on the premise that each electrode on the scalp records a linear sum of various underlying electrocortical and artifactual (i.e., non-electrocortical) signals (Makeig et al., 1996). Linearly decomposing the electrode signals into a set of maximally temporally independent source signals reveals these underlying

processes, which can then be classified as artifactual or electrocortical (Jung et al., 2000a; Jung et al., 2000b). Furthermore, electrocortical source signals are dipolar (Delorme et al., 2012) and can be localized within cortical grey matter using an inverse modeling approach based on a boundary element head model (Oostenveld and Oostendorp, 2002).

The following five chapters each contain a complete manuscript that is independent of the other chapters. In each chapter the methods are similar. Noninvasive electrical neuroimaging is achieved by using high-density EEG and ICA. Each chapter asks a different question with a different purpose. The first three chapters evaluate the feasibility of using high-density EEG and ICA to record cortical neural activity during human locomotion by studying healthy subjects standing, walking and running on a treadmill while concurrently performing a cognitive task. In Chapter 2, comparisons of cognitive event-related electrocortical dynamics between stationary and ambulatory conditions assess the quality of electrocortical recordings during locomotion. In Chapter 3, patterns of electrocortical activity that are synchronized to the gait cycle during walking are characterized; providing the first intra-stride measurements of human brain activity recorded during walking. Chapter 4 evaluates how reducing the number of EEG channel signals affects the electrocortical source signals that can be parsed from EEG recorded during standing and walking. In Chapters 5 and 6, I study healthy subjects performing a variety of lower-limb muscle contractions while seated. Chapter 5 demonstrates differences in the electrocortical activity as a function of the type of muscle action and assesses the trial-by-trial consistency of these electrocortical

dynamics by decoding muscle action from the recorded EEG. Chapter 6 examines the causal relationship between electrocortical processes and lower limb electromyographic signals.

Chapter 2: Removal of Movement Artifact from High-Density EEG Recorded During Walking and Running

This chapter has been previously published:
Gwin JT, Gramann K, Makeig S, Ferris DP. *Journal of Neurophysiology*. 103: 3526-3534, 2010.

Abstract

Though human cognition often occurs during dynamic motor actions, most studies of human brain dynamics examine subjects in static seated or prone conditions. EEG signals have historically been considered to be too noise prone to allow recording of brain dynamics during human locomotion. Here we applied a channel-based artifact template regression procedure and a subsequent spatial filtering approach to remove gait-related movement artifact from EEG signals recorded during walking and running. We first used stride time warping to remove gait artifact from high density EEG for 8 subjects recorded during a visual oddball discrimination task performed while walking and running. Next, we applied infomax independent component analysis (ICA) to parse the channel-based noise reduced EEG signals into maximally independent components (ICs) and then performed component-based template regression. Applying channel-based or channel-based plus component-based artifact rejection significantly reduced EEG spectral power in the 1.5 – 8.5 Hz frequency range during walking and running. In walking conditions, gait-related artifact was insubstantial: event-related potentials (ERPs), which were nearly identical to visual oddball discrimination events while

standing, were visible before and after applying noise reduction. In the running condition, gait-related artifact severely compromised the EEG signals: stable average ERP time-courses of IC processes were only detectable after artifact removal. These findings demonstrate that high-density EEG can be used to study brain dynamics during whole-body movements and that mechanical artifact from rhythmic gait events may be minimized using a template regression procedure.

Introduction

A non-invasive method for recording human electrocortical brain dynamics during mobile activities could have far reaching benefits (Makeig et al., 2009). Cognitive neuroscientists exploring embodied cognition could study brain dynamics associated with cognitive processes during whole-body interactions within natural environments. Studies of human motor control would no longer be limited to studies of constrained movements. Bioengineers might be able to employ such a method to derive control signals for neurorehabilitation and prosthetic technologies. An unanswered question in neuroscience is to what extent human cortex participates in the generation of rhythmic motor behaviors, in particular those motor behaviors associated with locomotion. The answer seems to lie in a multifaceted control strategy including descending, peripheral, and central control (Yang and Gorassini, 2006). An ability to measure brain dynamics during locomotion may provide additional information regarding the significance of descending control.

Electroencephalography (EEG) is the only non-invasive brain imaging modality that uses sensors that are light enough to wear during locomotion and have sufficient time resolution to record brain activity on the time scale of natural motor behavior. However, EEG has historically been considered to be too noise prone to allow such recordings. Mechanical artifact in EEG signals, associated with head movements during locomotion, can have amplitude that is an order of magnitude larger than the underlying brain related EEG signals.

A similar phenomenon occurs during simultaneous EEG and functional magnetic resonance imaging (fMRI). In this situation, alternating magnetic fields (gradients) of the MR scanner cause large repetitive artifact in EEG signals. Artifact template subtraction procedures have been used successfully to remove fMRI gradient artifact from EEG signals (Allen et al., 2000). Unlike fMRI gradient artifact which is relatively invariant over time (Garreffa et al., 2004), mechanical artifact associated with locomotion is time varying. Kinematics and kinetics of human walking exhibit both short-term (step to step) and long-term (over many steps) variability (Hausdorff et al., 1995; Hausdorff et al., 1996; Jordan et al., 2006, 2007). Time varying sources of EEG noise, such as the ballistocardiogram artifact in EEG recorded in a strong magnetic field, have been extracted from EEG signals using channel-based template subtraction procedures and subsequent spatial filtering (Debener et al., 2007; Debener et al., 2005). This combined method was shown to be more effective than channel-based template subtraction (Niazy et al., 2005) or spatial filtering (Benar et al., 2003; Eichele et al., 2005) alone.

Here, we implemented a two-step approach to removing locomotion induced mechanical artifact in high-density EEG signals recorded while subjects walked and ran on a treadmill while simultaneously performing a visual oddball discrimination task. We first removed stride phase-locked mechanical artifact using a channel-based template regression procedure. To address slow fluctuations (over many strides) in the time profile of the gait-related artifact, we used moving time-window averaging of the stride phase-locked data to compute an artifact template for each stride and each channel. To address step-to-step fluctuations in the phase and amplitude of the gait-related artifact resulting from variability in gait kinematics and kinetics, we regressed out the artifact template signals from each EEG signal. Next, we applied an adaptive independent component analysis (ICA) mixture model algorithm [AMICA] (Palmer et al., 2006; Palmer et al., 2008), generalizing infomax (Bell and Sejnowski, 1995; Lee et al., 1999a) and multiple mixture (Lee et al., 1999b; Lewicki and Sejnowski, 2000) ICA approaches, to parse EEG signals into spatially static, maximally independent component (IC) processes (Makeig et al., 1996).

Unlike more spatially stationary artifacts in EEG signals arising from eye movements, scalp muscles, fMRI gradients, etc (Debener et al., 2007; Debener et al., 2005; Jung et al., 2000a; Jung et al., 2000b), which may be resolved by ICA decomposition into a subspace of one or more ICs, we found that gait-related movement artifact remained in many if not most of the independent components. This prevented us from removing only a small subset of components capturing the movement artifacts. Instead, we applied the template regression procedure (previously

applied to the channel data) to the IC processes, reversed the time-warping to produce artifact-reduced ICs, and applied the ICA mixing matrix to recover a second set of artifact-reduced EEG signals.

To evaluate the combined effects of channel-based and channel-based plus component-based artifact removal, we computed the power spectral density of the resulting signals and compared spectral power in the 1.5 to 8.5 Hz frequency band before and after artifact removal, finding no sign of overcorrection of the EEG signals. We also compared the artifact-reduced stimulus event-related potentials (ERPs) in walking and running conditions to uncorrected ERPs recorded while standing. We found that in walking conditions, ERPs that were nearly identical to visual oddball discrimination events while standing, were visible before and after applying noise reduction, while in the running condition, stable average ERP time-courses of IC processes were only detectable after artifact removal.

Methods

Subjects

Eight healthy volunteers with no history of major lower limb injury and no known neurological or locomotor deficits completed this study (7 males and 1 female, age range 21-31 years). All subjects provided written informed consent prior to the experiment. All procedures were approved by the University of Michigan Internal Review Board and complied with the standards defined in the Declaration of Helsinki.

Task

Subjects stood, walked (0.8 m/s and 1.25 m/s), and ran (1.9 m/s) on a force measuring treadmill facing a monitor placed at eye level about 1 m in front of them. Standard (80%) and oddball (20%) stimuli (vertical or 45° rotated black crosses on a white background, respectively) were displayed for 500 ms. The stimuli occupied about 75% of the display area (14° of visual angle). The inter-stimulus interval between successive presentations varied randomly between 500 ms and 1500 ms. For each gait condition (standing, slower walking, faster walking, running) subjects performed two experimental blocks. In the first block, subjects were asked to press a button on a wireless Wii controller (Nintendo, Kyoto, Japan) held in their right hand whenever the target ('oddball') stimulus appeared. In the second block, subjects were asked to silently count the number of target stimuli presented, without producing a manual response. Each session began with the standing condition, followed by the other three conditions in random order. The standing blocks lasted 5 minutes each while walking and running blocks lasted 10 minutes each.

Recording Brain and Body Dynamics

EEG was recorded using a compact ActiveTwo amplifier and 248-channel active electrode array (BioSemi, Amsterdam, The Netherlands). Electrodes were affixed to the scalp using a custom made whole-head cap (Figure 2-1). During the experimental setup, electrode impedance was measured, and electrode gel was used to ensure that the impedance was less than 20 KΩ for each channel. EEG signals were sampled at 512 Hz and after collection were high-pass filtered above 1 Hz. All processing and analysis was

performed in Matlab (The Mathworks, Natick, MA) using scripts based on EEGLAB 7.1.4 (sccn.ucsd.edu/eeglab), an open source environment for processing electrophysiological data (Delorme and Makeig, 2004).

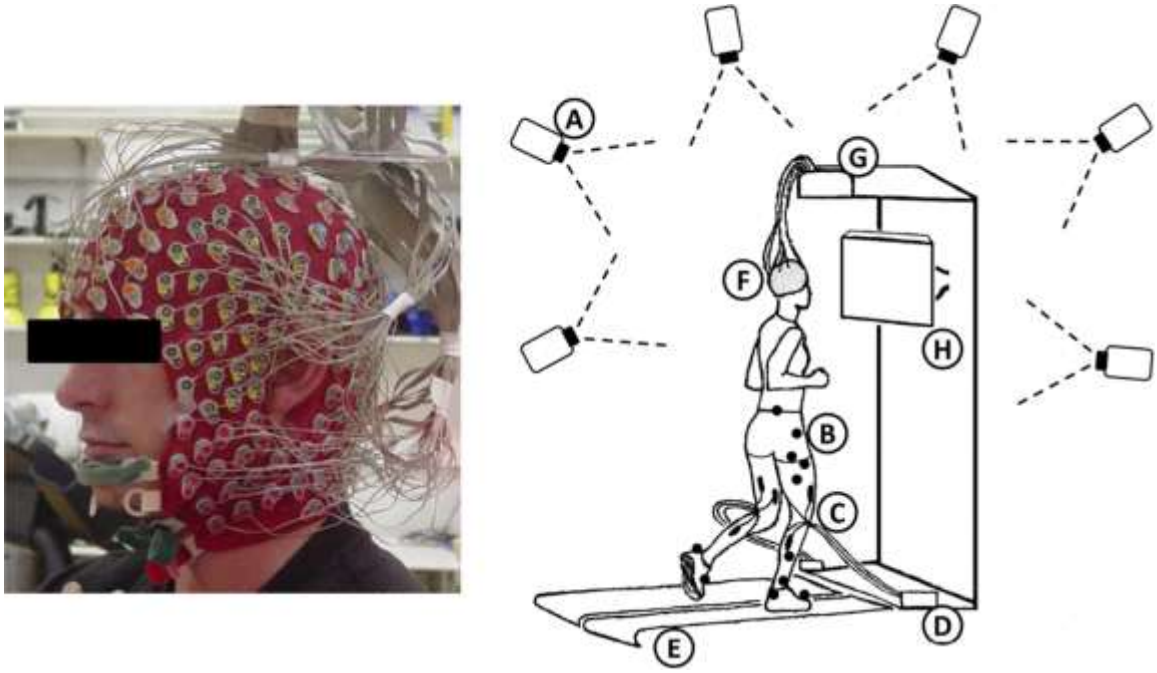

Figure 2-1: (Left) a subject wearing a 248-channel electrode cap and (right) experimental setup sketch showing (A) motion capture cameras and (B) markers, (C) lower limb electromyography (EMG) (not used in this study), (D) the EMG amplifier, (E) the dual-belt in-ground force measuring treadmill, (F) the electrode head-cap, (G) the EEG amplifier, and (H) the display for the visual stimuli.

For 2 of 8 subjects, EEG signals could not be recorded during the running condition because the electrode cap did not stay in place during running (i.e., it was too big for the subject). For the remaining 6 subjects, channels exhibiting substantial noise throughout the collection were removed from the data in the following manner: First, channels with std. dev. > 1000 μV were removed; then any channel whose kurtosis was more than 5 std. dev. from the mean was removed; finally, channels that were uncorrelated ($r < 0.4$) with nearby channels for more than 1% of the time-samples were removed. On average 130 EEG channel signals were retained after visual inspection and removal of noisy

channels (range, 89-164; std. dev., 24.6). The data were then re-referenced offline to the average of the remaining channels. Visual stimulus events were delivered and their latencies incorporated into the EEG data stream using DataSuite (A. Vankov, sccn.ucsd.edu/wiki/DataSuite).

Subjects walked and ran on a custom built, dual-belt, force measuring treadmill with two 24” wide belts mounted flush with the floor (Collins et al., 2009). The distance between the belts was 0.75”. The average belt speed variation while adult subjects walk on this treadmill at 1.25 m/s is 1.8%. The lowest natural frequency of the force treadmill is 41 Hz (for mediolateral forces). Each belt has a separate force platform mounted as its base for measuring ground reaction forces from each leg independently with a sample rate of 1200 Hz.

We used an eight-camera, 120 frames/sec, motion capture system (Motion Analysis Corporation, Santa Rosa, CA) to record the position of 25 reflective markers (low pass filtered at 6 Hz to remove movement artifact) on the lower limbs and pelvis. From these marker positions the kinematics of the ankle, knee, and hip joints were computed using Visual-3D software (C-Motion, Germantown, MD). Event detection algorithms within Visual-3D were used to determine when heel strikes occurred based on vertical ground reaction forces. If force platform signals were compromised because the subject drifted across the centerline of the dual belt treadmill, a kinematic-based pattern recognition technique within Visual-3D was used to identify heel strikes (Stanhope et al., 1990).

Removal of Gait-Related Movement Artifact

EEG signals were epoched, time-locked to single gait cycles (left heel strike to left heel strike), and linearly time-warped using EEGLAB processes (Makeig et al., 2007) so that after time-warping heel strike events (left then right) occurred at the same adjusted latencies in each epoch. For each channel and each stride, a gait-related artifact template was created by averaging the neighboring 20 time-warped stride-locked epochs (10 future epochs and 10 past epochs). This artifact template was then linearly scaled to best fit the time-warped EEG signal in a least-squares sense and was subtracted from the data to form artifact-reduced time-warped data. These cleaned data were then reverse time-warped to produce artifact-reduced continuous time EEG channel signals. We refer to this process as *channel-based artifact removal* (Figure 2-2).

In addition, we performed ICA decomposition on the concatenated single-trial data (including all experimental conditions) for each subject separately using AMICA. Prior to performing ICA decomposition, time-periods of EEG with substantial artifact, based on the z-transformed power across all channels at a given time-point being larger than 0.8, were rejected using EEGLAB. The rejected frames were then inspected visually and regions of fewer than 50 accepted frames between any two sets of rejected frames were also rejected. The resulting ICA unmixing matrix was multiplied with the cleaned EEG channel signals, giving a set of maximally independent component (IC) process time courses. These ICs were then subjected to the same noise reduction algorithm that was first applied to the channel data. Multiplying the further artifact-reduced ICs by the ICA mixing matrix (the inverse of the unmixing matrix) resulted in a second set of further

cleaned EEG channel signals. We refer to this process as *IC-based artifact removal* (Figure 2-2).

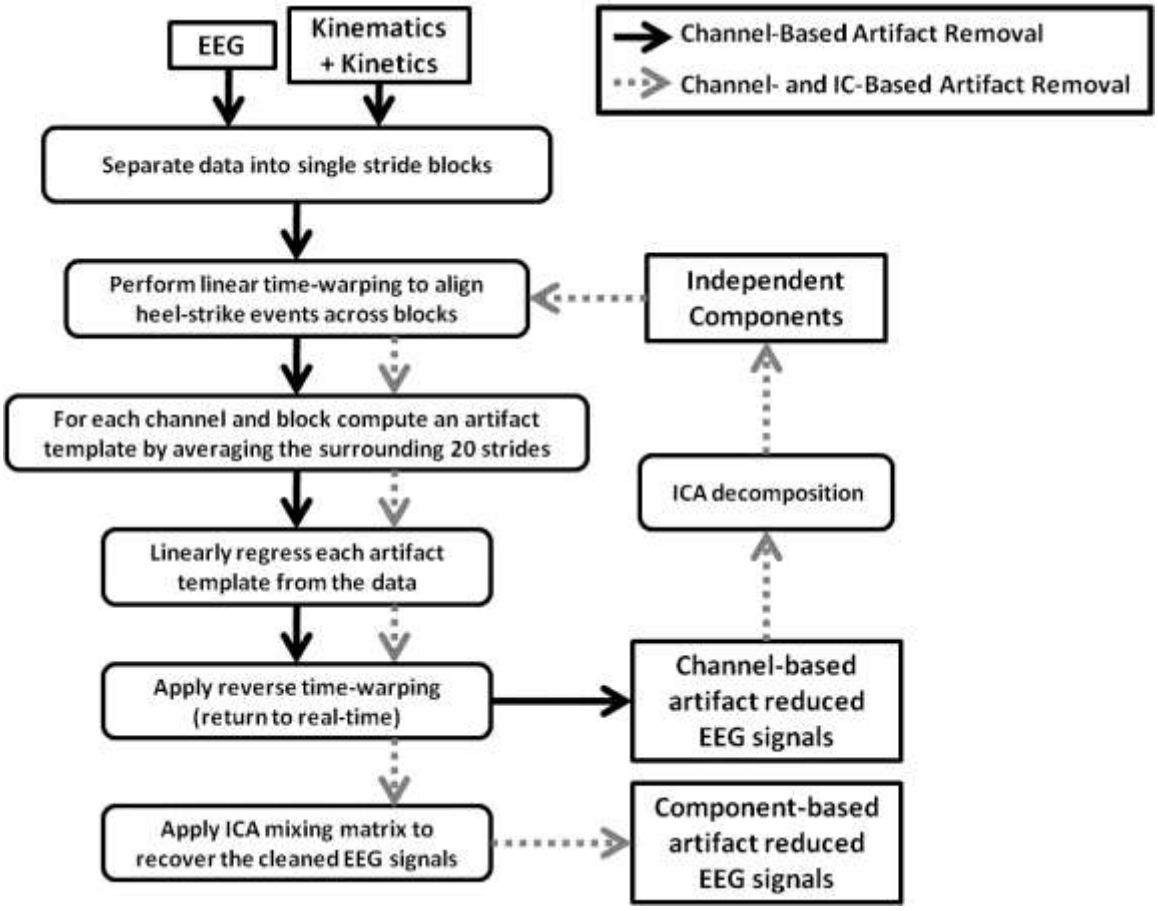

Figure 2-2: Flow chart of the channel-based and component-based artifact removal procedures. For component-based artifact removal, the independent components were derived from channel-based artifact removed EEG signals.

Power Spectral Density

For each gait condition (standing, slower walking, faster walking, running) and each method of artifact removal (before artifact removal, after channel-based removal, after further IC-based removal), we computed the power spectral density for each EEG channel using Welch's method. For illustrative purposes, we computed the power spectral envelope for each subject, defined as the maximum and minimum spectral

density at each frequency over all EEG channels. We analyzed spectral power in the 1.5 Hz to 8.5 Hz range to assess the efficacy of the gait-related artifact removal methods. This frequency band was selected because: 1) in all gait conditions for all subjects it encompassed the step frequency and the first two harmonics of the step frequency, 2) its lower cutoff (1.5 Hz) was greater than the high-pass filter cutoff frequency (1 Hz) that was applied to all EEG signals prior to analysis, and 3) frequencies above 8.5 Hz accounted for less than 6% of the total spectral power in the artifact templates for all gait conditions (slow walking, 6.2%; faster walking, 5.1%; running, 5.5%)(Figure 2-3).

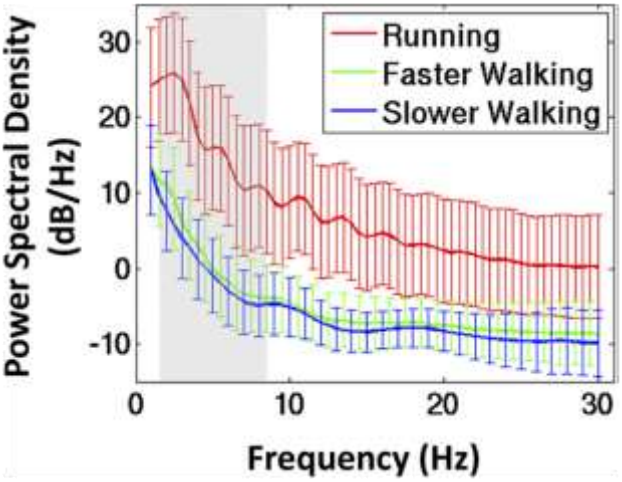

Figure 2-3: Grand average power spectral density of the IC-based artifact templates that were removed from the EEG signals during (blue line) walking at 0.8 m/s, (green line) walking at 1.25 m/s, and (red line) running at 1.9 m/s. The shaded region indicates the frequency band (1.5 Hz to 8.5 Hz) used in subsequent statistical analyses. Error bars show ± 1 standard deviation.

We used a 4-by-1 analysis of covariance (ANCOVA) to assess changes in the power spectra of the EEG signals across gait conditions prior to performing gait-related artifact removal. Spectral frequency was treated as a covariate. To test the hypothesis that the gait-related artifact removal procedures would decrease the spectral power in the EEG signals for all locomotion conditions (slower walking, faster walking, and running), we used the same ANCOVA model and introduced method of artifact removal (before artifact removal, after channel-based removal, after further IC-based removal) as a repeated measure. All statistical analysis was performed in SPSS 17.0 (SPSS Inc.,

Chicago, IL). Significance was set at $\alpha = 0.05$ *a priori*. Bonferroni correction was used to address the problem of multiple comparisons.

Stimulus-Locked Event Related Potentials

EEG signal epochs were extracted, time-locked from -600 ms to +1000 ms relative to visual stimulus onsets. Epochs containing artifacts not related to locomotion (such as eye movements and line noise) were excluded from further analysis using EEGLAB routines that determined the probability of occurrence of each trial by computing the probability distribution of EEG channel signals. Epochs with a probability of occurrence greater than 3 std. dev. from the mean across all epochs were rejected from further analysis (Delorme et al., 2007). The remaining epochs were averaged to form EEG channel-based event-related-potentials (ERPs). Additionally, these epochs were multiplied by the ICA unmixing matrix to form IC activity epochs and then averaged across epochs to form IC-based ERPs.

Here, an alternative approach would have been to remove ocular, electrocardiac, and other non gait-related artifacts using ICA (Jung et al., 2000a; Jung et al., 2000b). However, if ICA-based artifact removal techniques had been implemented it would have been difficult to isolate the effects of the template regression procedure on the channel power spectra from the effects of ICA-based artifact removal techniques. The artifact rejection procedure that we implemented ensured that gait-related artifact, which was present in all trials, remained whereas other artifact events such as eye blinks and line noise were minimized in the data analyzed.

Next, ICs were clustered across subjects using EEGLAB routines implementing k-means clustering on vectors jointly coding differences in IC scalp maps, power spectra, and ERPs; the resulting joint vector was reduced to 10 principal dimensions using principal component analysis (PCA) (Gramann et al., 2009; Jung et al., 2001). Previous analysis of a similar visual oddball discrimination task for seated subjects demonstrated that brain processes projecting maximally to the frontal midline would contribute substantially to the ERP, particularly to the post-motor positivity (Makeig et al., 2004). Visualizations of grand average IC-based ERPs confirmed that the mediofrontal IC cluster (comprised of components projecting maximally to the frontal midline) had a clear and substantial stimulus-locked ERP. Additionally, at least one IC from each subject was contained in this cluster. Therefore, the ICs in the mediofrontal cluster were selected for further analysis of the artifact removal procedures. For all ICs in the mediofrontal cluster, each gait condition, and each stage of artifact removal, we computed stimulus-locked IC-based ERPs and compared their time profiles across conditions.

Results

Power spectral density of the recorded EEG signals increased with step frequency (Figure 2-4). A 4-by-1 ANCOVA, with spectral frequency (1.5 Hz to 8.5 Hz) as the covariate, demonstrated significant differences in spectral power across gait conditions before gait-related artifact removal ($F(3,1) = 14824$, $p < 0.001$). Grand mean spectral powers were 3.45 $\mu V^2/Hz$, 4.43 $\mu V^2/Hz$, 5.49 $\mu V^2/Hz$, and 65.01 $\mu V^2/Hz$ during standing, slow walking, faster walking, and running, respectively. In the running condition, the

amplitude of EEG signals before artifact removal could be an order of magnitude larger than after artifact removal (Figure 2-5).

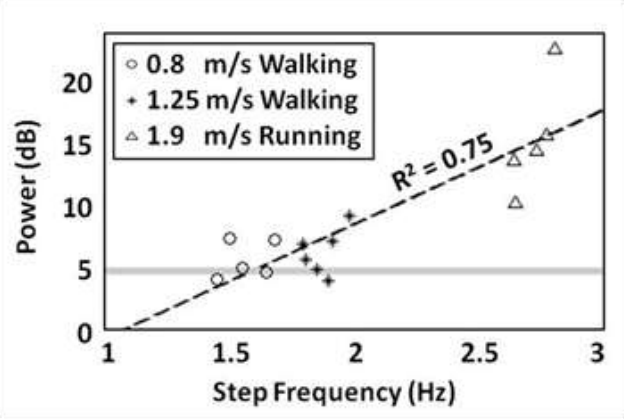

Figure 2-4: Grand average EEG spectral power in the 1.5 Hz to 8.5 Hz band for each subject and each gait condition plotted versus the subject-specific step frequency. (Circle) walking at 0.8 m/s, (star) walking at 1.25 m/s, and (triangle) running at 1.9 m/s. The gray horizontal line indicates the grand mean spectral power in the 1.5 to 8.5 Hz range for the standing condition. The black dashed line indicates a best fitting line through the data ($R^2 = 0.75$).

The gait-related artifact removed was quasi-periodic at the stride frequency. The most pronounced gait-related artifacts tended to be 180-degrees out of phase with vertical center-of-mass displacement as estimated from the displacement of motion-capture markers on the pelvis (Gard et al., 2004). However, spectral power in the gait-related artifact template was not isolated to the mean step frequency and its harmonics. This likely reflects the complex dynamic interaction between the EEG sensors, the EEG wires, the head cap, and the head, as well as to step-to-step variations in stride duration. For example, stride duration varied from roughly 720 ms to 800 ms for the running subject shown in Figure 6. In addition, the amplitude of the movement artifact steadily increased over many strides. The template regression procedure was developed to account for these slow (over many strides) and fast (stride-to-stride) fluctuations in gait-related artifact (Figure 2-6). After performing removal of gait-related artifact, the EEG signals appeared much cleaner (Figure 2-6).

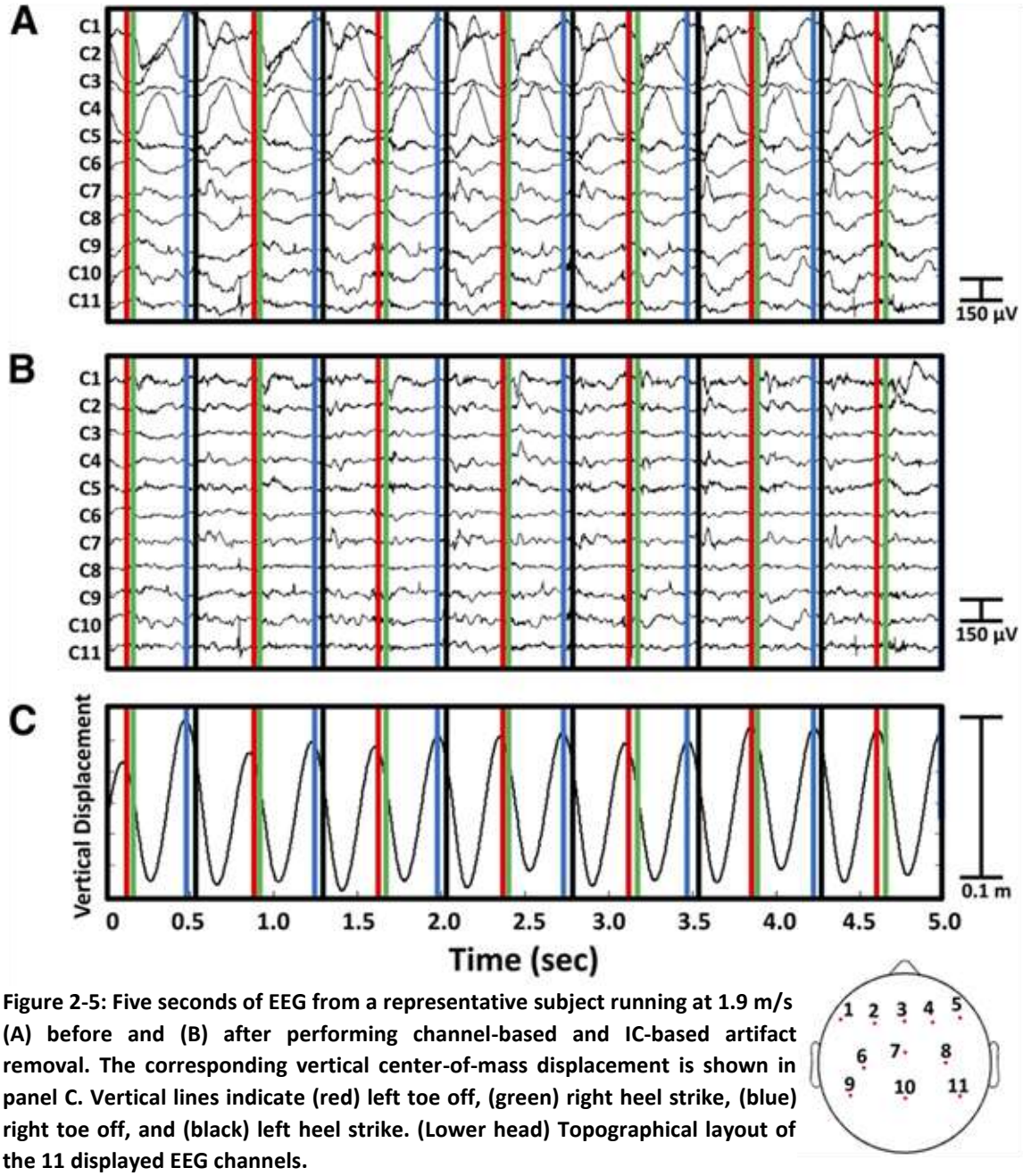

Figure 2-5: Five seconds of EEG from a representative subject running at 1.9 m/s (A) before and (B) after performing channel-based and IC-based artifact removal. The corresponding vertical center-of-mass displacement is shown in panel C. Vertical lines indicate (red) left toe off, (green) right heel strike, (blue) right toe off, and (black) left heel strike. (Lower head) Topographical layout of the 11 displayed EEG channels.

To evaluate the effects of the artifact removal procedures on the EEG signal power spectra, we introduced artifact removal method into our ANCOVA model as a repeated measure. Across all gait conditions, spectral power in the EEG signals decreased with each iteration of the artifact removal procedure ($F(2,1) = 16797$, $p < 0.001$). In both

walking conditions (0.8 m/s and 1.25 m/s), gait-related artifact removed from the EEG signals was minimal (Figure 2-7 A+B). However, in the running condition (1.9 m/s) the EEG signals exhibited substantial increases in spectral power across a broad spectrum and particularly at the mean step frequency and its harmonics. This artifact was reduced but not eliminated by the channel-based and IC-based artifact rejection procedures (Figure 2-7 C).

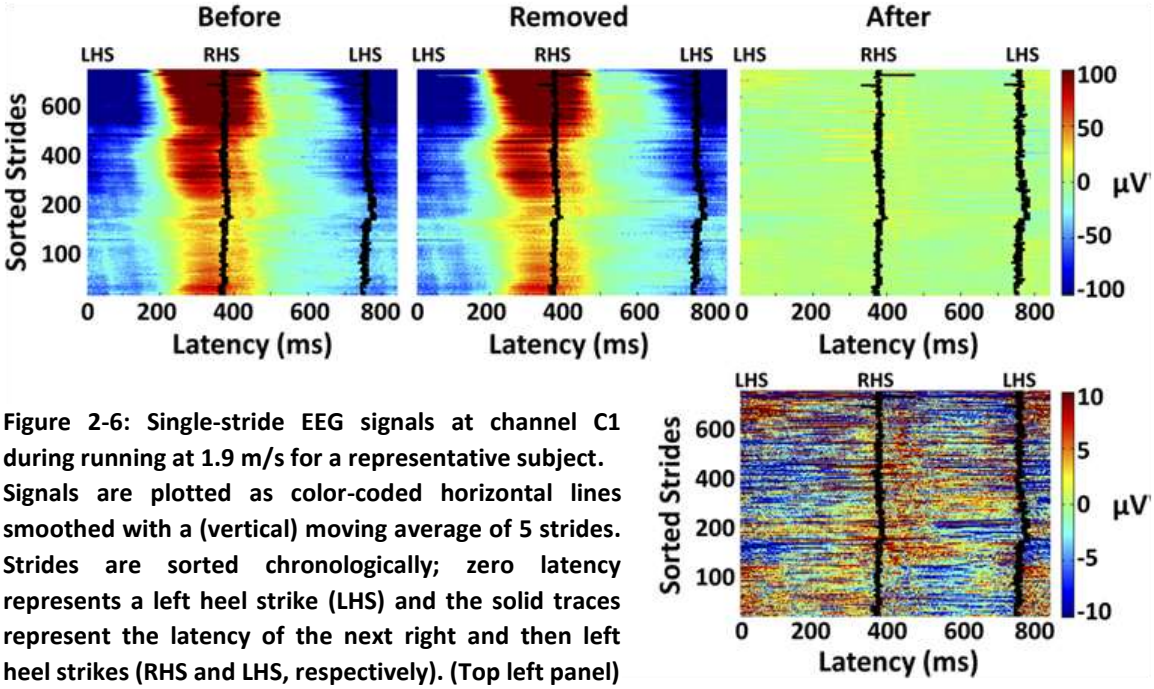

Figure 2-6: Single-stride EEG signals at channel C1 during running at 1.9 m/s for a representative subject. Signals are plotted as color-coded horizontal lines smoothed with a (vertical) moving average of 5 strides. Strides are sorted chronologically; zero latency represents a left heel strike (LHS) and the solid traces represent the latency of the next right and then left heel strikes (RHS and LHS, respectively). (Top left panel) The EEG signals before artifact removal; (top center panel) the gait-related artifact templates removed; (top right panel) the EEG signals remaining after channel- and IC-based artifact removal; (bottom right panel) the EEG signals remaining shown on a 10-times finer color scale than the top panels. The location of channel C1 is shown in Figure 2-5.

After IC-based artifact removal the grand mean spectral powers were 3.5 $\mu V^2/Hz$, 3.9 $\mu V^2/Hz$, and 31.7 $\mu V^2/Hz$ for slow walking, faster walking, and running, respectively. The differences in the grand mean spectral power between the standing condition and the movement conditions remained significant for running ($p < 0.001$) and fast walking ($p < 0.001$) but not for slow walking ($p = .756$).

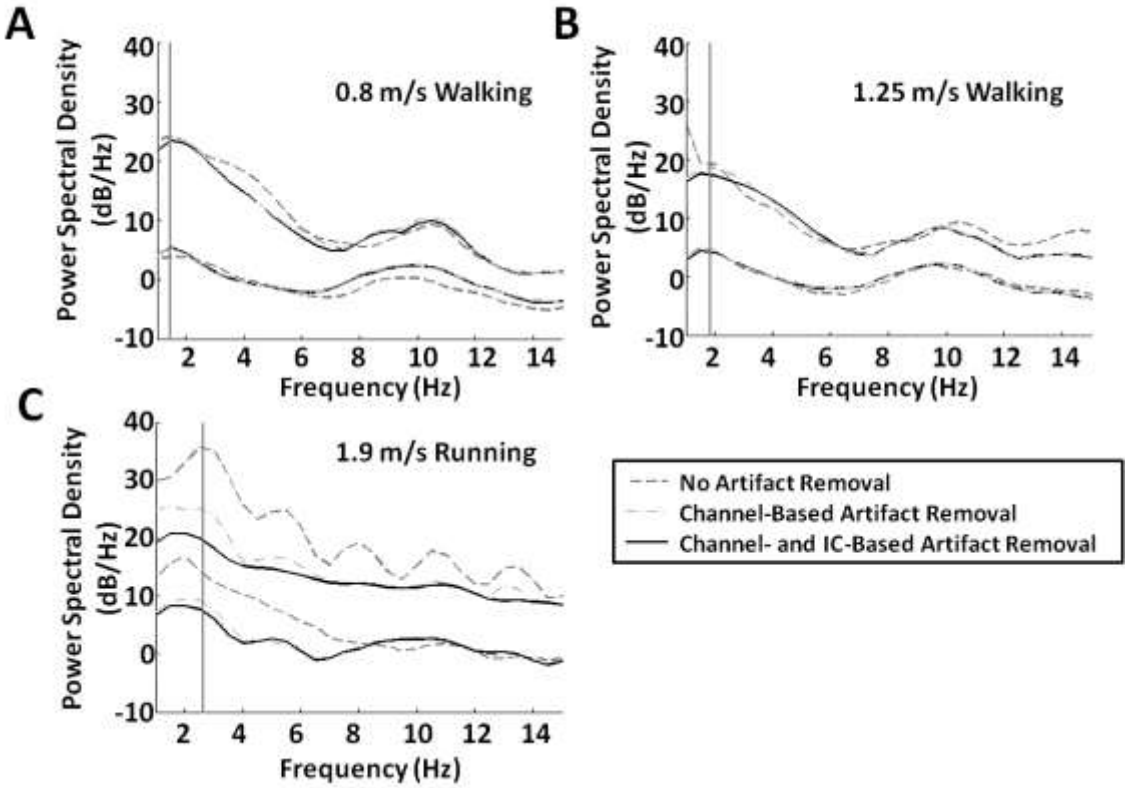

Figure 2-7: EEG channel power spectral density envelopes (max and min channel spectra). (Dashed line) before artifact removal, (dash-dot line) after performing channel-based artifact removal, and then (solid line) after performing IC-based artifact removal for a representative subject (A) walking at 0.8 m/s, (B) walking at 1.25 m/s, and (C) running at 1.9 m/s. Gray vertical lines indicate the mean step frequency in each condition.

There was a significant interaction between subject and artifact removal method ($F(5,2) = 644$, $p < 0.001$). Specifically, further decreases in spectral power after IC-based removal (compared to spectral power after channel-based artifact removal) were evident for some (3) but not all (6) subjects (Figure 2-8).

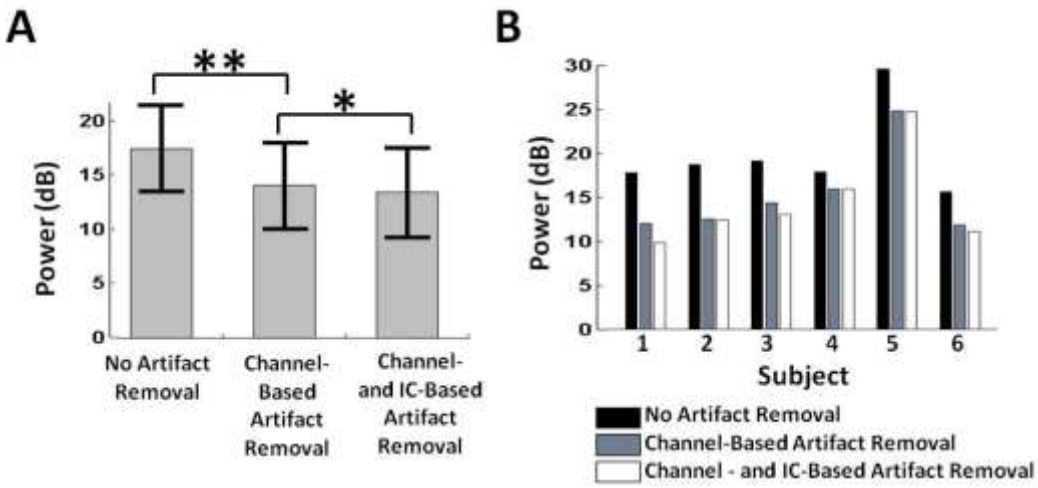

Figure 2-8: Average spectral power in the 1.5 Hz to 8.5 Hz band during 1.9 m/s running (A) for all channels and subjects, and (B) for all channels for each subject separately: (black) before artifact removal; (grey) after channel-based artifact removal; (white) after subsequent IC-based artifact removal. Error bars show ±1 standard deviation, * p < 0.01 , ** p < 0.001.

EEG signal epochs were extracted from -600 ms before to +1000 ms after visual stimulus onsets; these epochs were then averaged to form EEG channel ERPs. In the running condition, channel ERPs appeared cleaner after gait-related artifact removal than before artifact removal (Figure 2-9).

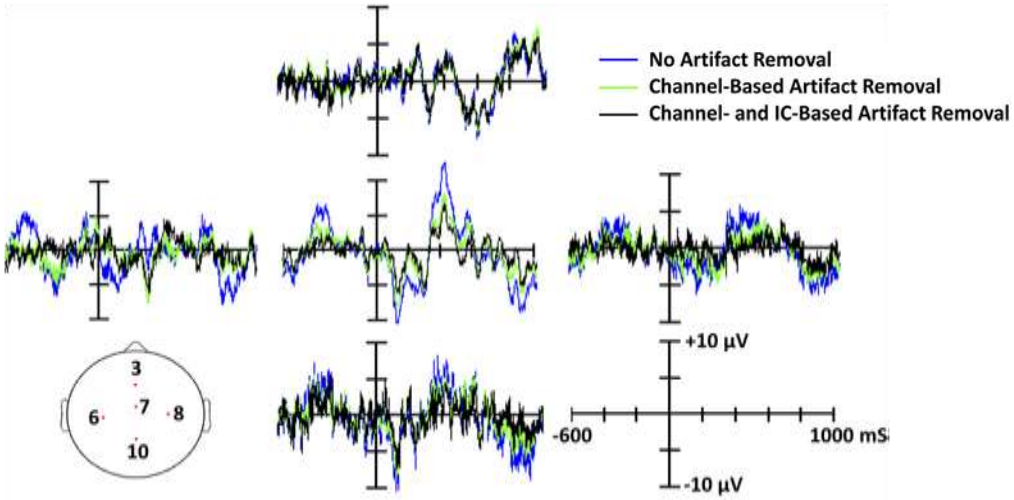

Figure 2-9: Mean target ERPs of 5 EEG channels from a representative subject during running at 1.9 m/s. The scalp locations of the 5 EEG channels are shown in the bottom left panel. In each panel, three stages of analysis are shown: before artifact removal (blue trace); after performing channel-based artifact removal (green trace); after subsequent IC-based artifact removal (black trace). Zero latency represents the onset of the visual target stimulus.

In both walking conditions, ERPs time-locked to visual target stimulus onsets for ICs in the mediofrontal cluster, before and after artifact removal, appeared similar in time profile and amplitude to ERPs for the same ICs recorded in the standing condition. Before artifact removal, the amplitudes and time profiles of the IC ERPs in the running condition did not resemble those in the standing condition; after artifact removal, the IC ERPs in the running and standing conditions appeared similar (Figure 2-10).

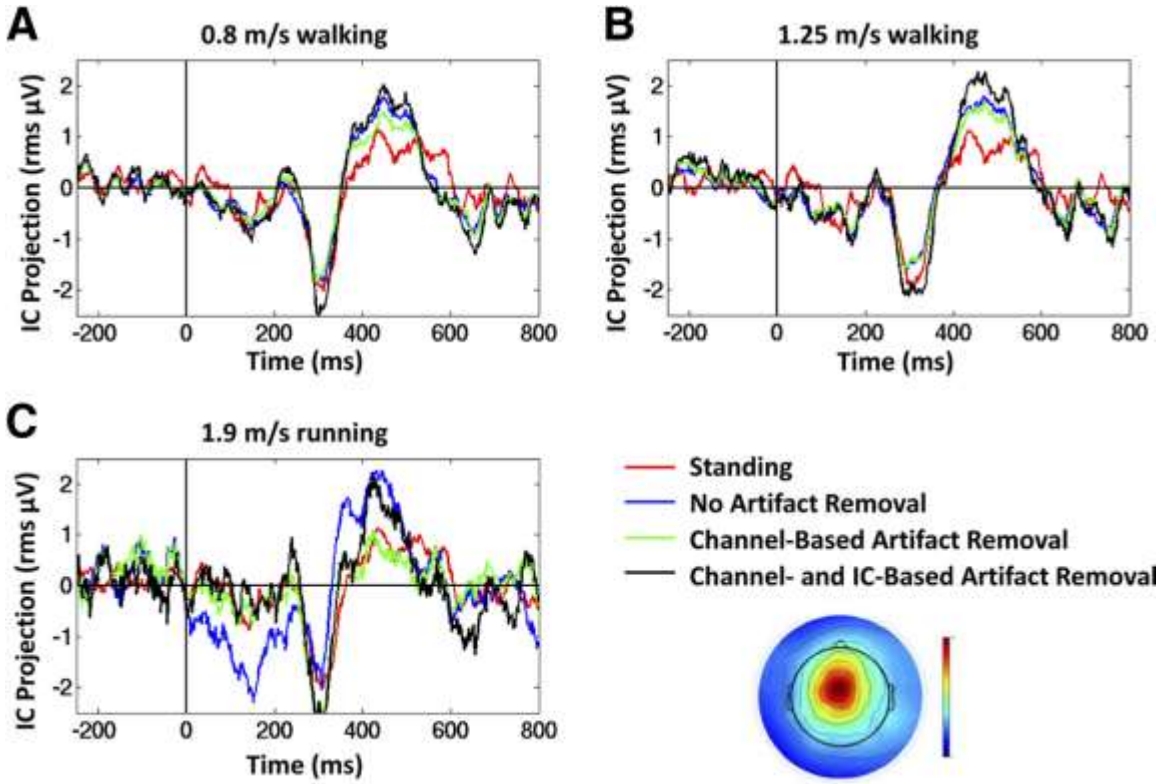

Figure 2-10: Mean target ERP of a mediofrontal independent component from a representative subject. The scalp topography of the selected IC is shown below the legend. Traces show ERPs in three gait conditions: (A) walking at 0.8 m/s; (B) walking at 1.25 m/s; (C) running at 1.9 m/s. In each panel, the ERP while standing is shown (red traces) along with ERPs in three stages of analysis: before artifact removal (blue traces); after performing channel-based artifact removal (green traces); after subsequent IC-based artifact removal (black traces). Zero latency represents the onset of the visual target stimulus. Vertical axis units: root-mean square microvolt projection of the IC process to all the scalp electrodes.

Discussion

To our knowledge, this is the first study of EEG and ERPs from a cognitive task recorded during human locomotion. Our results demonstrate the feasibility of removing gait-related movement artifact from EEG signals so that electrocortical processes that are associated with cognitive, motor, or perceptual tasks performed during locomotion can be studied. Specifically, we have demonstrated that by using high-density EEG recordings with (≤ 248) active electrodes synchronized to motion capture and mechanical force measurements it is possible to analyze EEG and derived ERP signals during walking, and that for a visual oddball task these have similar continuous and event-related dynamics as in a standing subject condition. Further, in a more active locomotor condition (1.9 m/s running), we demonstrated successful application of artifact removal techniques that take into account the time-varying nature of the gait-related artifact to separate brain EEG signals from gait-related noise. In the running condition, similar average ERP time-courses of IC processes were only detectable after artifact removal.

To do this we modified existing artifact removal techniques, designed for time-invariant noise sources (Allen et al., 2000), and applied them to EEG signals containing time-varying gait-related movement artifact. The artifact removal method that we implemented was intended to remove artifacts that were phase-locked to the gait cycle. Other artifacts (e.g., line noise, eye movement, and muscle activities) were not removed by these means. These artifacts can be addressed by other methods, such as by

identifying independent components (ICs) that explain the portions of the EEG associated with these processes (Jung et al., 2000a; Jung et al., 2000b).

The artifact removal method implemented here involved: 1) performing a linear time-warping procedure to align heel strike events to a common latency template prior to performing artifact removal, 2) computing an artifact template for each stride based on the surrounding 20 strides, 3) using linear regression to fit a channel-based artifact template to the recorded signals for each stride, 4) performing ICA decomposition on the continuous data, 5) using linear regression to remove a component-based artifact template from recorded signals for each stride, 6) applying reverse time warping to the artifact-reduced component signals, and 7) applying the ICA mixing matrix to recover the artifact-reduced channel signals (Figure 2-2). We found that in 3 of the 6 subjects, applying the second stage of artifact removal (IC-based artifact removal, steps 4-7 above) provided a clear further reduction in gait-related movement artifact. The head cap may have fit some subjects better than others, and the running mechanics of certain subjects may have lead to more dramatic head accelerations. Nevertheless, it is not entirely clear why these further reductions were evident in some but not all subjects.

The artifact removal method that we implemented requires considerable computational resources. In order to run ICA, enough RAM must be available to load all EEG signals for each subject into the Matlab workspace (up to 248 channels X 512 samples/sec X 70 minutes, occupying 2 GB in single precision). Using 16-GB nodes of a computer cluster, we encountered no memory problems. AMICA is designed to run in parallel over several nodes, and computation time scales near-linearly with the number

of nodes available. By processing in parallel over 8 nodes, we were able to run AMICA for each subject overnight.

While 248 channels of EEG were recorded for each subject, on average only 130 channels were retained for analysis. A contributing factor here was that only a single electrode cap was available. While attempts were made to recruit subjects with appropriately sized heads, in some cases the head cap was too large for the subject (particularly in the posterior neck region). Because of un-resolvable artifact caused by loose electrode placements, particularly noticeable in the running condition, 55 of the 248 electrodes were rejected more than 75% of the time; these electrodes were highly concentrated in the posterior neck region. The custom head cap was designed to cover regions of the head and neck below the level of the inion (Figure 2-1). This design was useful for recording neck muscle contributions to ongoing EEG in looking and pointing tasks (Gramann et al., 2009; Makeig et al., 2009) but it was not optimal for recording EEG during locomotor tasks, as it did not allow the head and posterior neck portions of the cap to move with respect to each other.

There are many areas for further study that arise from the work presented here. We used active electrodes for this study that passed high-level signals through the electrode cables. Undoubtedly, passive electrodes would be more prone to movement artifacts arising from cable sway. Whether or not the artifact removal method that we implemented could be used to remove movement artifact from EEG recorded with passive electrodes during walking and running should be studied. In addition, wireless EEG systems, now in development in many places, would likely reduce, but likely not

eliminate, movement artifact. When possible, the artifact removal method proposed here should be re-evaluated using wireless electrodes. Furthermore, we selected a 20-stride moving window for the artifact template because we found that this provided enough steps to generate a smooth template yet was still sensitive to the long-term (over many steps) variations in the movement artifact. Further parametric analysis to determine the optimal number of strides to include in the artifact template is recommended. Finally, we have applied the artifact removal method to EEG collected during a visual oddball task. Future studies should examine other types of tasks.

We evaluated the efficacy of the procedure on EEG collected during treadmill walking and running, relatively rhythmic motor tasks. However, the artifact removal procedure we implemented is not inherently limited to removing quasi-rhythmic motor artifacts. It may be possible to use a related procedure to remove mechanical artifact from bio-electric signals recorded during other locomotor tasks, such as tasks involving rapid directional changes or responses to ground perturbations, provided enough trials are available for creation of an appropriate set of artifact templates and movement-related kinematic signals are available for performing appropriate time-warping. Here, a simple stride-order based moving average template was effective. In conditions involving locomotor challenges, extraction of mean templates might for instance be based on moving averages of trials sorted by challenge as well as time on task. Further, if head kinematics were recorded and synchronized to the EEG data stream in real time, it might be possible to perform mechanical artifact removal online, with a delay limited

only by the duration of the mechanical artifact template. These are avenues of inquiry worthy of pursuit.

Mobile recordings of EEG signals during natural behaviors may provide a foundation for further exploration into the complex links between distributed brain dynamics and motivated natural behavior. Makeig and colleagues have proposed a wearable mobile brain/body imaging (MoBI) system and new data-driven analysis methods to model the complex resulting data (Makeig et al., 2009). The artifact removal procedures demonstrated here may enable the use of MoBI in more dynamic environments than previously thought.

Chapter 3: Electrocortical Activity is coupled to Gait Cycle Phase during Treadmill Walking

This chapter has been previously published:
Gwin JT, Gramann K, Makeig S, Ferris DP. *Neuroimage* 54: 1289-1296, 2011.

Abstract

Recent findings suggest that human cortex is more active during steady-speed unperturbed locomotion than previously thought. However, techniques that have been used to image the brain during locomotion lack the temporal resolution necessary to assess intra-stride cortical dynamics. Our aim was to determine if electrocortical activity is coupled to gait cycle phase during steady-speed human walking. We used electroencephalography (EEG), motion capture, and a force-measuring treadmill to record brain and body dynamics while eight healthy young adult subjects walked on a treadmill. Infomax independent component analysis (ICA) parsed EEG signals into maximally independent component (IC) processes representing electrocortical sources, muscle sources, and artifacts. We calculated a spatially fixed equivalent current dipole for each IC using an inverse modeling approach, and clustered electrocortical sources across subjects by similarities in dipole locations and power spectra. We then computed spectrograms for each electrocortical source that were time-locked to the gait cycle. Electrocortical sources in the anterior cingulate, posterior parietal, and sensorimotor cortex exhibited significant ($p<0.05$) intra-stride changes in spectral power. During the

end of stance, as the leading foot was contacting the ground and the trailing foot was pushing off, alpha- and beta-band spectral power increased in or near the left/right sensorimotor and dorsal anterior cingulate cortex. Power increases in the left/right sensorimotor cortex were more pronounced for contralateral limb push-off (ipsilateral heel-strike) than for ipsilateral limb push-off (contralateral heel-strike). Intra-stride high-gamma spectral power changes were evident in anterior cingulate, posterior parietal, and sensorimotor cortex. These data confirm cortical involvement in steady-speed human locomotion. Future applications of these techniques could provide critical insight into the neural mechanisms of movement disorders and gait rehabilitation.

Introduction

Vertebrate legged locomotion requires dynamic interaction between peripheral sensors, central pattern generators, and supraspinal locomotion centers (Grillner et al., 2008; Rossignol et al., 2006). It is generally accepted that humans use a multifaceted locomotion control strategy, including descending, peripheral, and central inputs (Dietz, 2003; Dietz and Duysens, 2000; Drew et al., 2004; Nielsen, 2003; Yang and Gorassini, 2006). Spinal locomotor networks in humans and other vertebrates are capable of generating rhythmic muscle activity (Dietz, 2003; Dimitrijevic et al., 1998; Grillner, 1985; Rossignol, 2000; Rossignol et al., 2006; Shik and Orlovsky, 1976). However, activating this network in humans without functional descending motor pathways has proven to be difficult (Dietz et al., 1995; Ferris et al., 2004; Fong et al., 2009; Wirz et al., 2001). Some supraspinal locomotor centers are organized hierarchically in the brainstem,

cerebellum, and cortex. This hierarchical structure facilitates integration of multi-sensory information for dynamic control during gait (Fong et al., 2009; Rossignol et al., 2006). However, primates (including humans) also have a monosynaptic corticospinal pathway connecting the motor cortex to spinal motoneurons.

Several research areas have provided indirect evidence of cortical involvement in human locomotion. Dual-task experiments have demonstrated that balance during walking can be negatively affected by concomitant information processing (Woollacott and Shumway-Cook, 2002). Positron emission tomography (PET) and functional magnetic resonance imaging (fMRI) have demonstrated that during rhythmic foot or leg movements the primary motor cortex is activated, consistent with expected somatotopy, and that during movement preparation and anticipation frontal and association areas are activated (Christensen et al., 2000; Dobkin et al., 2004; Heuninckx et al., 2005; Heuninckx et al., 2008; Luft et al., 2002; Sahyoun et al., 2004). Furthermore, electrophysiological studies of similar tasks have demonstrated lower limb movement related electrocortical potentials (Wieser et al., 2010), as well as coherence between electromyographic and electroencephalographic signals (Hansen and Nielsen, 2004; Raethjen et al., 2008). These studies can be extrapolated to make predictions about locomotion.

Direct evidence for cortical involvement in human locomotion comes from studies using functional near-infrared spectroscopy (fNIRS) and PET. Using fNIRS, researchers demonstrated increases in oxygenated hemoglobin in the frontal, premotor, and supplementary motor cortex during walking (Harada et al., 2009; Miyai et al., 2001;

Suzuki et al., 2008; Suzuki et al., 2004). In a recent study using PET before and immediately after imagined and real walking, researchers found that imagined 20 second bouts of walking beginning from stance activated an indirect pathway via the supplementary motor cortex and basal ganglia loop, while 20 minutes of real steady speed walking activated a direct corticospinal pathway via the primary motor cortex (la Fougere et al., 2010). The authors suggested that the direct corticospinal pathway is responsible for execution of locomotion in a non-modulatory state while the indirect pathway is responsible for planning and modulation of locomotion. In that framework, intra-stride phasic cortical activity associated with integration of afferent sensory information and maintenance of a steady gait might be expected. However, it is difficult to disentangle differences between real and imagined locomotion from differences between short bouts of walking initiated from stance and long bouts of steady speed walking.

Transcranial magnetic stimulation (TMS) facilitates direct study of intra-stride modulations in corticospinal excitability. Studies using transcranial magnetic stimulation (TMS) have shown that activation of inhibitory circuits in the motor cortex during steady walking disrupts ongoing cortico-muscular interaction and reduces lower limb (plantar- and dorsi-flexor) activity (Capaday et al., 1999; Christensen et al., 2001; Petersen et al., 2001; Schubert et al., 1999; Schubert et al., 1997), as well as upper-limb (posterior deltoid) activity (Barthelemy and Nielsen, 2010). In addition, motor evoked potentials (MEPs) in plantar- and dorsi-flexors evoked by TMS are evident only during phases of the gait cycle where a particular muscle is active; for example MEPs in the soleus are

present during stance and absent during swing (Capaday et al., 1999; Schubert et al., 1997). At least part of this MEP modulation is caused by changes in excitability of monosynaptic corticospinal cells (Petersen et al., 2001).

In animal models, microwire electrode arrays implanted into the cortex have provided evidence of intra-stride modulations of neuronal firing rates. In feline posterior parietal cortex (Andujar et al., 2010; Beloozerova and Sirota, 2003; Lajoie et al., 2010) and motor cortex (Armstrong and MarpleHorvat, 1996; Drew, 1993; Drew et al., 2002; Widajewicz et al., 1994) neuronal firing rates exhibit peaks that are synchronized to the gait cycle. These studies suggest that feline posterior parietal cortex likely plays a role in visuo-motor integration during locomotion while motor cortex contributes to gait execution. Additionally, lower limb muscle activations and joint angles have been decoded from motor cortex neuronal firing rates in rhesus monkeys during bipedal walking (Fitzsimmons et al., 2009). Taken together these studies demonstrate the existence of intra-stride modulations in cortical activity in various vertebrate animals.

Electroencephalography (EEG) is the only non-invasive brain imaging modality that uses sensors that are light enough to wear during ambulation and have sufficient time resolution to record intra-stride changes in brain activity (Makeig et al., 2009). Independent component analysis (ICA) combined with magnetic resonance based head models can be used to overcome electromyographic, electroocular, movement artifact, and line noise contamination of EEG signals (Delorme and Makeig, 2004; Delorme et al., 2007; Gwin et al., 2010b; Jung et al., 2000a; Jung et al., 2000b; Makeig et al., 1996; Makeig et al., 2009; Onton et al., 2006). We have previously demonstrated that high-

density EEG can be used to record electrocortical dynamics associated with cognitive tasks during walking and running (Gwin et al., 2010b). Specifically, we identified a visually evoked target response in human electrocortical activity during walking and running that was similar to the visually evoked target response during standing. The purpose of this study was to use high-density EEG to examine patterns of intra-stride electrocortical dynamics during steady-speed human walking. Our hypothesis was that electrocortical dynamics, particularly in the sensorimotor cortex, would exhibit intra-stride patterns of activation and deactivation. In addition to providing insight into how the human central nervous system coordinates locomotion, we believe that in the long run these dynamics may be of use for brain-machine interface (BMI) based neurorehabilitation (Daly and Wolpaw, 2008; Yang and Gorassini, 2006) and that future applications of these techniques could provide critical insight into the neural mechanisms of movement disorders and gait rehabilitation.

Methods

Data Collections

Eight healthy volunteers with no history of major lower limb injury and no known neurological or locomotor deficits completed this study (7 males and 1 female, age range 21-31 years). All subjects provided written informed consent prior to the experiment. All procedures were approved by the University of Michigan Internal Review Board and complied with the standards defined in the Declaration of Helsinki.

Subjects stood, walked (0.8 m/s and 1.25 m/s), and ran (1.9 m/s) on a force measuring treadmill (Collins et al., 2009) facing a monitor placed at eye level about 1 m in front of them while we recorded 248-channel electroencephalography (EEG), lower limb kinematics, and ground reaction forces. One objective of this data collection was to test the feasibility of recording cognitive brain processes during human locomotion (Gwin et al., 2010b). In order to do this standard (80%) and target (20%) stimuli (vertical or 45° rotated black crosses on a white background, respectively) were displayed on the monitor for 500 ms with a random inter-stimulus interval between 500 ms and 1500 ms. For each gait condition (standing, slower walking, faster walking, running) subjects performed an experimental block wherein they were asked to press a handheld button whenever the target stimulus appeared and a control block wherein no manual response to the target stimulus was required. Each session began with the standing condition, followed by the other three conditions in random order. The standing blocks lasted 5 minutes each while the walking and running blocks lasted 10 minutes each. For the present study we analyzed data from the walking control conditions. Data collected during running were not used due to the presence of large mechanical artifacts in the EEG signals.

We recorded EEG using an ActiveTwo amplifier and a 248-channel active electrode array (BioSemi, Amsterdam, The Netherlands). The BioSemi software sampled the EEG signals at 512 Hz per channel. Prior to data collection, we measured electrode impedance and used electrode gel to ensure that the impedance was less than 20 KΩ for each channel. After data collection we high-pass filtered the EEG signals above 1 Hz. As

in (Gwin et al., 2010b) EEG signals exhibiting substantial noise throughout the collection were removed from the data in the flowing manner: 1) channels with std. dev. > 1000 μV were removed, 2) any channel whose kurtosis was more than 5 std. dev. from the mean was removed, and 3) channels that were uncorrelated ($r < 0.4$) with nearby channels for more than 1% of the time-samples were removed. On average 130.4 EEG channels were retained for analysis (range, 89-164; std. dev., 24.6). These remaining channel signals were then re-referenced to an average reference. All processing and analysis was performed in Matlab (The Mathworks, Natick, MA) using scripts based on EEGLAB 7.1.4 (sccn.ucsd.edu/eeglab), an open source environment for processing electrophysiological data (Delorme and Makeig, 2004).

We recorded the positions of 25 reflective markers on the lower limbs and the pelvis using an eight-camera motion capture system (Motion Analysis Corporation, Santa Rosa, CA). Marker positions were sampled at 120 Hz and low pass filtered at 6 Hz to remove movement artifact. Visual-3D software (C-Motion, Germantown, MD) computed the kinematics of the ankle, knee, and hip joints based on these marker positions. Event detection algorithms within Visual-3D determined when heel-strike and toe-off occurred based on vertical ground reaction forces and lower limb kinematics (Stanhope et al., 1990).

Data Analyses

We applied an adaptive mixture independent component analysis (ICA) algorithm [AMICA] (Palmer et al., 2006; Palmer et al., 2008) that generalizes infomax (Bell and Sejnowski, 1995; Lee et al., 1999a) and multiple mixture (Lee et al., 1999b; Lewicki and

Sejnowski, 2000) ICA approaches, to parse EEG signals into spatially static, maximally independent component (IC) processes (Makeig et al., 1996). Prior to performing ICA decomposition, time-periods of EEG with substantial artifact, as defined by z-transformed power across all channels in a given time window being larger than 0.8, were rejected using EEGLAB.

DIPFIT functions within EEGLAB (Oostenveld and Oostendorp, 2002) computed an equivalent current dipole model that best explained the scalp topography of each IC using a boundary element head model based on the Montreal Neurological Institute (MNI) template (the average of 152 MRI scans from healthy subjects, available at www.mni.mcgill.ca). We excluded ICs from further analysis if the projection of the equivalent current dipole model to the scalp accounted for less than 80% of the scalp map variance, or if the topography and time-course of the IC was reflective of eye movement artifact (Jung et al., 2000a; Jung et al., 2000b). The remaining ICs were classified as electrocortical sources or muscle sources based on inspection of their power spectra and the locations of their equivalent current dipoles. Next, electrocortical sources were clustered across subjects using EEGLAB routines implementing k-means clustering on vectors jointly coding differences in equivalent dipole locations and power spectra; the resulting joint vector was reduced to 10 principal dimensions using principal component analysis (Gramann et al., 2009; Jung et al., 2001).

We generated spectrograms for each electrocortical source during each gait cycle for each subject. For comparison purposes we selected a subset of muscle sources located around the left and right mastoid processes (possibly representing left and right

sternocleidomastoid EMG) and computed similar spectrograms. The single-trial spectrograms were then linearly time-warped so that both right and left heel-strikes occurred at the same adjusted latencies in each epoch (Makeig et al., 2007). To visualize intra-stride changes in the spectrograms, we subtracted the average log spectrum for all gait cycles from the log spectrogram for each gait cycle. We refer these changes from baseline as gait event related spectral perturbations (ERSP) (Makeig, 1993). We generated grand average mean ERSP plots for each cluster of electrocortical sources at each walking speed. Significant gait ERSPs ($p<0.05$) were identified using a bootstrapping method available within EEGLAB (Delorme and Makeig, 2004). In order to visualize the relative timing of spectral power fluctuations we computed the average gait ERSP for each electrocortical source in the alpha (8-12 Hz), beta (12-30 Hz), and high-gamma (50-150 Hz) frequency bands. We displayed these average ERSPs in separate line plots for each frequency band.

Results

Clusters of electrocortical sources that were identified by ICA and inverse source modeling were spatially localized to the prefrontal cortex (5 electrocortical sources), left and right sensorimotor cortex (7 and 6 sources), anterior cingulate cortex (9 sources), and posterior parietal cortex (13 sources) (Figure 3-1). Electrocortical sources were also identified in the left premotor cortex, left/right temporal lobe, and left/right occipital lobe, but these sources were found in less than half of our subjects and so were not included in subsequent analysis. Gait ERSPs revealed small but significant modulations

of spectral power within IC clusters localized in or near the anterior cingulate, posterior parietal, and left/right sensorimotor cortex (Figure 3-2). Finding no significant differences between gait ERSPs for 0.8 and 1.25 m/s walking, we averaged the gait ERSPs across walking speeds.

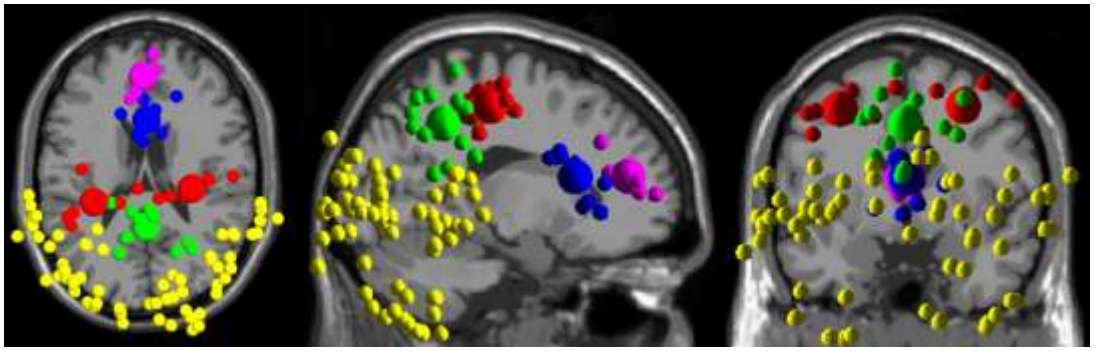

Figure 3-1: Clusters of electrocortical sources localized to the anterior cingulate cortex (blue), prefrontal cortex (purple), posterior parietal cortex (green), and sensorimotor cortex (red). Small spheres indicate the equivalent current dipole locations for single electrocortical sources for single subjects; larger spheres indicate geometric cluster centroids. The locations of the equivalent current dipoles for muscle sources are shown in yellow.

Cortical local field potential activity represents net potentials within complex local thalamocortical and cortico-cortical networks with many modulatory influences. Cortically generated far-field EEG activity recorded at scalp electrodes reflects partial synchrony of local field potentials across a compact cortical domain (on the order of a cm^2) that is far larger than a few neurons. Increased EEG power relative to the mean baseline, shown in Figure 3-2 by warm colors, may reflect a mean increase in the degree of local synchrony within the source domain, a change in the size of the source domain, and/or stronger local field activity within the source domain. Decreased power is indicated by cool colors.

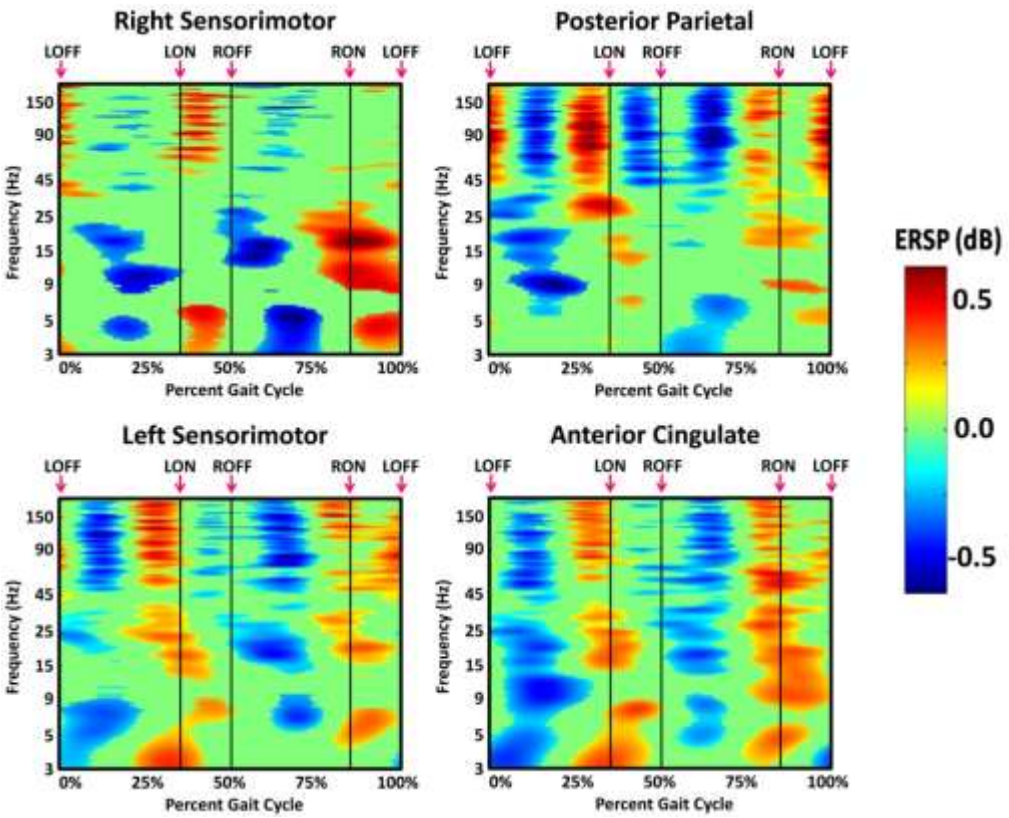

Figure 3-2: Gait event-related spectral perturbation (ERSP) plots showing average changes in spectral power during the stride cycle relative to the full gait cycle baseline for (top left) the right sensorimotor cluster, (top right) the posterior parietal cluster, (bottom left) the left sensorimotor cluster, and (bottom right) the anterior cingulate cluster. The gait cycle begins and ends with left toe-off (LOFF). Vertical lines indicate the timing of left heel-strike (LON), right toe-off (ROFF), and right heel-strike (RON). Non-significant differences (p>0.05) have been set to 0 dB (green).

Significant alpha- and beta-band power increases in or near the left/right sensorimotor and dorsal anterior cingulate cortex occurred during the end of stance as the leading foot was contacting the ground and the trailing foot was pushing off. Power increases in the left/right sensorimotor cortex were more pronounced for contralateral limb push-off (ipsilateral heel-strike) than for ipsilateral limb push-off (contralateral heel-strike) (Figure 3-2). Within the alpha- and beta-bands, spectral fluctuations for all four electrocortical sources were in phase with each other. Peaks in beta-band spectral power preceded peaks in alpha-band spectral power by roughly 8% of the gait cycle;

beta-band peaks occurred at heel-strike while alpha-band peaks occurred roughly half-way through the double support phase (Figure 3-3). Power increases in the high-gamma band occurred for all clusters (Figure 3-2). With the exception of the right sensorimotor source, high-gamma spectral fluctuations across the electrocortical domains were in phase with each other and exhibited more peaks per gait cycle than the alpha- and beta-band spectral fluctuations. High-gamma spectral fluctuations in the right sensorimotor source were out of phase with high-gamma fluctuations in the other electrocortical domains (Figure 3-3).

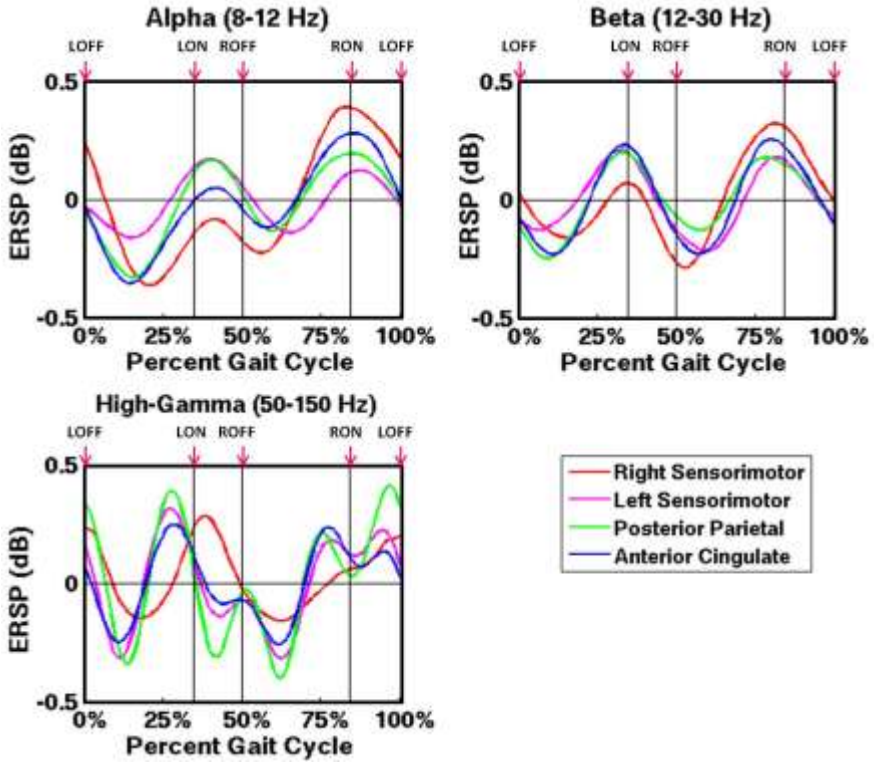

Figure 3-3: Average gait event-related spectral perturbation (ERSP) line plots for the (top left) alpha (8-12 Hz), (top right) beta (12-30 Hz), and (bottom left) high-gamma frequency bands. Each cluster of electrocortical sources is represented by a colored trace: (red) right sensorimotor cluster, (magenta) left sensorimotor cluster, (green) posterior parietal cluster, and (blue) anterior cingulate cluster. The gait cycle begins and ends with left toe-off (LOFF). Vertical lines indicate the timing of left heel-strike (LON), right toe-off (ROFF), and right heel-strike (RON).

To highlight the importance of extracting neck muscle contributions from the EEG signals, we have also shown gait ERSP plots for groups of muscle sources that were localized to the region around the left/right mastoid processes (Figure 3-4). Muscle sources exhibited larger intra-stride spectral power changes than electrocortical sources; as such, the color scale in Figure 3-4 is four times coarser than in Figure 3-2. The broad spatial distribution of all neck muscle sources (Figure 3-1) is reflective of the fact that many neck muscles contribute to head stabilization during walking (Cromwell et al., 2001). Only one subset of these neck muscle sources is represented in Figure 3-4, with the intent of demonstrating that the magnitude of electromyographic spectral fluctuations can be at least 4X greater than the magnitude of electrocortical spectral fluctuations.

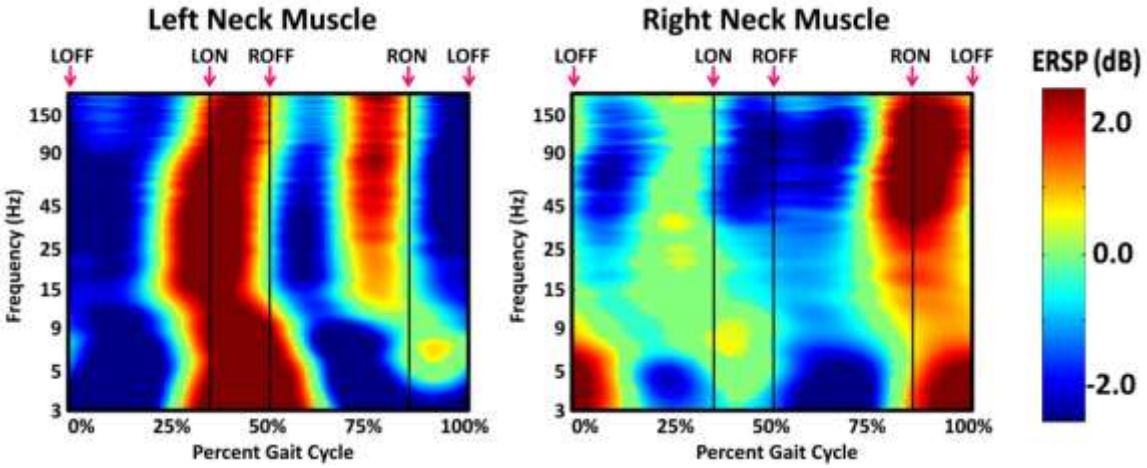

Figure 3-4: Gait event-related spectral perturbation (ERSP) plots showing average changes in spectral power relative to a full gait cycle baseline for a subset of neck muscle components localized to the region around the left (shown left) and right (shown right) mastoid processes. These clusters may represent left and right sternocleidomastoid EMG and are shown for comparison with Figure 2. Note that the color scale is coarser than Figure 2. The gait cycle begins and ends with left toe-off (LOFF). Vertical lines indicate the timing of left heel-strike (LON), right toe-off (ROFF), and right heel-strike (RON). Non-significant differences (p> 0.05) have been set to 0 dB (green).

Discussion

To our knowledge, this is the first study to report intra-stride patterns of spatially resolved human brain activation during walking. ICA decomposition parsed scalp EEG into activities generated in separate cortical domains, individual neck and scalp muscles, and other non-brain artifact sources (eyes, heart, line noise, etc.). We found that small but significant changes in the power spectra of various electrocortical processes, which were disentangled from scalp EEG by ICA, occurred during particular phases of the gait cycle.

Significant alpha- and beta-band power increases in or near the left/right sensorimotor and dorsal anterior cingulate cortex occurred during the end of stance as the leading foot was contacting the ground and the trailing foot was pushing off. Findings from electrophysiological and imaging studies have suggested that dorsal anterior cingulate cortex may be the brain's center for error detection and correction (Bush et al., 2000; O'Connell et al., 2007; Walton et al., 2007). In our study, therefore, the increased beta activity in or near anterior cingulate during foot placement could be related to foot trajectory error detection and correction. A future experiment that examines a walking task requiring more controlled foot placement and step-to-step adjustment (e.g., walking on stepping stones or marks on the floor) could test this hypothesis. An alternate hypothesis is that medial frontal processes are implicated in the transition from flexion to extension (akin to the stance to swing transition in normal walking). This hypothesis is supported by a recent study of scalp EEG topography during

a rhythmic multi-joint lower-limb movement task designed to mimic walking (Wieser et al., 2010).

Power increases in the left/right sensorimotor cortex were most pronounced during the end of contralateral limb stance when maximum lower limb muscle power is required (Kuo et al., 2005) but somatosensory attention may shift from the contralateral limb to the ipsilateral limb about to be raised (Pfurtscheller et al., 1996). It is possible that increased sensorimotor cortex EEG power during push-off indexes stronger lower limb muscle recruitment. If so, future studies examining biomechanical perturbations to gait might identify correlations between muscle recruitment and electrocortical dynamics during walking. Interestingly, electrocortical sources were broadly distributed in the lower and upper limb regions of the somatosensory cortex. This may be reflective of different attentional strategies between subjects who are more or less accustomed to treadmill walking. Future studies examining simultaneous lower and upper limb motor tasks could test whether high density EEG and ICA can effectively disentangle sources in the upper limb region of the somatosensory cortex from sources in the lower limb region.

Broad high-gamma (50-150 Hz) changes in electrocortical power intra-stride were evident in all four electrocortical clusters including the posterior parietal cortex. Prior research has suggested that high-gamma activity is increased in human cortex during selective attention (Ray et al., 2008), in motor cortex accompanying finger movements (Pfurtscheller et al., 1996), and selectively in different cortical regions during various imagined emotion states (Onton and Makeig, 2009). Others have proposed that during

rhythmic sensory tasks the brain favors a 'rhythmic mode of operation' that includes entrainment of lower-frequency oscillations to task dynamics and temporal alignment of high-frequency oscillations to attended rhythmic events as a means of enhancing responses that are in-phase with attended events and suppressing responses that are out-of-phase with attended events (Schroeder and Lakatos, 2009). It has also been suggested that during dynamic force production the sensorimotor system shifts towards gamma frequencies to rapidly integrate multi-sensory information that is required to produce the appropriate motor command (Omlor et al., 2007).

Posterior parietal cortex has been associated with visuo-motor integration and bimanual coordination. Prior research using functional magnetic resonance imaging has implicated the posterior parietal cortex in upper-limb reaching (Filimon et al., 2009) and in coordination of left and right wrist movements (Wenderoth et al., 2005). In addition, microwire arrays implanted into feline posterior partial and motor cortex during flat ground and precision walking have suggested that visuo-motor integration during locomotion is critically dependent on posterior parietal and motor cortex networks (Andujar et al., 2010; Beloozerova and Sirota, 2003; Drew et al., 2002; Lajoie et al., 2010). In our study, we found (with one exception) that within a given frequency band (alpha, beta, or high-gamma) spectral power fluctuations were synchronous across all four electrocortical domains but were not uniformly significant (i.e. periods of significant spectral fluctuations occurred in different regions of the gait cycle for different electrocortical domains, Figure 3-2). The exception was that high-gamma fluctuations in the right sensorimotor cortex were out of phase with high-gamma fluctuations in the

other three regions (left sensorimotor, anterior cingulate, and posterior parietal). This is consistent with convincing evidence that bilateral coordination preferentially recruits the left hemisphere and that the left hemisphere regulates limb position and posture (Serrien et al., 2006). Synchronous spectral power fluctuations across the anterior cingulate, posterior parietal and left sensorimotor cortex may be reflective of visuo-motor integration and error monitoring networks.

In this study we showed intra-stride changes in spectral power of neck and scalp muscle sources to demonstrate the importance of spatially filtering EEG signals. Muscle source spectral power changes were substantially larger than electrocortical spectral power changes. Interestingly, neck muscle sources located around the left and right mastoid processes (possibly representing left and right sternocleidomastoid EMG) exhibited increased spectral power from ipsilateral heel-strike through contralateral toe-off, which may be reflective of head stabilization during locomotion. The sternocleidomastoid is only one of several muscles that contribute to head stabilization during walking (Cromwell et al., 2001). A more thorough analysis of neck muscle EMG, including EMG sources extracted from EEG by the methods presented herein, is needed to characterize intra-stride patterns of neck muscle activation and to assess the possibility of incomplete decontamination of electrocortical sources.

The intra-stride changes in electrocortical spectral power identified in this study are small, on the order of 0.5 dB (corresponding to a mean 2.5% amplitude increase). Nevertheless, the existence of significant intra-stride patterns of activation and deactivation suggests that the human cortex is actively engaged during steady-speed

locomotion. Given that corticospinal excitability is modulated during the human gait cycle (Capaday et al., 1999; Petersen et al., 2001; Schubert et al., 1997) it is likely that direct corticospinal pathways contribute to locomotor execution. This hypothesis is also supported by a recent PET study of imagined and real walking (la Fougere et al., 2010). However, tonic descending inputs to spinal networks from the mesencephalic locomotor region of the brainstem can also generate rhythmic muscle activation and may be modulated by afferent sensory signals processed in the cortex (Rossignol et al., 2006). In an *in-vitro* isolated lamprey brainstem the mesencephalic locomotor region has recently been shown to modulate sensory transmission (Le Ray et al., 2010) and rhythmic motor tasks have been shown to activate the sensorimotor cortex even when performed passively (Christensen et al., 2000). Given these prior results, our finding of intra-stride cortical spectral power fluctuations in humans, while novel, is not entirely surprising. Furthermore, our finding does not indicate whether human cortex is actively involved in controlling locomotion via direct pathways or whether human cortex processes sensory afferents that are used to modulate a descending signal to spinal generators via the mesencephalic locomotor region. We expect that human cortex in fact performs both of these functions. Studying walking under challenging conditions, with either increased or decreased sensory demands or availability, may provide a means of further testing these hypotheses. It may be easier to discern the precise nature of attended sensory events during challenging walking conditions than during normal locomotion. For example, close examination of these data revealed no relationship between the timing of intra-stride power increases and step-to-step

changes in step duration for any of the clusters of electrocortical sources. We expect that 1) walking through more complex environments with obstacles and varied terrain requires more input from supraspinal centers than steady-speed treadmill walking, and 2) steady-speed treadmill walking on a flat consistent surface should demand less cortical control and adjustment, indexed by less within-stride variation in high-frequency EEG source activity. However, our data suggest that even under steady-speed walking conditions the cortex shows moment-to-moment adjustments in activity tone. The locations of the electrocortical sources that were active during walking are mostly consistent with results of prior studies using fNIRS and PET. Unlike recent PET results (la Fougere et al., 2010), but as expected for scalp EEG data, we did not detect EEG source activity in parahippocampal or cerebellar regions.

In a clinical setting, the ability to quantify brain activation patterns during gait in neurologically impaired patients could be helpful as it might allow clinicians to better diagnose subsets of patients with similar EEG symptomatology (Alexander et al., 2009; Boyd et al., 2007). Most behavioral variables of motor performance (e.g. over-ground preferred walking speed) have large inter-subject and intra-subject variability, making them coarse measures of motor learning and neural plasticity. Even when behavioral measures are robust enough to test the efficacy of therapeutic interventions, methods to quantify brain plasticity (versus spinal plasticity or muscle plasticity) are needed for studying the underlying mechanisms of motor recovery (Gorassini et al., 2009; Norton and Gorassini, 2006; Yang and Gorassini, 2006). Spatially resolved EEG measures might help clinicians choose rehabilitation strategies with a better chance of success and might

also allow researchers and clinicians to track brain plasticity during interventions to gauge the success of an intervention (Boyd et al., 2007; Mielke and Szelies, 2003; Weiller, 1998; Yang and Gorassini, 2006). Another potential use of the technique presented here would be to identify neural mechanisms of freezing gait in Parkinson's patients.

In closing, our study suggests that high-density EEG recorded simultaneously with body motion capture during ambulation and then spatially resolved using independent component analysis can provide insight into the cortical contributions to locomotor control and might provide useful information regarding brain activation supporting gait in clinical settings.

Chapter 4: How many electrodes are really needed for EEG-based mobile brain imaging?

This chapter has been accepted for publication:

*Lau TM, *Gwin JT, Ferris DP. *Journal of Brain and Behavioral Science.* [In Press].

*These authors contributed equally to this manuscript. JG contributed the sections on "assessing changes in IC scalp projections." TL contributed the section on "assessing changes in IC activations."

Abstract

A noninvasive method for imaging the human brain during mobile activities could have far reaching benefits for studies of human motor control, for research and treatment of neurological disabilities, and for brain-controlled powered prosthetic limbs or orthoses. Several recent studies have demonstrated that electroencephalography (EEG) can be used to image the brain during locomotion provided that signal processing techniques, such as independent Component Analysis (ICA), are used to parse electrocortical activity from artifact contaminated EEG. However, these studies used high-density 256-channel EEG sensor arrays, which are likely too time-consuming to setup in a clinical or field setting. Therefore, it is important to evaluate how reducing the number of EEG channel signals affects the electrocortical source signals that can be parsed from EEG recorded during standing and walking while concurrently performing a visual oddball discrimination task. Specifically, we computed temporal and spatial correlations between electrocortical sources parsed from high-density EEG and electrocortical sources parsed from reduced-channel subsets of the original high-density EEG. For this task, our results indicate that on average an EEG montage with as few as

35 channels may be sufficient to record the two most dominate electrocortical sources (temporal and spatial $R^2 > 0.9$). Correlations for additional electrocortical sources decreased linearly such that the least dominant sources extracted from the 35 channel dataset had temporal and spatial correlations of approximately 0.7. This suggests that for certain applications the number of EEG sensors used for mobile brain imaging could be vastly reduced, but researchers and clinicians must consider the expected distribution of relevant electrocortical sources when determining the number of EEG sensors necessary for a particular application.

Introduction

Electroencephalography (EEG) has long been used to record electrocortical activity within the brain because it is a safe and non-invasive tool (Klimesch, 1999; Makeig et al., 2009; Rabbi et al., 2009). EEG is used to monitor ictal and inter-ictal activity in seizure patients (Buechler et al., 2008; Rudzinski and Meador, 2011) and to assess cognitive processes during neuroscience and psychology experiments (De Raedt et al., 2008; Santesso et al., 2008). In addition, EEG is used in brain computer interface devices, which enable command of an electronic device by brain activity modulation (Jerbi et al., 2011; Müller et al., 2008; Patil and Turner, 2008; Sullivan et al., 2008). Current EEG systems can have as few as four electrodes (Sullivan et al., 2008) or as many as 256 electrodes. Until recently, the use of EEG has been limited to stationary settings (i.e., settings where the subject is seated or prone) because of the susceptibility of EEG electrodes to movement and electromyographic artifacts (Godlove, 2010; Jung et al.,

2000a). However, we have recently demonstrated that these artifacts can be removed from high-density (256-channel) EEG using advanced computational methods; thus enabling the use of EEG during walking (Gramann et al., 2011a; Gwin et al., 2010a, b). When combined with kinematic motion capture, this novel paradigm has been referred to as Mobile Brain Imaging (MoBI) (Makeig et al., 2009) and is gaining traction as a viable technique to study the human brain under non-stationary conditions. MoBI will open the door to a plethora of new research areas including cognitive control of locomotion, brain-body interactions in neurological disorders, and advancements in the field of brain-machine interfaces.

The use of Independent Component Analysis (ICA), a technique that parses independent component (IC) signals from correlated time-series data (Delorme and Makeig, 2004; Delorme et al., 2007; Gwin et al., 2010b; Jung et al., 2000a; Makeig et al., 1996; Palmer et al., 2006; Palmer et al., 2008), has been particularly helpful to the development of MoBI. ICA of EEG is based on the premise that each electrode on the scalp records a linear sum of various underlying electrocortical signals, as well as electromyographic, electroocular, electrocardiographic, and movement artifacts. ICA can generate one maximally independent source signal (which may reflect an electrocortical or artifactual source) for each EEG channel signal recorded; the more EEG channels recorded, the more ICs produced (Palmer et al., 2006; Palmer et al., 2008). Therefore, it is desirable to record from as many EEG sensors as possible if the intent is to capture as many electrocortical processes as possible.

Increasing the number of EEG electrodes used is not trivial, and the increase is not without drawbacks. For high-density EEG systems, data processing can take a significant amount of time, even on large computing clusters. In addition, more electrodes mean higher costs and more difficult experimental setups. Lastly, in experimental setups involving movement and in many real-world settings, wireless transmission of EEG signals is desirable. Increasing the number of electrodes challenges existing wireless transmission systems. Given these drawbacks, a question naturally arises: how many electrodes are needed for MoBI? The answer will likely depend on the tasks being performed and nature of the cognitive activity involved, but we can begin to estimate the number for common situations.

In this study, we assessed how reducing the number of EEG channel signals affects the electrocortical source signals that can be parsed from EEG recorded during standing and walking using ICA. We performed this assessment using data from (Gwin et al., 2010b). This study involved subjects standing and walking while performing a visual oddball discrimination task. We incrementally reduced the number of channels from the EEG montage that were used in the analysis and evaluated changes in the temporal and spatial properties of the resulting electrocortical source signals.

Methods

Data Collections

Twelve healthy volunteers with no history of major lower limb injury and no known neurological or locomotor deficits completed this study (11 males and 1 female, age

range 20-31 years). All subjects provided written informed consent prior to the experiment. All procedures were approved by the University of Michigan Internal Review Board and complied with the standards defined in the Declaration of Helsinki.

Subjects stood, walked (0.8 m/s and 1.25 m/s), and ran (1.9 m/s) on an in-ground treadmill (Collins et al., 2009) while we recorded 248-channel electroencephalography at 512 Hz (ActiveTwo, BioSemi, Amsterdam, The Netherlands). Concurrently, standard (80%) and target (20%) stimuli (vertical or 45° rotated black crosses on a white background, respectively) were displayed on a monitor placed at eye level about 1 m in front of the subjects. For each gait condition (standing, slower walking, faster walking, running) subjects performed an experimental block wherein they were asked to press a handheld button whenever the target stimulus appeared and a control block wherein no manual response to the target stimulus was required. Each data collection session began with the standing condition, followed by the other three conditions in random order. The standing blocks lasted 5 minutes each while the walking and running blocks lasted 10 minutes each. For the present study, data collected during running were not used due to the presence of large mechanical artifacts in the EEG signals.

EEG Processing

All processing and analysis was performed in Matlab (The Mathworks, Natick, MA) using scripts based on EEGLAB (sccn.ucsd.edu/eeglab), an open source environment for processing electrophysiological data (Delorme and Makeig, 2004).

After data collection we high-pass filtered the EEG signals above 1 Hz. As in (Gwin et al., 2010a, b), EEG signals exhibiting substantial noise throughout the collection were

removed from the data in the flowing manner: 1) channels with std. dev. > 1000 μV were removed, 2) any channel whose kurtosis was more than 5 std. dev. from the mean was removed, and 3) channels that were uncorrelated ($r < 0.4$) with nearby channels for more than 1% of the time-samples were removed. Datasets containing fewer than 125 channels after channel rejection were not included in this analysis (data for 7 subjects, all males, were retained). For each remaining subject, a subset of 125 channels was selected so that the electrodes were uniformly distributed across the scalp (due to channel rejection the electrode arrays differed slightly among subjects). Next, for each subject, a subset of 115 channels was selected from the 125 channel subset so that the electrode distribution remained maximally uniform. We continued this processes, selecting nested subsets of channels, until we had 11 EEG subsets per subject (125, 115… 25 channels). For each subject and each channel subset, the channel signals were re-referenced to an average reference.

We applied an adaptive mixture ICA algorithm [AMICA] (Palmer et al., 2006; Palmer et al., 2008) to each subset of EEG signals. ICA parses EEG signals into spatially static, maximally independent component processes (Makeig et al., 1996). Prior to performing ICA decomposition, time-periods of EEG with substantial artifact, as defined by z-transformed power across all channels in a given time window being larger than 0.8, were rejected using EEGLAB. DIPFIT functions within EEGLAB (Oostenveld and Oostendorp, 2002) computed an equivalent current dipole model that best explained the scalp topography of each IC using a boundary element head model based on the

Montreal Neurological Institute (MNI) template (the average of 152 MRI scans from healthy subjects, available at www.mni.mcgill.ca).

The datasets with 125 channels were considered to be benchmark datasets to which the reduced channel datasets (115, 105 … 25 channels) were compared. For this purpose, each of the 125 ICs for the 125-channel ICA decompositions were categorized as electrocortical activity, muscle activity, eye movement artifact, or noise in the following manner. First, if the projection of the equivalent current dipole model to the scalp accounted for less than 85% of the scalp topography variance the component was considered to be noise (scalp topography refers to a mapping of electrode coefficients for each IC onto a 2-dimensional head-map). Second, the scalp topography and time-course of each IC was visually inspected to identify ICs that were reflective of eye movement artifact (Jung et al., 2000a). Third, the remaining ICs were classified as electrocortical sources or muscle sources based on inspection of their power spectra and the locations of their equivalent current dipoles.

Assessing changes in IC scalp projections

To assess changes in the scalp topography of the ICs, as a function of the number of EEG channels used, the scalp topographies of ICs from the reduced channel datasets were interpolated at each EEG channel location in the 125-channel electrode montage. Next, for each subject, pairwise correlations were computed between IC scalp topographies for the 125-channel ICA decomposition and each of the reduced-channel ICA decompositions, using the Hungarian method. Only ICs representing electrocortical activity from the 125-channel dataset were considered. ICs were paired based on the

maximum absolute IC scalp topography correlation. In other words, ICs from the reduced-channel datasets were paired with ICs from the 125-channel dataset that had similar scalp topography, irrespective of polarity. Finally, IC pairs were sorted by absolute IC scalp topography correlation and averaged across subjects. We also computed the percentage of electrocortical and electromyographic sources that were retained for each reduced-channel dataset. The percentage of electrocortical sources retained was defined as the number of electrocortical sources in the 125-channel dataset that were correlated with a source in the reduced-channel dataset ($r > 0.85$); the percentage of electromyographic sources retained was similarly defined.

Assessing changes in IC activations

To assess changes in IC activation (i.e., timeseries) as a function of the number of channels used, pairwise correlations (for each subject) were computed between 125-channel IC activations and reduced-channel IC activations, using the Hungarian method. Only ICs representing electrocortical activity from the 125-channel dataset were considered. ICs were paired based on the maximum correlation. In other words, ICs from the reduced-channel datasets were paired with ICs from the 125-channel dataset that had similar activations. Finally, IC pairs were sorted by IC activation correlation and averaged across subjects.

Assessing changes in visual target discrimination electrocortical dynamics

Previous analysis of a similar visual target discrimination task for seated subjects showed that brain processes projecting maximally to the frontal midline would contribute substantially to the event related potential (ERP), particularly to the post-

motor positivity (Makeig et al., 2004). Prior visualizations of grand average IC-based ERPs from our dataset confirmed that mediofrontal ICs (projecting maximally to the frontal midline) had a clear and substantial stimulus-locked ERP (Gwin et al., 2010b).

In this study, the IC that projected most strongly to the frontal midline for each subject was identified from the 125-channel IC decomposition by inspecting the scalp topographies. Next, the corresponding paired ICs from the reduced-channel datasets were identified. For each IC, signal epochs were extracted, time-locked from -200 to 800 ms relative to visual stimulus onsets, using data from only the active walking conditions (i.e., the conditions in which subjects were walking and actively responding to the oddball stimuli by pressing a handheld trigger). A signal-to-noise ratio was computed for each trial as the peak magnitude in the range of 300 to 600 ms after the stimulus divided by the pre-stimulus standard deviation (Debener et al., 2007). For each subject and each dataset (i.e., the 125-channel dataset and the reduced-channel datasets) the mean signal-to-noise was computed. Analysis of variance was used to compare the grand mean signal-to-noise ratio across datasets.

Results

Of the 12 subjects who participated in this study, 7 had 125 or more EEG channels after rejection of noisy channels. For these subjects, 9.0 ± 1.3 electrocortical sources, 10.9 ± 2.3 electromyographic sources, and 2.4 ± 1.6 electroocular sources, were identified for the 125-channel datasets (mean ± std. dev.). In general, the scalp

topographies for electrocortical sources were more distorted by reducing the number of EEG channels than the scalp topographies for electromyographic sources (Figure 4-1).

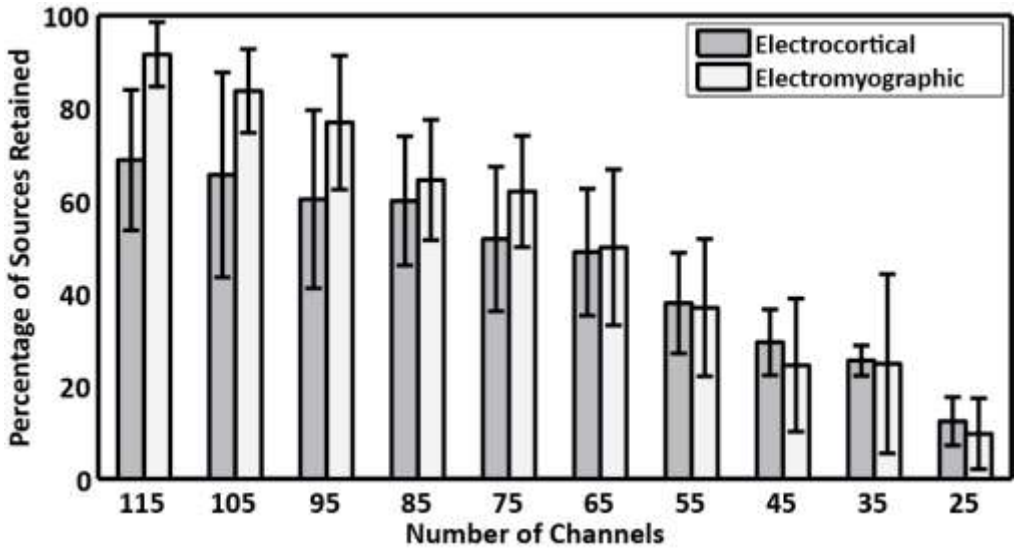

Figure 4-1: Percentage of brain and muscle sources retained for the reduced-channel datasets. containing 115, 105 … 25 EEG channels.The percentage of electrocortical sources retained was defined as the number of electrocortical sources in the 125-channel dataset that were correlated with a source in the reduced-channel dataset (R > 0.85); the percentage of electromyographic sources retained was similarly defined

The average correlation between electrocortical source scalp topographies for the reduced channel datasets (115, 100 … 25 channels) and the 125-channel dataset decreased from 0.90 ± 0.09 for the 115-channel dataset to 0.70 ± 0.14 for the 25-channel dataset (mean ± std. dev.) (Figure 4-2). Scalp topographies of four electrocortical sources, from an example subject, are shown for the 125-channel, 105-channel … 25-channel datasets (Figure 4-3). The average correlation between electrocortical source activation for the reduced-channel datasets and the 125-channel dataset decreased from 0.86 ± 0.03 for the 115-channel dataset to 0.63 ± 0.04 for the 25-channel dataset (Figure 4-4). The visual target discrimination ERP signal-to-noise ratio did not change significantly (P = 0.65) as a function of the number of channels

removed. The mean (std. dev.) signal-to-noise ratio across all subjects and all datasets was 3.08 (0.09).

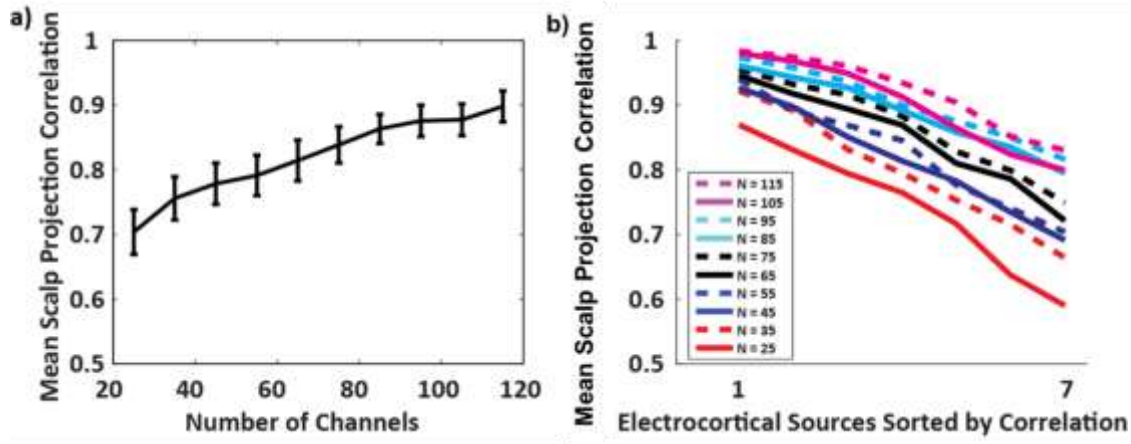

Figure 4-2: Correlation between reduced channel and 125-channel electrocortical scalp projections. A) Grand average absolute correlation between electrocortical source scalp projections for the reduced channel datasets and the 125-channel dataset (error-bars, 2 S.E.), and B) average absolute correlation between electrocortical source scalp projections for the reduced-channel datasets and the 125-channel dataset ordered by the magnitude of correlation; traces are color coded by the number of channels in the reduced-channel dataset. Data for the 7 best correlated sources are shown.

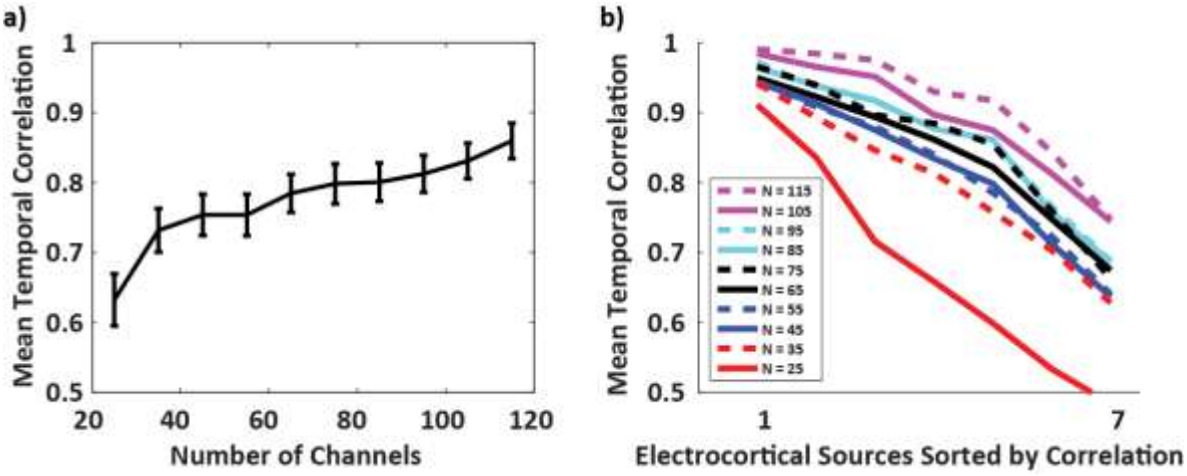

Figure 4-3: Correlation between reduced channel and 125-channel electrocortical source activations. A) Grand average absolute correlation between electrocortical source temporal signals for the reduced channel datasets and the 125-channel dataset (error-bars, 2 S.E.), and B) average absolute correlation between electrocortical source temporal signals for the reduced-channel datasets and the 125-channel dataset ordered by the magnitude of correlation; traces are color coded by the number of channels in the reduced-channel dataset. Data for the 7 best correlated sources are shown.

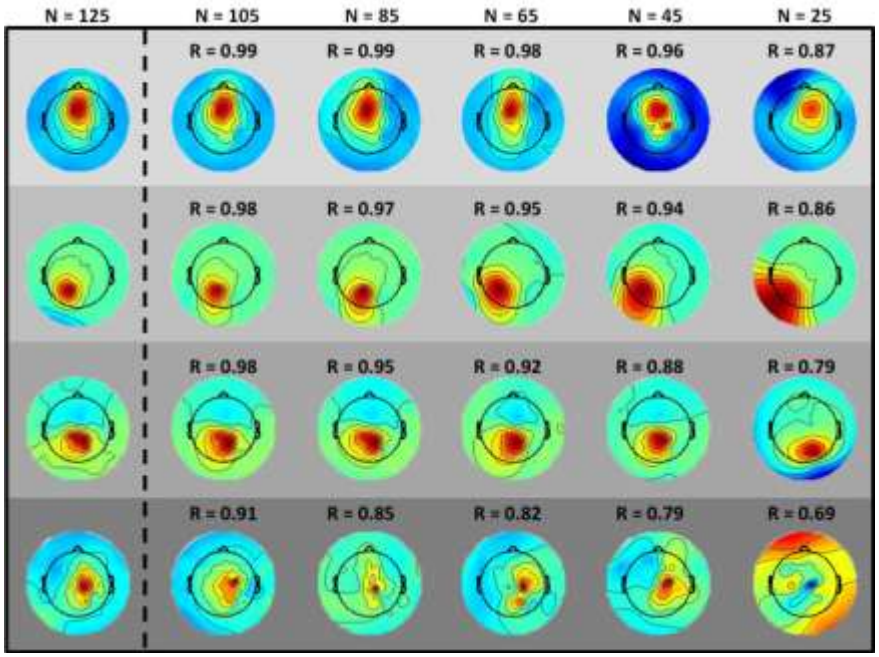

Figure 4-4: Electrocortical scalp projections for an example subject from the (columns, left to right) 125-channel, 105-channel … 25-channel datasets, (rows) four electrocortical sources are shown for each dataset. Correlation values between the reduced-channel scalp projections and the 125-channel scalp projection are shown.

Discussion

This work demonstrates a distinct relationship between the number of EEG electrodes used and the quality of electrocortical source signals that can be parsed from scalp EEG, recorded during standing and walking, using ICA. By systematically reducing the number of channels used, we implemented a straightforward paradigm to assess how reducing the number of EEG channel signals affected the electrocortical source signal estimates derived from ICA. We evaluated the scalp topography (i.e., the electrode coefficients mapped to the scalp), the timeseries activation of the electrocortical signals, and the signal-to-noise ratio of an IC-based visual target discrimination ERP.

Correlations between scalp topographies from the benchmark (125-channel) dataset and the reduced-channel datasets fell off linearly with the number of channels used. The correlation between the electrocortical source activations also weakened as the number of channels used was reduced. Figure 4-4 demonstrates that small reductions in scalp topography correlation can lead to qualitatively different topographies.

It is important not to over-interpret the spatial or the temporal performance results. These measures must be considered collectively. Topographical comparisons do not reflect the absolute contributions to the IC from each channel. For example, if a patch of EEG channels remained relatively silent (or absolutely zero) than any combination of weights for those electrodes would return (nearly) the same IC activation. In addition, temporal correlations, measured over the entire experimental time-course, may not reflect the true accuracy of the electrocortical source signal because events time-locked to cortical processes may be better reconstructed than the entire activation time series. Furthermore, the correlations evaluated here do not indicate whether causal relationships between various electrocortical sources are maintained as channels are reduced.

Our results suggest that, for the concurrent locomotor and cognitive tasks studied here, the two most robust electrocortical sources can be well captured (temporal and spatial $R^2 > 0.9$) using an electrode montage with as few as 35 channels. The anterior cingulate cortex source, which contributes strongly to the visual target discrimination ERP, is a robust component that was well captured by the reduced-channel IC decompositions. Therefore, it is not surprising that the signal-to-noise ratio of the IC-

based ERP did not change significantly as the number of channels was reduced. This is an encouraging result for those interested in analyzing ERPs during mobile activities for BMI applications or for research purposes.

Another consideration is that despite the use of a 256-channel EEG system on average only 125 channels were usable. Poor recordings in the other channels were due to large movement artifacts and/or degrading electrode-scalp connections, which likely resulted from forces on the electrode head cap from moving electrode wires. As sensor technologies improve (i.e., dry electrode sensors and wireless transmission) a higher percentage of electrodes will yield clean usable signals.

An emerging field of study in neuroscience approaches the brain as a complex network of dynamic oscillators. ICA has already been utilized to formulate these network nodes for various analyses (Calhoun et al., 2008; Damoiseaux et al., 2008; Londei et al., 2007). The number of ICs extracted is of critical importance when studying brain activity with these methods. ICA can decode and anatomically locate sources of EEG activity; therefore, physiologically realistic maps can be generated when the density of anatomical nodes is sufficient. Therefore, while reducing the number of EEG channels may be sufficient for analysis of ERPs during mobile tasks, researchers interested in network analysis will likely want to maximize the number of EEG signals recorded.

Another area in which ICA of EEG has proved useful is seizure detection and localization (Nam et al., 2002). Seizures are often marked by large amounts of movement artifact that can pose similar challenges as locomotion to the interpretation of EEG recordings (Urrestarazu et al., 2004). The use of ICA to remove movement

artifact from seizure EEG and to localize the anatomical source of seizure activity can be beneficial to this field. We can only speculate how the results of this study will transfer to seizure analysis. However, during seizure, the seizure-related EEG activity is dominant in the EEG channel signals. Therefore, just as the anterior cingulate source was well captured by the reduced-channel electrode montages in this study, seizure activity may be well captured with a reduced number of EEG sensors. We believe that applying the analysis approach presented in this study to seizure-related EEG would answer this question and, therefore, should be pursued.

The results of this study are important because they provide useful information for researchers and developers who are interested in implementing MoBI. While additional EEG electrodes (at least up to 125 channels, as shown here) will improve the ICA decomposition, task specific placement of electrodes may bypass the need for added channels. For example, the cognitive state of a subject can be extracted from a few usable ICs, negating the benefit of additional channels (Patil and Turner, 2008; Sullivan et al., 2008). We plan to evaluate the relative effects of strategic placement of EEG electrodes in future work.

Chapter 5: An EEG-based study of discrete isometric and isotonic human lower limb muscle contractions

This chapter has been accepted for publication:
Gwin JT, Ferris DP. *Journal of Neuroengineering and Rehabilitation*. [In Press].

Abstract

Electroencephalography (EEG) combined with independent component analysis enables functional neuroimaging in dynamic environments including during human locomotion. This type of functional neuroimaging could be a powerful tool for neurological rehabilitation. It could enable clinicians to monitor changes in motor control related cortical dynamics associated with a therapeutic intervention, and it could facilitate noninvasive electrocortical control of devices for assisting limb movement to stimulate activity dependent plasticity. Understanding the relationship between electrocortical dynamics and muscle activity will be helpful for incorporating EEG-based functional neuroimaging into clinical practice. The goal of this study was to use independent component analysis of high-density EEG to test whether we could relate electrocortical dynamics to lower limb muscle activation in a constrained motor task. A secondary goal was to assess the trial-by-trial consistency of the electrocortical dynamics by decoding the type of muscle action.

We recorded 264-channel EEG while 8 neurologically intact subjects performed isometric and isotonic, knee and ankle exercises at two different effort levels. Adaptive mixture independent component analysis (AMICA) parsed EEG into models of underlying source signals. We generated spectrograms for all electrocortical source signals and used a naïve Bayesian classifier to decode exercise type from trial-by-trial time-frequency data.

AMICA captured different electrocortical source distributions for ankle and knee tasks. The fit of single-trial EEG to these models distinguished knee from ankle tasks with 80% accuracy. Electrocortical spectral modulations in the supplementary motor area were significantly different for isometric and isotonic tasks ($p<0.05$). Isometric contractions elicited an event related desynchronization (ERD) in the α-band (8-12 Hz) and β-band (12-30 Hz) at joint torque onset and offset. Isotonic contractions elicited a sustained α- and β-band ERD throughout the trial. Classifiers based on supplementary motor area sources achieved a 4-way classification accuracy of 69% while classifiers based on electrocortical sources in multiple brain regions achieved a 4-way classification accuracy of 87%.

In conclusion, independent component analysis of EEG reveals unique spatial and spectro-temporal electrocortical properties for different lower limb motor tasks. Using a broad distribution of electrocortical signals may improve classification of human lower limb movements from single-trial EEG.

Introduction

Functional neuroimaging could be a powerful tool for neurological rehabilitation. Being able to quantify how task specific brain activation is different in neurologically impaired patients compared to healthy individuals would inform clinical practice, would help clinicians choose a rehabilitation strategy with the best chance of success, and would facilitate tracking of brain plasticity during an intervention (Boyd et al., 2007; Weiller, 1998; Yang and Gorassini, 2006). In addition, functional neuroimaging may facilitate brain-based control of devices that assist limb movement and thus stimulate activity dependent plasticity (Daly and Wolpaw, 2008; Wang et al., 2010).

Regaining the ability to walk after neurological injury is a fundamental rehabilitation goal that can vastly improve a patient's lifestyle. This recovery is dependent on our ability to strengthen and modulate cortical inputs for lower limb motor control (Enzinger et al., 2009; Yang and Gorassini, 2006). In addition, the contribution of these cortical inputs, relative to spinal networks, is dependent on task specific body dynamics (Maegele et al., 2002). To get the most clinical benefit from functional neuroimaging during neurological rehabilitation, it is necessary to establish relationships between electrocortical dynamics and muscle activity in neurologically intact humans during a variety of lower limb motor tasks including individual muscle contractions, coordinated stepping, and locomotion.

Electrical neuroimaging with electroencephalography (EEG) is the only non-invasive brain imaging modality that uses sensors that are light enough to wear while performing dynamic motor tasks and have sufficient time resolution to record changes in brain

activity on the timescale of natural human movements (Makeig et al., 2009). An alternate imaging technique that can be used during dynamic task performance is near-infrared spectroscopy (NIRS). However, NIRS records cortical hemodynamics with a temporal resolution on the order of several seconds (Irani et al., 2007; Villringer and Chance, 1997) while EEG records electrocortical processes with a temporal resolution on the order of several ms (Michel et al., 2009). Due to these advantages, electrical neuroimaging is well suited for implementation in a clinical rehabilitation setting.

To effectively study electrocortical dynamics using EEG it is necessary to implement signal processing techniques that parse electrocortical contributions to EEG signals from other contributing sources, such as electroocular, electrocardiographic, electromyographic, and movement artifacts. There are many approaches to this problem. Our preferred approach is independent component analysis (ICA). ICA is a blind source separation technique that optimizes a set of maximally independent source signals from linearly mixed recordings. When applied to EEG, ICA parses underlying electrocortical source signals from artifact contaminated electrical potentials on the scalp (Delorme et al., 2007; Jung et al., 2000a; Jung et al., 2000b; Makeig et al., 1996; Onton et al., 2006). An advantage of this approach is that electrocortical source signals are analyzed, as opposed to EEG channel signals that reflect the summed contribution of multiple electrocortical sources. In addition, we have recently demonstrated that ICA of EEG allows for functional neuroimaging during human locomotion (Gramann et al., 2011a; Gwin et al., 2010a, b). Therefore, this technique can be used throughout the rehabilitation process as the patient progresses toward more dynamic, real world tasks.

In addition to monitoring cortical plasticity, another potential application of functional neuroimaging for neurological rehabilitation is brain-based control of devices that assist limb movement with the goal of stimulating activity dependent plasticity (Daly and Wolpaw, 2008; Wang et al., 2010). ICA of EEG may be beneficial for these brain-machine interfaces (BMIs) (Hammon et al., 2008; Kachenoura et al., 2008). While early BMIs focused mainly on signals from primary motor cortex, there is an emerging consensus that a broad distribution of signals, and a better understanding of underlying cortical physiology, will improve the information transfer rate in these devices (Leuthardt et al., 2009). ICA identifies a broad distribution of electrocortical signals from scalp recordings. In addition, incorporating spatial, spectral, and temporal features of electrocortical signals, across multiple cortical areas, can improve the fidelity of classification algorithms (Besserve et al., 2011; Muller-Gerking et al., 1999; Qin et al., 2004; Ramoser et al., 2000; Wentrup et al., 2005; Zhang et al., 2007).

A common approach to the study of electrocortical source signals is to evaluate modulations in spectral power that are time-locked to an event of interest. One well established phenomenon is that oscillatory cortical activity in the α-band (8–12 Hz) and β-band (12–30 Hz) is suppressed during dynamic movements (Allen and MacKinnon, 2010; MacKay, 2005; Pfurtscheller and Lopes da Silva, 1999). This phenomenon is referred to as event-related desynchronization (ERD) and has been studied extensively for upper limb movements and to a lesser degree for foot and toe movements (Muller-Putz et al., 2007; Neuper et al., 2006; Pfurtscheller et al., 1997). Most studies evaluate ERD in EEG channel signals. Electrocorticography provides a more direct measure of the

underlying electrocortical sources, but electrocorticography is also affected by volume conduction of multiple electrocortical source signals (Whitmer et al.). ICA provides a means to evaluate spectral modulations in the underlying electrocortical processes themselves. In one study, ICA of EEG was shown to enhance the detection of the ERD associated with finger movements (Foffani et al., 2004).

In this study, we used ICA of high-density EEG to examine electrocortical dynamics while 8 healthy subjects performed isometric and isotonic, knee and ankle, flexor and extensor muscle contractions at two different effort levels. The goals of this study were to characterize differences in spatial and spectro-temporal electrocortical dynamics associated with these muscle activations, as well as to assess the trial-by-trial (i.e., single exercise repetition) consistency of these differences by decoding the type of muscle activation from the recorded brain signals. Specifically, we tested 1) whether the fit of single-trial EEG to different ICA mixture models could distinguish knee from ankle contractions; 2) if muscle contraction related electrocortical spectral modulations in the motor cortex would differ between isometric and isotonic tasks, and between flexion and extension tasks; 3) if tasks requiring a greater muscular effort would elicit a more pronounced ERD; and 4) if muscle contraction type could be distinguished from single-trial electrocortical spectrograms.

Studying these electrocortical dynamics will provide a better understanding of lower limb motor control and may inform our interpretation of earlier results regarding electrocortical spectral modulations during human walking. The techniques that we have implemented in this study can be used throughout the rehabilitation process to

study both discrete lower limb muscle activations and more dynamic tasks, such as coordinated non-weight-bearing stepping or normal locomotion. Therefore, we believe that the results of this study may have implications for neurorehabilitation of gait, including monitoring cortical plasticity and providing real-time control of robotic lower limb exoskeletons.

Methods

Tasks

Eight healthy volunteers with no history of major lower limb injury and no known neurological or musculoskeletal deficits completed this study (7 males; 1 female; age range 21–31 years). Subjects provided written informed consent prior to the experiment. The University of Michigan Internal Review Board approved all procedures, which complied with the standards defined in the Declaration of Helsinki.

Subjects sat on a bench while performing isometric muscle activations (activation without limb movement) and isotonic movements (activation with limb movement, concentric followed by eccentric) of the knee and ankle joints (Figure 5-1). Subjects performed both flexion and extension; except for isotonic knee flexion, which could not be accommodated by the test apparatus. They completed two sets of 20 repetitions of each exercise. One set was performed at high effort and the second set was performed at low effort. For high effort isotonic exercises, we applied the following weights: 9.1 kg (20 lbs) on top of the knee for plantar flexion; 3.2 kg (7 lbs) on the dorsal surface of the foot for dorsiflexion; 9.1 kg (20 lbs) on the anterior shank just proximal to the ankle for

knee extension. For low effort isotonic exercises, we did not apply weight (movement was inhibited only by the mass of the limbs). For high effort isometric exercises, we instructed subjects to “press as hard as you can using only your leg, keep your arms and torso still, and don’t grab the exercise bench with your hands.” For low effort isometric exercises, we instructed subjects to “push approximately 25% as hard as you did for the high effort set.” Subjects were not given visual feedback of the force or torque they exerted. A few practice repetitions allowed subjects to acclimate to 25% effort.

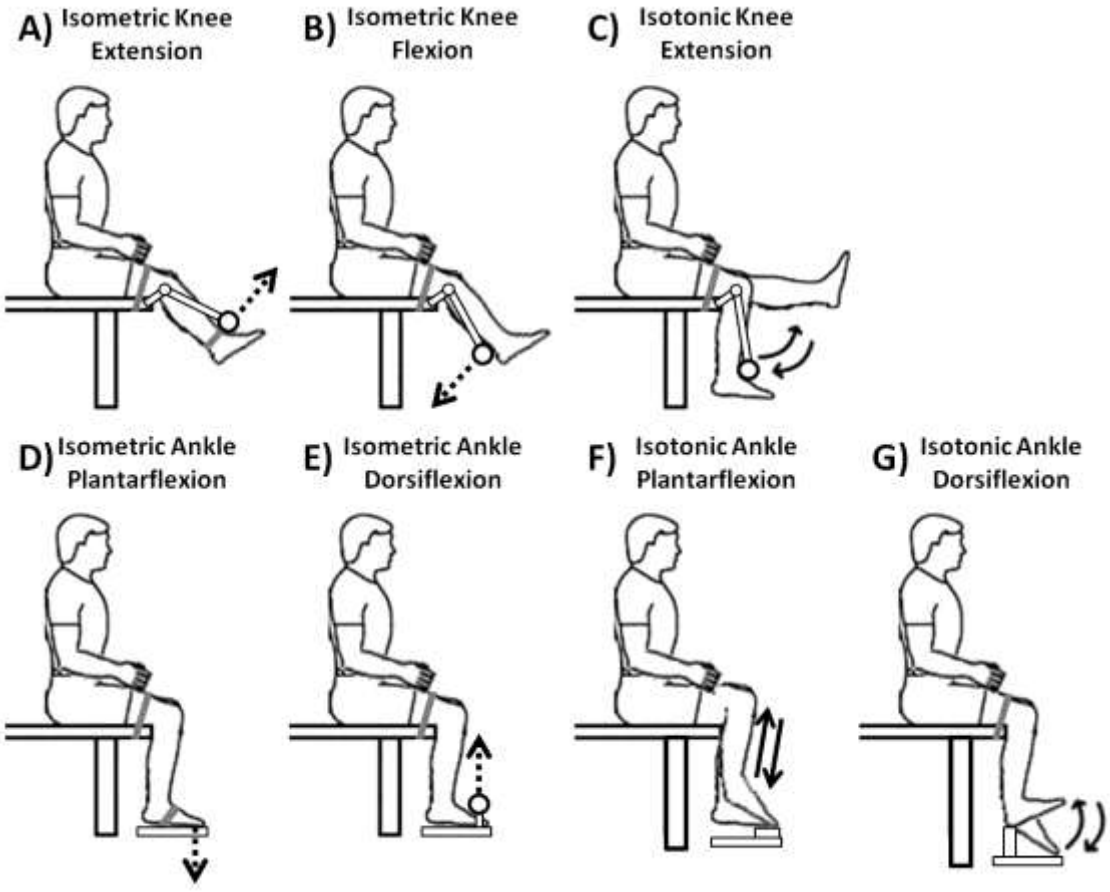

Figure 5-1: A sketch of the experimental setup for performing knee and ankle exercises. A) isometric knee extension, B) isometric knee flexion, C) isotonic knee extension, D) isometric ankle plantar flexion, E) isometric ankle dorsiflexion, F) isotonic ankle plantar flexion, and G) isotonic ankle dorsiflexion. For isometric exercises the direction of the applied force is indicated by a dashed arrow. For isotonic exercises the direction of movement is indicated by solid arrows.

Isometric and isotonic exercise repetitions were performed over roughly 3 seconds. For isotonic tasks the concentric and eccentric contractions were performed continuously (i.e., immediate direction change after the concentric contraction) and took a total of 3 seconds. Subjects paused for 5 seconds between repetitions. We did not provide timing cues because we did not want to confound electrocortical dynamics with an audio or visual task. As a result, exercise timing was approximate. Subjects performed isometric ankle exercises at a neutral ankle angle and isometric knee exercises at 45 degrees of flexion. All exercises were performed with the right lower limb only. We screened subjects for handedness, by asking them their preferred writing hand, and footedness, by asking which foot they would kick a ball with. All were right handed and right footed.

Recording EEG and lower limb dynamics

We recorded EEG at 512 Hz using an ActiveTwo amplifier and a 264-channel active electrode array (BioSemi, Amsterdam, The Netherlands). A digitizer (Polhemus, Colchester, VT, USA) localized the 256-channel EEG head cap, as well as 8 electrodes that were external to the head cap, with respect to anatomic head reference points (nasion, left preauricular point, and right preauricular point). After data collection, we applied a zero phase lag 1 Hz high-pass Butterworth filter to the EEG signals to remove drift. We removed EEG signals exhibiting substantial noise throughout the collection in a manner similar to (Gwin et al., 2010a, b). Channels with standard deviation ≥ 1000 μV were removed. Any channel whose kurtosis was more than 3 standard deviations from the mean was removed. Channels that were uncorrelated ($r \leq 0.4$) with nearby channels

for more than 0.1% of the time-samples were removed. On average, 191 channels were retained (range: 134–240; standard deviation: 34.6). The remaining channels were evenly distributed around the head; the mean (standard deviation) channel rejection rate was 72.4% (20.2%). The remaining channels were re-referenced to an average reference. We performed all processing and analysis in Matlab (The Mathworks, Natick, MA) using scripts based on EEGLAB (Delorme and Makeig, 2004), an open source Matlab toolbox for processing electrophysiological data. For isotonic exercises, we measured ankle and knee angles using electrogoniometers (Biometrics, Gwent, England). For isometric exercises, we measured force production using a load cell (Omegadyne, Sunbury, OH, USA). We sampled the load cell and electrogoniometers at 1000 Hz, and synchronized EEG and biomechanics signals offline.

Adaptive Mixture Independent Component Analysis

For each subject, we merged EEG signals from all conditions into a single dataset. We submitted these data to an adaptive mixture ICA algorithm [AMICA] (Palmer et al., 2006; Palmer et al., 2008), which generalizes infomax (Bell and Sejnowski, 1995; Lee et al., 1999a) and multiple mixture (Lee et al., 1999b; Lewicki and Sejnowski, 2000) ICA approaches. AMICA is an open source plugin for EEGLAB that generates a predetermined number of mixture models each of which captures a competition selected subset of the data. Based on the known somatotopic distribution of the sensorimotor cortex (Kandel et al., 2000) we had an *a priori* hypothesis that ankle and knee muscle actions would elicit different electrocortical source spatial distributions. Therefore, we allowed AMICA to generate 2 mixture models. For each subject, we

separately computed model probabilities for the subset of data containing all ankle trials and the subset of data containing all knee trials. Model probability reflects the likelihood that a given model best fits a particular subset of data (on a scale of 0 to 1) and was computed based on the posterior log-likelihood using Matlab functions in the AMICA plugin for EEGLAB. Analysis of variance assessed whether the model probabilities were significantly different across all subjects.

DIPFIT functions within EEGLAB computed an equivalent current dipole model that best explained the scalp topography of each independent component using a boundary element head model based on the Montreal Neurological Institute (MNI) template (the average of 152 MRI scans from healthy subjects, available at http://www.mni.mcgill.ca) (Oostenveld and Oostendorp, 2002). We aligned digitized electrode locations with the head model by scaling and rotating the head coordinate system so that the digitized anatomical reference points matched the head model anatomic reference points. We excluded independent components if the projection of the equivalent current dipole to the scalp accounted for less than 85% of the scalp map variance, or if the topography, time-course, and spectra of the independent component were reflective of eye movement or electromyographic artifact (Jung et al., 2000a; Jung et al., 2000b). The remaining independent components reflected electrocortical sources. These sources were clustered across subjects using EEGLAB routines that implemented k-means clustering on vectors coding differences in equivalent dipole locations and the topography of the dipole projection to the scalp. Scalp topography was reduced to 10 principal dimensions using principal component analysis. To account for differences in

the dimensions of the dipole locations compared to the scalp topography, we gave dipole locations a weight of 3 and topography principle components a weight of 1 prior to clustering, as in (Gwin et al., 2010a, b). We retained clusters that contained electrocortical sources from at least 6 of 8 subjects; electrocortical sources that were not included in these clusters were excluded from all further analyses.

Electrocortical Source Time-Frequency Analysis

To test the hypothesis that different types of muscle activations have different electrocortical spectro-temporal features, we generated spectrograms for each electrocortical source, each muscle contraction, and each subject. We performed time-frequency analysis using Morlet wavelets with 500 ms sliding windows and 25 ms of overlap. Frequencies were divided into 220 log spaced bins from 3 to 150 Hz. We time-locked single-trial spectrograms to the start of each trial and then linearly time-warped them so that the end of the trial occurred at the same adjusted latency in each spectrogram. We determined the start and end of isometric trials based on the onset and offset of applied force (load cell measurements). We determined the start and end of isotonic trials based on the onset and offset of joint rotation (electrogoniometer measurements). We normalized each spectrogram by subtracting the average log spectrum for a pre-trial baseline (1000 ms to 500 ms prior to onset) from the spectrogram (this is a static baseline, each exercise repetition was preceded by a 5 second pause). We then generated grand average normalized spectrograms in the α- and β-bands for electrocortical sources in the contralateral medial sensorimotor cortex for flexion, extension, isometric, and isotonic trials. We performed pairwise

comparisons of these spectrograms using a bootstrapping method available within EEGLAB (Delorme and Makeig, 2004). Finding no significant differences in these spectrograms for knee and ankle muscle trials or for flexion and extension trials, we averaged the spectrograms across these conditions yielding distinct grand average spectrograms for the following four conditions: isometric low effort, isometric high effort, isotonic low effort, and isotonic high effort. Significant fluctuations from baseline in these grand average spectrograms were identified using EEGLAB bootstrapping methods (Delorme and Makeig, 2004). Last, within contraction type (i.e., isometric or isotonic) T-tests compared the means of the α- and β-band time-frequency points that exhibited a significant spectral change from baseline for low effort versus high effort trials.

4-way Classification of Single Trial Electrocortical Source Spectrograms

We evaluated two 4-way linear naïve Bayesian classifiers for grouping single trial data as isometric or isotonic and high or low effort. The first classifier was based only on the cluster of electrocortical sources in the supplementary motor area and the second classifier was based on all electrocortical sources except for those in the visual cortex. The second classifier was included to evaluate the extent to which the addition of electrocortical sources that were not in the supplementary motor area would improve the fidelity of the classification algorithm. For this classifier, electrocortical sources in the visual cortex were excluded for control purposes. Subjects were instructed not to look at the lower limb during testing but differences in eye gaze between conditions could have biased electrocortical dynamics in the visual cortex.

For both classifiers, feature vectors were generated by reducing the resolution of the normalized spectrograms by a factor of 10 (in both time and frequency) and identifying significant time-frequency points from the reduced resolution spectrograms across trials for each subject and each type of muscle activation. The decibel values at the time-frequency points that were significant across trials were selected in each trial and formed the single-trial feature vector. Next, we trained and tested subject specific linear naïve Bayesian classifiers (i.e., classifiers were trained and tested on single subject data) using the Matlab Statistics Toolbox. For each subject, a 10-fold cross validation was performed. The confusion matrices for each subject and each fold were then averaged to form a grand average confusion matrix for each classifier.

Results

Differences between the two AMICA model probabilities were significant for the subset of data for knee tasks and the subset of data for ankle tasks ($p < 0.01$). In other words, one model best explained the data during knee exercises and the other model best explained the data during ankle exercises (Figure 5-2).

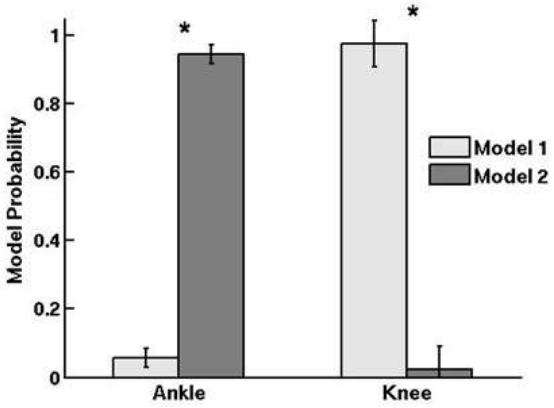

Figure 5-2: AMICA model probabilities for ankle trials (left) and knee trials (right). Error bars show 1 SD. * p< 0.01.

For clarity, these AMICA models are referred to as the knee model and the ankle model, respectively, for the remainder of this manuscript. However, it is critical to recall

that these models were trained on the entire dataset without knowledge of the underlying muscles being activated. On a trial-by-trial basis, the fit of the recorded EEG to the AMICA mixture models distinguished knee contractions from ankle contractions with 80% accuracy.

The knee and ankle ICA mixture models parsed an average of 23.8 and 21.8 electrocortical sources from the EEG signals, respectively. The number of sources per subject was not significantly different between the two models (ANOVA, $p = 0.66$). Clusters containing electrocortical sources from at least 6 of 8 subjects were localized to the anterior cingulate, posterior cingulate, supplementary motor, left dorsal premotor, right dorsal premotor, posterior parietal, and visual cortex. All of these clusters were present in both the knee and ankle ICA models (Figure 5-3). Talairach coordinates for the cluster centroids are shown in Table 5-1.

Table 5-1: Talairach coordinates for the geometric cluster centroids. The cluster numbers correspond to the numeric labels in Figure 5-3.

		Knee Model		Ankle Model	
Cluster	Nearest Grey Matter (Brodmann Area)[1]	Talairach Coordinates	Distance to Nearest Grey Matter (mm)[1]	Talairach Coordinates	Distance to Nearest Grey Matter (mm)[1]
1: supplementary motor	BA 6	(-6, -2, 58)	1	(-4, -21, 55)	0
2: left dorsal premotor	BA 6	(-25,-10,53)	0	(-31, -14, 55)	2
3: right dorsal premotor	BA 6	(20, -13, 55)	3	(26, -16, 47)	5
4: posterior cingulate	BA 23, 31	(5, -26, 28)	0	(10, -36, 31)	3
5: posterior parietal	BA 7	(-1, -58, 44)	0	(-2, -65, 41)	1
6: anterior cingulate	BA 24, 32	(2, 6, 40)	2	(2, 7, 43)	4
7: visual	BA 18	(3, -77, 18)	0	(-2, -74, 10)	0

[1] Determined using the freely downloadable Talairach Client (www.talairach.org) (Lancaster et al., 2000)

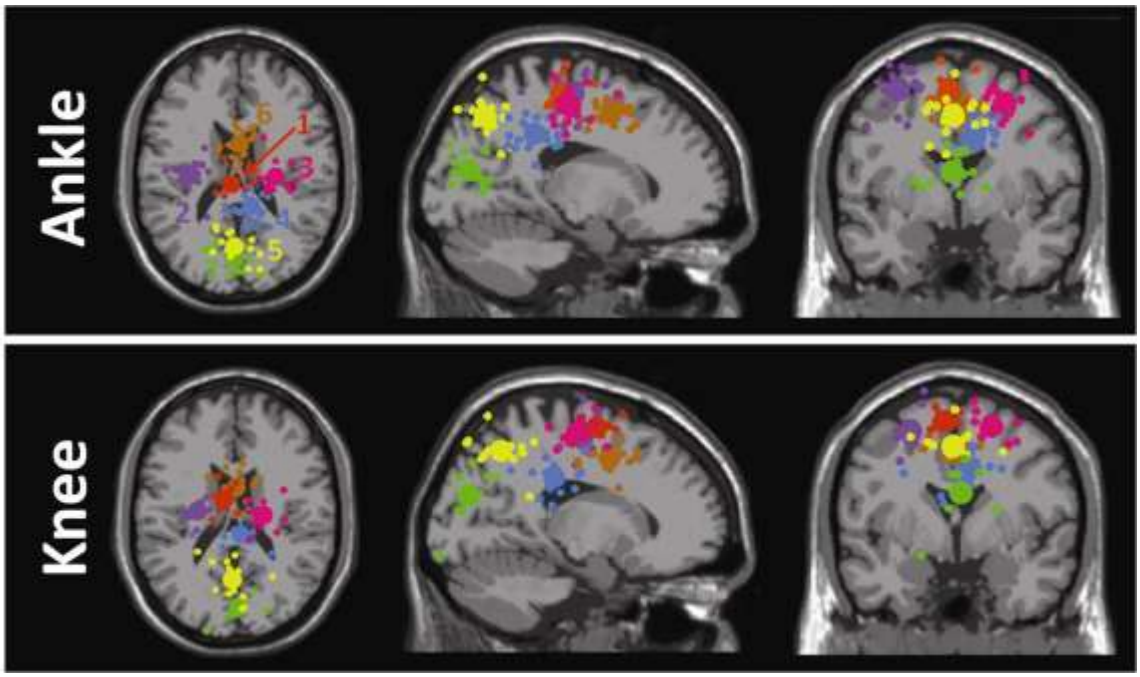

Figure 5-3: Clusters of electrocortical source equivalent current dipoles for knee and ankle exercises. Clusters were localized to the (1: orange) supplementary motor area, (2: purple) left dorsal premotor area, (3: magenta) right dorsal premotor area, (4: blue) posterior cingulate, (5: yellow) posterior parietal, (6: brown) anterior cingulate, and (7: green) visual cortex. Two dipole models are shown; (top) the model best fitting the EEG signals during ankle exercises and (bottom) knee exercises. Small spheres indicate dipole locations for single electrocortical sources for single subjects; larger spheres indicate geometric cluster centroids.

Isometric and isotonic contractions elicited significantly different α- and β-band spectral power modulations for the cluster of electrocortical sources in the supplementary motor area (cluster 1: orange in Figure 5-3). Specifically, isometric contractions elicited α- and β-band ERD at trial onset and offset while isotonic contractions elicited a sustained α- and β-band ERD throughout the trial (Figure 5-4). Finding no significant differences in these spectrograms for knee and ankle muscle trials or for flexion and extension trials, we averaged the spectrograms across these conditions. For both isometric and isotonic contractions, high effort tasks elicited a slightly but significantly ($p < 0.01$, power > 0.99) more pronounced ERD (Figure 5-5).

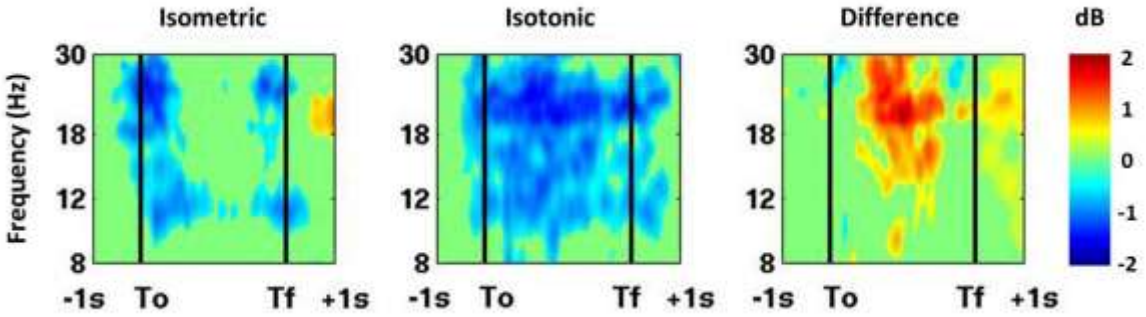

Figure 5-4: Grand average spectrograms for supplementary motor area electrocortical sources showing average changes in spectral power during the task relative to a pre-trial baseline for isometric (left) versus isotonic (middle) trials. The right panel shows the difference between isometric and isotonic conditions. The horizontal axis begins 1 s prior to trial onset (T_o; first black vertical line) and ends 1 s after trial offset (T_f; second black vertical line). The times between the onset and offset of the trials were warped to align these latencies across all trials. Non-significant changes from baseline ($p > 0.05$) were set to 0 dB (green).

We evaluated two 4-way linear naïve Bayesian classifiers for grouping single trial data as isometric or isotonic and high or low effort. Finding no significant differences in the spectrograms for flexion and extension we did not attempt to decode these conditions. The first classifier was based on electrocortical sources in the supplementary motor area (cluster 1: orange in Figure 5-3), and the second classifier was based on all electrocortical sources except for those in the visual cortex.

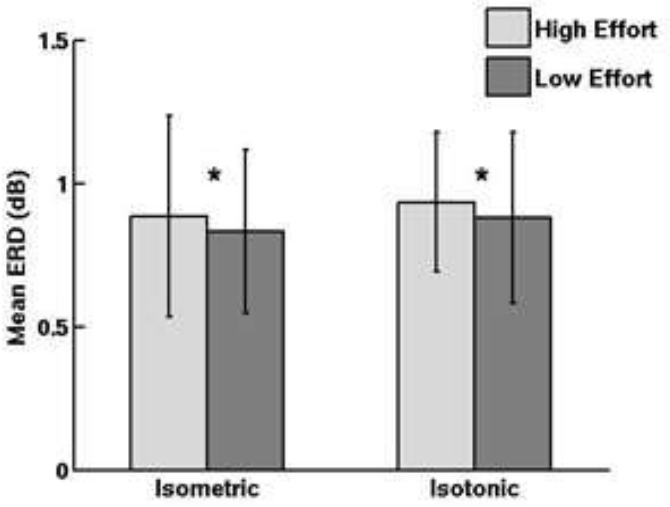

Figure 5-5: Average event-related desynchronization for high effort and low effort muscle contractions shown separately for isometric (left) and isotonic (right) conditions. Error bars show 1 SD. * $p < 0.01$.

Grand average spectrograms for each cluster of electrocortical sources used in the second classifier are shown in Figure 5-6. Spectrograms for the anterior cingulate cortex are excluded because no significant differences from baseline were found for this cluster. The accuracies of these classifiers were 68.8 ± 9.3% and 87.1 ± 9.0% (mean ± SD), respectively. The grand average normalized confusion matrices, averaged across 10 folds and 8 subjects, are shown in Table 5-2 and Table 5-3, respectively.

Table 5-2: Grand average normalized confusion matrix for the 4-way linear naïve Bayesian classifier using electrocortical sources in the supplementary motor area.

	Predicted			
Actual	High Effort Isometric	Low Effort Isometric	High Effort Isotonic	Low Effort Isotonic
High Effort Isometric	20.0%	4.7%	2.8%	3.0%
Low Effort Isometric	4.4%	19.4%	2.7%	2.9%
High Effort Isotonic	2.3%	2.4%	15.9%	2.2%
Low Effort Isotonic	1.1%	1.0%	1.4%	13.8%

Table 5-3: Grand average normalized confusion matrix for the 4-way linear naïve Bayesian classifier using all electrocortical sources except those in the visual cortex.

	Predicted			
Actual	High Effort Isometric	Low Effort Isometric	High Effort Isotonic	Low Effort Isotonic
High Effort Isometric	25.8%	2.7%	1.3%	1.7%
Low Effort Isometric	2.1%	24.8%	1.0%	1.0%
High Effort Isotonic	0.5%	0.5%	19.0%	1.0%
Low Effort Isotonic	0.2%	0.3%	0.9%	17.3%

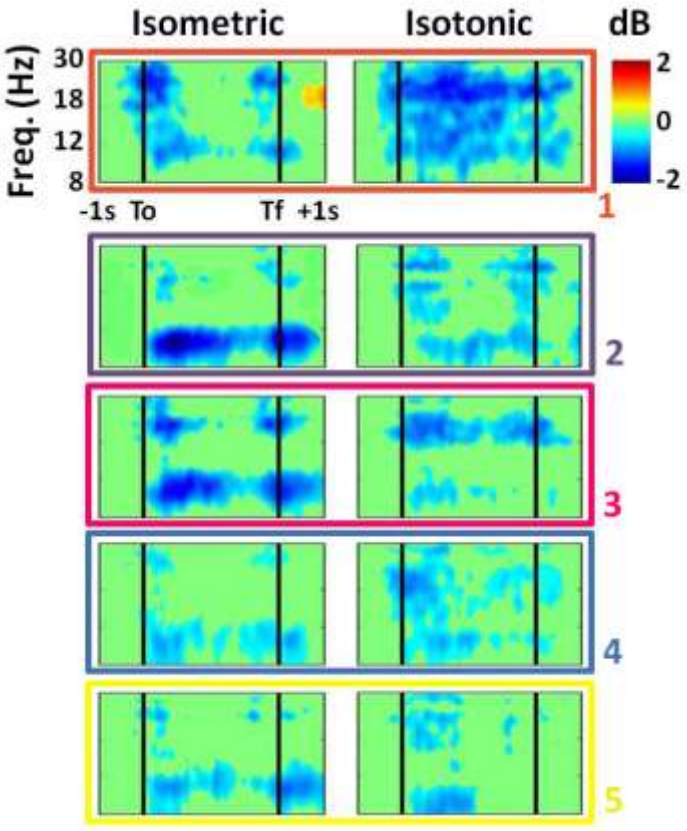

Figure 5-6: Grand average normalized spectrograms for clusters of electrocortical sources. (Top row) supplementary motor area, (second row) left dorsal premotor cortex, (third row) right dorsal premotor cortex, (fourth row) posterior cingulate, and (fifth row) posterior parietal cortex showing average changes in spectral power during the task relative to a -1000 ms to -500 ms baseline for isometric (left) and isotonic (right) trials. The color of the border and the numeric label for each row corresponds to the color and numeric label of the dipoles for the corresponding cluster shown in Figure 3. The horizontal axis begins 1 s prior to trial onset (T_o; first black vertical line) and ends 1 s after trial offset (T_f; second black vertical line). The times between the onset and offset of the trials were warped to align these latencies across all trials. Non-significant changes from baseline ($p > 0.05$) were set to 0 dB (green).

Discussion

We used high-density EEG to study voluntary lower limb isometric and isotonic, ankle and knee, flexor and extensor muscle contractions in eight healthy subjects. The goals of this study were to characterize differences in electrocortical dynamics between these muscle actions and to assess the trial-by-trial consistency of these differences by decoding the type of muscle action from recorded brain signals.

For all subjects, AMICA captured different spatial distributions of electrocortical sources for ankle and knee actions. The somatotopic arrangement of the sensory and motor cortices is well established (Kandel et al., 2000). Therefore, from a physiological perspective it is not surprising that knee and ankle muscle actions would elicit different distributions of underlying electrocortical sources. The supplementary motor area (cluster 1: orange in Figure 5-3) is of particular interest because this region of the premotor cortex projects to distal limb motor nuclei while the dorsal premotor area (clusters 2 and 3: purple and magenta in Figure 5-3) projects mainly to motor nuclei innervation the proximal limb musculature (Krakauer and Ghez, 2000). The location of face, hand, and foot areas of the human supplementary motor area follow an anterior-posterior shift (Chainay et al., 2004). Therefore, the posterior shift of the supplementary motor area ankle cluster compared to the knee cluster is consistent with expected somatotopy; though supplementary motor area somatotopy has not been formalized to the extent that primary motor cortex somatotopy has been. However, we do not believe that the data collected here provides a sufficient basis for a physiological explanation for the subtle location shift of this cluster between the two models. Future work should evaluate the use of subject specific head models (derived from individual magnetic resonance images) to improve the accuracy of source localization. Nevertheless, AMICA provides a novel data driven way to derive distinct source distributions. In this study, we could have separated the ankle and knee data *a priori* and submitted these data to two distinct ICA decompositions. The benefit of AMICA is that *a priori* knowledge of different source distributions is not required. For this reason we choose to evaluate AMICA in this

study. Our results suggest that AMICA of high-density EEG has sufficient spatial resolution to distinguish electrocortical process for knee tasks from those for ankle tasks.

We used the fit of single-trial EEG to the AMICA mixture models to distinguish knee from ankle tasks with modest success. Isometric knee exercises could be distinguished from isometric ankle exercises with 91% accuracy, but isotonic exercises could only be distinguished with 62% accuracy. For some subjects (3 of 8), 100% accuracy was achieved for both isometric and isotonic exercises. For other subjects, isometric exercises were accurately categorized but isotonic exercises were not. We expect that for these subjects, the isotonic exercises elicited a distribution of electrocortical activity that was different from that elicited by the isometric exercises. It might be helpful for future studies to allow the AMICA algorithm to identify additional mixture models, but this might require larger data sets. In fact, this observation highlights an important benefit of the AMICA algorithm

Spectrograms for electrocortical sources in the supplementary motor area differed between isometric and isotonic contractions, but did not differ significantly between flexion and extension trials. Specifically, isometric contractions elicited an ERD in the α- and β-band at force onset and offset while isotonic contractions elicited a sustained α- and β-band ERD throughout the trial. In addition, high effort trials (i.e., greater muscle activation) elicited a slightly but significantly more pronounced desynchronization than low effort trials. This result is consistent with the understanding that oscillatory cortical activity in the α- and β-bands reflects steady-state sensorimotor processing that is

reduced during dynamic movement (Allen and MacKinnon, 2010; MacKay, 2005; Pfurtscheller and Lopes da Silva, 1999). Regarding the ERD during isometric contractions at onset and offset, it is important to note that the onset of an isometric contraction consists of dynamic muscle shortening and tendon lengthening until the desired level of force is achieved, and the offset of an isometric contraction consists of muscle lengthening and tendon shortening until rest is achieved (Fukunaga et al., 2002). In addition, some limb movement is inevitable as the test apparatus and the soft tissues of the lower limb becomes loaded and then unloaded at the onset and offset of each trial. To our knowledge this is the first comparison of electrocortical dynamics associated with isometric and isotonic lower limb muscle activations.

Several observations can be made from the electrocortical cluster spectrograms shown in Figure 5-6. First, while the α-band ERD for isometric trials occurred only at trial onset and offset for the supplementary motor area cluster (first row of Figure 5-6), the α-band ERD was persistent throughout the isometric trials for the dorsal premotor area clusters that were located more laterally in the premotor cortex (second and third row of Figure 5-6, respectively). This may be the result of dynamic torso stabilization throughout the trial. Second, significant ERD for the supplementary motor area cluster preceded trial onset by roughly 400 ms but significant ERD for all other electrocortical source clusters did not begin until after trial onset. Third, the supplementary motor area ERD was β-dominant for both the isometric and isotonic conditions; whereas the dorsal premotor clusters were α-dominant for the isometric condition and β-dominant for the isotonic conditions. Most importantly, electrocortical spectrograms in broadly

distributed brain regions contained information regarding the level of effort and the contraction type (isometric versus isotonic). This is evidenced by the fact that classifiers based only on supplementary motor area electrocortical sources achieved a 4-way classification accuracy of 69% while classifiers based on electrocortical sources in multiple brain regions achieved a 4-way classification accuracy of 87%. This findings supports the notion that a broad distribution of electrocortical signals will improve the information transfer rate in BMIs (Leuthardt et al., 2009).

In this study we used ICA to parse EEG signals recorded on the scalp into underlying electrocortical source signals and then evaluated the spectro-temporal characteristics of the source signals. However, this is certainly not the only way to study electrocortical dynamics associated with limb movements. Many informative findings have come from time-domain measures, such as motor-related cortical potentials (MRCPs). MRCPs have been shown to be greater and occur earlier for eccentric elbow contractions than for concentric contractions (Fang et al., 2001). In addition, MRCP amplitude has been shown to scale with the amount of torque produced (Siemionow et al., 2000) and to decrease with fatigue (Liu et al., 2005). In addition, coherence analysis of EEG and EMG could provide additional insight. In particular, such analysis could be used to localize active brain regions for knee and ankle tasks.

There are certain limitations of this study. First, it is possible that certain sources of electromyographic or electroocular artifact were present during ankle and not knee trials (or vice versa), even after removing artifacts using ICA. This would have positively influenced the prediction of knee vs. ankle action. To avoid this, subjects were seated in

the same position for all experimental conditions and were instructed to keep their gaze forward. In addition, they were instructed to engage only the right leg during each exercise (i.e., subjects were not permitted to grab the exercise bench to generate more force). Second, the exercises that were categorized as isotonic in this study are not truly isotonic (joint torque was not constant throughout the trial), and this could confound the interpretation of the data. Third, the methods of classification used in this study cannot be used for real-time classification. ICA mixture models were trained offline. It remains to be seen whether ICA mixture models are stable from day-to-day, in the presence of unavoidable differences in EEG head-cap setup. If the mixture models are stable from day-to-day then subject specific mixture models could be applied in real-time. In addition, classification of muscle contraction type was based on time-frequency data for the full (approximately 3 second) repetition. Real-time classification would require the use of a shorter duration of EEG activity. However, the purpose of decoding single-trial spectrograms in this study was to assess the trial-by-trial consistency of the task specific differences in the electrocortical spectrograms.

The results of this study demonstrate that ICA of high-density EEG can be used to monitor a broad distribution of electrocortical sources that contribute to lower limb muscle actions. In an earlier study we used a similar imaging technique during human locomotion and found spectral modulations in sensorimotor, anterior cingulate, and posterior parietal cortex that were locked to the gait cycle (Gwin et al., 2010a). It remains to be seen how these task specific electrocortical dynamics are affected by neurological injuries, such as stroke or spinal cord injury, or how they change in

response to motor rehabilitation. However, alternative imaging techniques suggest that functional recovery will rely on plasticity in multiple cortical regions and that the relative contribution of different regions will change throughout the course of rehabilitation (Eliassen et al., 2008; Enzinger et al., 2009; Kokotilo et al., 2009a; Kokotilo et al., 2009b; Miyai et al., 2006; Nishimura and Isa, In Press). The techniques used in this study may provide a means to better understand the cortical physiology underlying neurological rehabilitation and recovery.

Our results demonstrate that different types of lower limb muscle activation carry unique spatial and spectro-temporal electrocortical signatures, and that a broad distribution of electrocortical signals may improve classification of human lower limb movements from single-trial EEG data. Our findings may have implications for tracking cortical plasticity during neurorehabilitation. Specifically, the techniques presented here could be used to track changes in spectro-temporal and spatial properties of motor-related electrocortical signals during recovery. This could help researchers and clinicians gauge the success of a therapy or pharmaceutical treatment.

Chapter 6: Beta- and gamma-range human lower limb corticomuscular coherence

This chapter has been submitted for consideration of publication:
Gwin JT, Ferris DP. *Frontiers in Human Neuroscience*. [In Review].

Abstract

Coherence between electroencephalography (EEG) recorded on the scalp above the motor cortex and electromyography (EMG) recorded on the skin of the limbs is thought to reflect corticospinal coupling between motor cortex and muscle motor units. Beta-range (13-30 Hz) corticomuscular coherence has been extensively documented during static force output while gamma-range (31-45 Hz) coherence has been linked to dynamic force output. However, the explanation for this beta-to-gamma coherence shift remains unclear. We recorded 264-channel EEG and 8-channel lower limb electromyography (EMG) while 8 healthy subjects performed isometric and isotonic, knee and ankle exercises. Adaptive mixture independent component analysis (AMICA) parsed EEG into models of underlying source signals. We computed magnitude squared coherence between electrocortical source signals and EMG. Significant coherence between contralateral motor cortex electrocortical signals and lower limb EMG was observed in the beta- and gamma-range for all exercise types. Gamma-range coherence was significantly greater for isotonic exercises than for isometric exercises. We conclude that active muscle movement modulates the speed of corticospinal oscillations. Specifically, isotonic contractions shift corticospinal oscillations towards the gamma-

range while isometric contractions favor beta-range oscillations. Prior research has suggested that tasks requiring increased integration of visual and somatosensory information may shift corticomuscular coherence to the gamma-range. The isometric and isotonic tasks studied here likely required similar amounts of visual and somatosensory integration. This suggests that muscle dynamics, including the amount and type of proprioception, may play a role in the beta-to-gamma shift.

Introduction

Coherence is a commonly used statistic to estimate the causality between the input and output of a linear system. Coherence between electroencephalography (EEG) recorded on the scalp above the motor cortex and electromyography (EMG) recorded on the skin over muscles is thought to reflect corticospinal coupling between motor cortex and pooled motor units (Mima and Hallett, 1999; Negro and Farina, 2011). Corticomuscular coherence phase lags are consistent with the conduction time between the motor cortex and the respective muscle. This suggests that the motor cortex drives the motorneuron pool (Gross et al., 2000).

Studies of corticomuscular (EEG-EMG) coherence have largely focused on the upper limbs (Chakarov et al., 2009; Halliday et al., 1998; Kristeva-Feige et al., 2002; Kristeva et al., 2007; Mima et al., 2000; Omlor et al., 2007; Yang et al., 2009). The prevalence of monosynaptic corticospinal projections to the motor units of the upper limbs, and the hand in particular, contributes to the dexterity of the upper limbs compared to the lower limbs (Krakauer and Ghez, 2000). There have been a few studies investigating EEG-EMG coherence for lower limbs muscles (Hansen et al., 2002; Mima et al., 2000;

Raethjen et al., 2008; Vecchio et al., 2008). For both the upper and lower limbs, the existence of these causal descending signals reflects motor cortex control of voluntary movements via pyramidal pathways (Gross et al., 2000; Mima and Hallett, 1999; Negro and Farina, 2011).

The type of motor task affects the frequency band where corticomuscular coherence is most prominent. Beta-range (13-30 Hz) corticomuscular coherence measured using EEG has been extensively documented during static force output (Chakarov et al., 2009; Gross et al., 2000; Kristeva-Feige et al., 2002; Kristeva et al., 2007; Mima et al., 2000; Raethjen et al., 2008; Yang et al., 2009). Gamma-range (31-45 Hz) corticomuscular coherence has been studied to a lesser extent but has been linked to dynamic force output (Marsden et al., 2000; Omlor et al., 2007). Marsden et al. recorded electrocorticographic (ECoG) signals from non-pathological areas in humans with subdural electrodes in place for investigation of epilepsy. There was coherence between ECoG and simultaneously recorded EMG from upper limb muscles in the beta-range for isometric contractions and in the gamma-range for self-paced phasic contractions. Omlor et al. evaluated EEG–EMG coherence during constant and periodically modulated force production in a visuomotor task (i.e., tracking a sinusoidal force given visual force feedback). In both tasks, subjects attempted to achieve a target force given real-time visual feedback of force production. For the constant force condition, EEG-EMG coherence existed in the beta-range. For the periodically modulated force condition, the EEG-EMG coherence shifted toward higher (gamma-range) frequencies.

A complete explanation for the beta-to-gamma corticomuscular coherence shift for static versus dynamic tasks is lacking. Omlor et al. hypothesized that the shift toward higher frequencies for the dynamic force tracking task compared to the constant force task reflected that tracking a periodically modulated force requires more attentional resources and more complex integration of visual and somatosensory information than the constant force task. They suggested that higher frequency coherence might reflect the integration of multi-sensory information into the motor plan. However, Marsden et al. observed a beta-to-gamma shift for a self-timed task without visual feedback.

The purpose of the present study was to compare corticomuscular coherence for isometric and isotonic contractions when both contraction types were self-paced and in the absence of external force feedback. We hypothesized that despite similar visual and sensory motor integration demands for both tasks the isotonic contractions would elicit gamma-range corticomuscular coherence while the isometric contractions would elicit beta-range coherence. We based this hypothesis on the observation from Marsden et al. that self-paced phasic contractions shifted corticomuscular coherence to the gamma-range in the absence of visuomotor coordination. A novel aspect of our study is that we used independent components analysis (Delorme et al., 2012; Jung et al., 2000a; Makeig et al., 1996; Onton et al., 2006) to parse underlying electrocortical sources from mixed signals recorded on the scalp, rather than directly using EEG electrode signals for calculating corticomuscular coherence.

Methods

Data Collections

The experimental apparatus, testing protocol, and data collection procedures have been described previously (Gwin and Ferris, [In Press]) and are briefly summarized here. The subjects of this study were eight healthy right-handed and right-footed volunteers with no history of major lower limb injury and no known neurological or musculoskeletal deficits (7 males; 1 female; age range 21–31 years). These subjects sat on a bench while performing isometric muscle activations and isotonic movements (concentric followed by eccentric) of the right knee and right ankle joints. Exercise repetitions took approximately 3 seconds. For isotonic tasks concentric and eccentric contractions were performed continuously (i.e., immediate direction change after the concentric contraction). Subjects paused for 5 seconds between repetitions. We did not provide timing cues because we did not want to confound electrocortical dynamics with an audio or visual task. As a result, exercise timing was approximate.

We recorded 512 Hz EEG using an ActiveTwo amplifier and a 264-channel active electrode array (BioSemi, Amsterdam, The Netherlands). We recorded lower limb EMG at 1000 Hz (tibialis anterior, soleus, vastus lateralis, vastus medialus, medial gastrocnemius, lateral gastrocnemius, medial hamstring, and rectus femoris) using 8 surface EMG sensors and a K800 amplifier (Biometrics, Gwent, England), as well as a Vicon data acquisition system (Vicon, Los Angeles, US). The University of Michigan Internal Review Board approved all procedures, which complied with the standards defined in the Declaration of Helsinki.

EEG and EMG pre-processing

EEG was pre-processed in the same manner as (Gwin and Ferris, [In Press]) using Matlab (The Mathworks, Natick, MA) scripts based on EEGLAB, an open source environment for processing electrophysiological data (Delorme and Makeig, 2004). We applied a zero phase lag 1 Hz high-pass Butterworth filter to the EEG signals to remove drift. Next, we removed EEG signals exhibiting substantial noise throughout the collection; the channel rejection criteria were standard deviation greater than 1000 μV, kurtosis more than 3 standard deviations from the mean of all channels, or correlation coefficient with nearby channels less than 0.4 for more than 0.1% of the time-samples. The remaining channels were average referenced (191 ± 34.6 channels, mean ± standard deviation). For each subject, we submitted these channel signals to a 2-model adaptive mixture independent component analysis (AMICA) (Delorme et al., 2012; Palmer et al., 2006; Palmer et al., 2008). We have previously demonstrated that applying a 2-model AMICA decomposition to these data captures differences in the electrocortical source distribution for knee versus ankle exercises (Gwin and Ferris, 2011; Gwin and Ferris, [In Press]). DIPFIT functions (Oostenveld and Oostendorp, 2002) within EEGLAB computed an equivalent current dipole model that best explained the scalp topography of each independent component using a boundary element head model based on the Montreal Neurological Institute (MNI) template. We excluded independent components if the projection of the equivalent current dipole to the scalp accounted for less than 85% of the scalp map variance, or if the topography, time-course, and spectra of the independent component were reflective of eye movement or

electromyographic artifact (Jung et al., 2000a; Jung et al., 2000b). The remaining independent components reflected electrocortical sources. EEGLAB clustered electrocortical sources across subjects based on the equivalent current dipole models of the sources. We retained clusters that contained electrocortical sources from at least 6 of 8 subjects; the geometric means of these clusters were in the contralateral motor (2 clusters), ipsilateral motor, anterior cingulate, posterior cingulate, and parietal cortex (Gwin and Ferris, 2011; Gwin and Ferris, [In Press]). Electrocortical sources that were not included in these clusters were excluded from all further analyses. EMG signals were re-sampled at 512 Hz (the EEG sampling rate) using the Matlab resample function and then full-wave rectified. Full wave rectified surface EMG mimics the temporal pattern of grouped firing motor units (Halliday et al., 1995). The onset and offset of each exercise repetition were determined based on the onset and offset of applied force (Omegadyne load cell, Sunbury, OH, USA) for isometric exercises and joint rotation (Biometrics electrogoniometer, Gwent, England) for isotonic exercises.

Corticomuscular coherence

For each exercise set (i.e., 20 repetitions) the power spectra of rectified EMG, EEG, and electrocortical source signals were computed using Welch's method with 0.5 s non-overlapping Hanning windows (for a frequency resolution of 2 Hz). Only active data (i.e., between onset and offset of each exercise repetition) were used for power spectral estimation. Magnitude squared coherence was computed as follows for each EEG channel / EMG channel pair and for each electrocortical source / EMG channel pair:

$$coh_{c1,c2}(f) = \frac{|S_{c1c2}(f)|^2}{S_{c1c1}(f) \cdot S_{c2c2}(f)}$$

where S_{c1c1} and S_{c2c2} are the auto-spectra of each signal; and S_{c1c2} is the cross-spectra. Coherence was only computed for agonist muscles (i.e., for flexion exercises coherence was computed for tibialis anterior and medial hamstring, and for extension exercises coherence was computed for soleus, medial gastrocnemius, lateral gastrocnemius, vastus lateralis, vastus medialus, and rectus femorus). Coherence was considered to be significant if it was greater than the 95% confidence limit (CL), which was computed as follows (Rosenberg et al., 1989):

$$CL = 1 - 0.05^{\frac{1}{n-1}}$$

where n is the number of windows used for spectral estimation. In this study the number of windows was not the same for all spectral estimates because exercises were self-paced. Therefore, coherence values were linearly warped so that the 95% CL was the same for all coherence estimates.

Coherence scalp-maps visualizing the maximum EEG-EMG coherence in the mu-range (8-12 Hz), beta-range (13-30 Hz), and gamma-range (31-45 Hz) for each EEG channel / EMG channel pair were computed for each subject and exercise set. Grand average coherence scalp-maps were generated for isometric and isotonic exercises by first interpolating subject specific coherence maps to a standardized 64-channel electrode array (using spherical interpolation implemented in EEGLAB) and then averaging interpolated coherence maps across subjects. Interpolation to a standardized

64-channel electrode array was necessary because after EEG-channel rejection the electrode montages were not consistent across subjects.

Peak coherence in the beta- and gamma-range was computed for each electrocortical source / EMG channel pair. Student's t-tests were used to assess the significance of differences in grand average coherence peaks for isometric versus isotonic exercises. The significance criteria was set at $\alpha = 0.05$ *a priori* and Bonferroni correction was used to address the problem of multiple comparisons.

Results

Significant coherence between EEG-channel signals and lower limb EMG was observed in the beta- and gamma-range, but not in the mu-range, for all exercise types (Figure 6-1). Beta-range coherence for isometric exercises was broadly and bilaterally distributed over the medial sensorimotor cortex and favored the contralateral side (left column, middle row, Figure 6-1). Beta-range coherence for isotonic exercises was distributed less broadly and was significant only over the contralateral sensorimotor cortex (right column, middle row, Figure 6-1). Gamma-range coherence for isometric exercises was distributed narrowly over the medial motor cortex (left column, bottom row, Figure 6-1). Gamma-range coherence for isotonic exercises was distribute more broadly and favored the contralateral side (right column, bottom row, Figure 6-1).

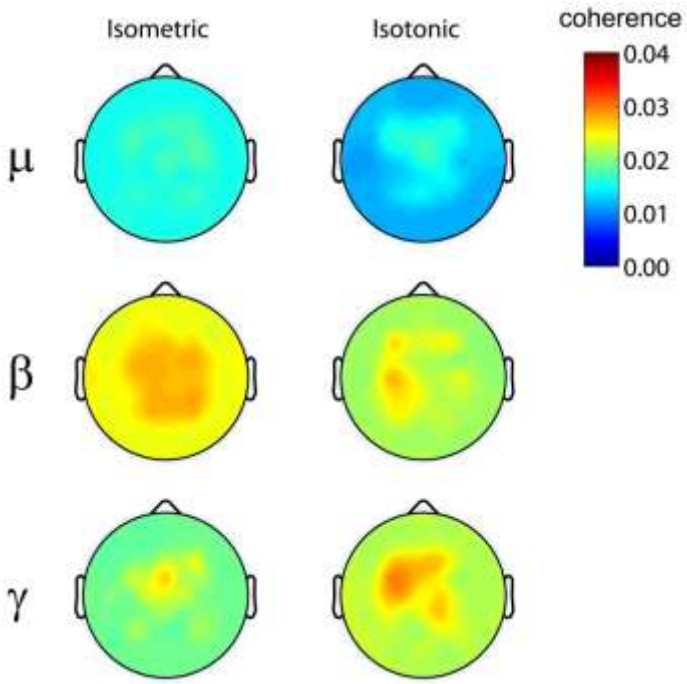

Figure 6-1: Grand average mu-range, beta-range, and gamma-range EEG-EMG coherence scalp-maps for (left) isometric and right (isotonic) exercises. 95% coherence confidence limit = 0.025.

Beta- and gamma-range coherence between contralateral motor cortex electrocortical source signals and lower-limb EMG was significant for all exercise types (Figure 6-2). In the gamma-range, coherence for isotonic exercises was significantly greater ($p < 0.05$) than coherence for isometric exercises. These coherence values are separated by muscle in Figure 6-3. The trend of increased gamma-range coherence for isotonic compared to isometric exercise was consistent across all muscles except vastus medialus and lateral gastrocnemius, which did not exhibit significant coherence for either condition. Anterior cingulate, posterior cingulate, posterior parietal, and ipsilateral sensorimotor electrocortical source signals did not exhibit significant coherence with EMG.

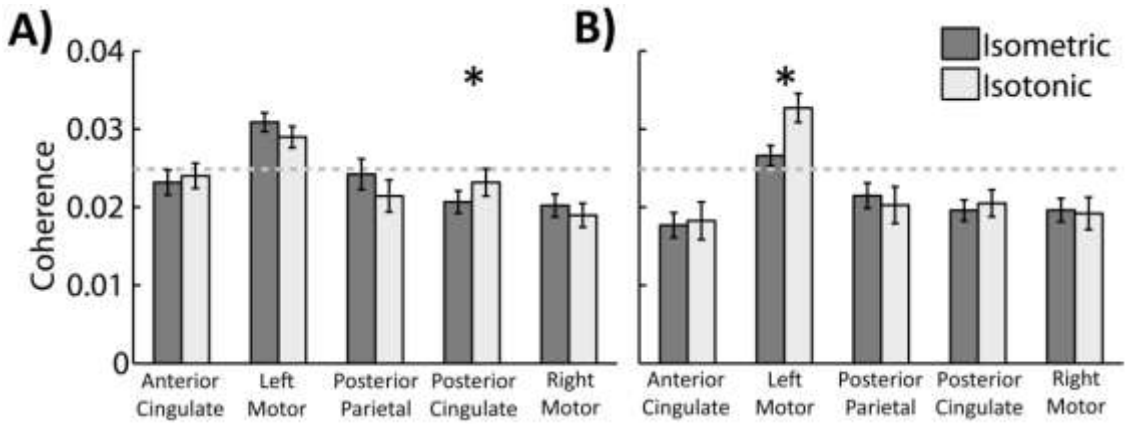

Figure 6-2: Grand average peak coherence between EMG and electrocortical source signals in the (A) beta-range and (B) gamma-range for (dark grey) isometric and (light grey) isotonic exercises. The 95% coherence confidence limit is indicated with a dashed grey line. Error bars show standard error of the mean. * indicates a significant difference between isometric and isotonic conditions ($p < 0.05$).

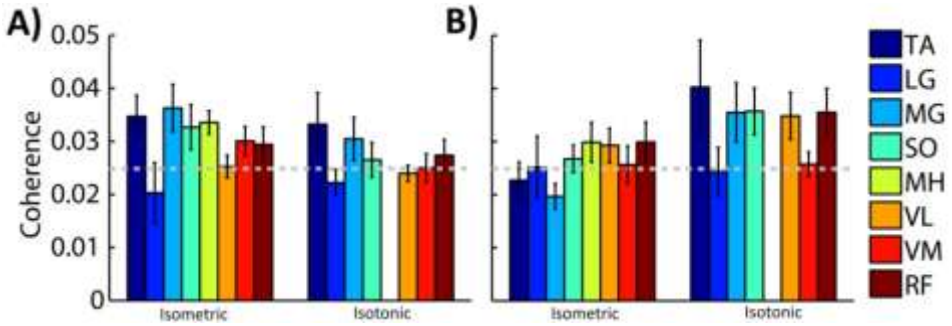

Figure 6-3: Grand average peak coherence for contralateral motor cortex electrocortical source signals in the (A) beta-range and (B) gamma-range for isometric and isotonic exercises. Colored bars represent (TA) tibialis anterior, (LG) lateral gastrocnemius, (MG) medial gastrocnemius, (SO) soleus, (MH) medial hamstring, (VL) vastus lateralis, (VM) vastus medialus, and (RF) rectus femoris muscles. The 95% coherence confidence limit is indicated with a dashed grey line. Error bars show the standard error of the mean. Isotonic knee flexion could not be accommodated by the test apparatus; therefore, no values are shown for isotonic MH coherence.

Discussion

We found that both isometric and isotonic, knee and ankle exercises elicited significant coherence between contralateral motor cortex electrocortical signals and lower limb EMG in the beta- and gamma-range. Gamma-range coherence was significantly greater for isotonic exercises than for isometric exercises. This finding is consistent with prior research using ECoG to study corticomuscular coherence during

tonic and phasic contractions (Marsden et al., 2000) and suggests that muscle dynamics and relative changes in proprioception may play a role in the beta-to-gamma shift of coherent frequencies for static versus dynamic force production.

Gamma-range corticomuscular coherence has also been observed using scalp EEG during an isometric force tracking task when subjects attempted to achieve a periodically modulated target force given real-time visual feedback of force production (Omlor et al., 2007). The authors of that study hypothesized that the shift toward higher (gamma-range) frequencies might have reflected the fact that tracking a periodically modulated force requires more attentional resources and more complex integration of visual and somatosensory information for control than tracking a constant force. We observed a similar beta-to-gamma shift but the isotonic task studied here did not require more visuomotor integration than the isometric task. Despite the fact that the external anatomy remains stationary, isometric force increases involve dynamic muscle shortening and tendon lengthening while isometric force decreases involve muscle lengthening and tendon shortening (Fukunaga et al., 2002). Therefore, the beta-to-gamma shift observed here may not be inconsistent with the beta-to-gamma shift for the periodically modulated isometric force production task used by Omlor et al. (2007).

Our findings of corticomuscular coherence were consistent across most of the lower limb muscles. We recorded EMG from tibialis anterior, soleus, vastus lateralis, vastus medialus, medial gastrocnemius, lateral gastrocnemius, medial hamstring, and rectus femoris muscles. We found that the beta-to-gamma coherence frequency shift was consistent across all muscles (i.e., isotonic contractions elicited greater gamma-

range coherence than isometric contractions) except vastus medialus and lateral gastrocnemius, which did not exhibit significant coherence for either condition. This observation is consistent with a common pyramidal pathway activating multiple coordinated muscles via spinal interneurons to achieve coordinated limb movement at a lower computational cost (Krakauer and Ghez, 2000; Ting and McKay, 2007).

Most EEG-based studies of corticomuscular coherence evaluate coherence between scalp EEG and surface EMG signals. However, many underlying source signals (including electrocortical, electroocular, electromyographic, and artifact sources) collectively contribute via volume conduction to the electrical potentials recorded on the scalp. These sources can be parsed from scalp EEG using blind source separation techniques and equivalent current dipole modeling (Delorme et al., 2012). In this study, multi-subject clusters of electrocortical sources were localized to the contralateral motor (2 clusters), ipsilateral motor, anterior cingulate, posterior cingulate, and parietal cortex. However, only the electrocortical sources in the contralateral motor cortex exhibited significant corticomuscular coherence. This finding is consistent with the knowledge that the corticospinal pathways originate in the motor cortex. The use of independent components analysis to separate out motor cortex sources rather than directly using EEG electrode signals for calculating corticomuscular coherence is beneficial because it ensures that mixing of various electrocortical processes, as well as neck and facial EMG signals, via volume conduction doesn't bias the analysis. Blind source separation techniques may be beneficial for future studies of corticomuscular coherence, particularly during dynamic motor tasks when scalp EEG signals can be highly

contaminated by electromyographic and movement artifacts (Gramann et al., 2011a; Gwin et al., 2010a, b).

In conclusion, significant coherence between contralateral motor cortex electrocortical signals and lower limb EMG was observed in the beta- and gamma-range for both isometric and isotonic self-paced knee and ankle exercises. However, gamma-range coherence was significantly greater for isotonic exercises than for isometric exercises. This beta-to-gamma shift was consistent across 6 of the 8 lower limb muscle EMG signals that we recorded. This suggests that active muscle movement may modulate the speed of corticospinal oscillations. Specifically, isotonic contractions shift corticospinal oscillations towards the gamma-range while isometric contractions favor beta-range oscillations.

Chapter 7: Discussion

The overarching objective of this dissertation was to evaluate electrocortical dynamics associated with lower limb motor tasks using a novel noninvasive electrical neuroimaging approach.

Chapter 2 demonstrated the feasibility of using high-density EEG and ICA to record cortical neural activity during human locomotion. This manuscript focused on recording brain dynamics associated with a cognitive task that was performed while healthy subjects stood, walked, and ran on a treadmill. A primary finding of Chapter 2 was that by using high-density EEG and ICA, cognitive event-related cortical potentials could be recorded during walking that were nearly identical to those during standing. This was the first demonstration of noninvasive electrical neuroimaging during human locomotion and led directly to a second, more in depth, study of cognitive event-related cortical potentials during walking (Gramann et al., 2011a).

There are many interesting avenues for further study of brain dynamics associated with cognitive tasks performed while walking. In particular, the techniques used in Chapter 2 enable novel studies using dual-task (cognitive and motor) experimental designs to assess brain dynamics associated with performing cognitive tasks while walking. In a completed but unpublished study from the Human Neuromechanics Laboratory at the University of Michigan using the data from Chapter 2 of this

dissertation, Granger causality was used to determine the effective connectivity between electrocortical sources. This study demonstrated that effective connectivity involving non-sensorimotor areas was stronger during walking than during standing when subjects were engaged in a simultaneous cognitive task. This suggests that performing a cognitive task while walking promotes greater interaction among cognitive neural substrates than performing the same task while standing. A limitation of this study and of Chapter 2 is that subjects performed a relatively simple visual target discrimination and response task. Active studies in the Human Neuromechanics Laboratory are examining more complex cognitive tasks, such as the Brooks spatial memory task, performed while walking. Finally, the techniques used in Chapter 2 are not limited to treadmill walking. Researchers at the Swartz Center for Computational Neuroscience at the University of California, San Diego, are implementing similar techniques to study subjects performing object identification during over ground navigation (Makeig et al., 2009). Further investigations using dual-task (cognitive and motor) experimental designs to assess brain dynamics associated with performing cognitive tasks while walking are warranted. Such studies would be particularly relevant for older adults because the population is rapidly aging and empirical evidence suggests that age-related performance decrements for certain combinations of cognitive and motor tasks are disproportionately greater than the additive age-related costs of performing the two tasks independently (Seidler et al., 2010).

A second important finding from Chapter 2 was that during running, gait-related artifact severely compromised the EEG signals to the point that even after applying ICA

stable cognitive event-related cortical potentials were not detectable. I solved this problem by implementing a channel-based artifact template regression procedure prior to ICA. After applying this procedure, stable cognitive event-related cortical potentials were detectable during running. This finding demonstrated that mechanical artifact from stereotyped movements may be minimized using a template regression procedure provided that movement-related kinematic signals are available for performing appropriate time-warping. A limitation of this approach is that only electrodynamics that are randomly out of phase with the movement artifact can be recovered; electrodynamics that are time locked to the movement artifact will be regressed from the data. There are many avenues for further study using this approach. Some researchers have expressed an interest in using this technique to study brain dynamics associated with evasive maneuvers such as jump-cut landings. Understanding the mechanisms of neuro-motor control during these evasive maneuvers is important because this type of movement carries a high ACL injury risk (McLean and Beaulieu, 2010).

Chapter 3 built on the results of Chapter 2 but focused on patterns of electrocortical activity that are synchronized to the gait cycle during walking. This study provided the first intra-stride measurements of human brain activity recorded during walking. Electrocortical sources in the anterior cingulate, posterior parietal, and sensorimotor cortex exhibited significant intra-stride changes in spectral power. During the end of stance, as the leading foot was contacting the ground and the trailing foot was pushing off, alpha- and beta-band spectral power increased in or near the left/right

sensorimotor and dorsal anterior cingulate cortex. These data confirmed cortical involvement in steady-speed human locomotion.

The existence of significant intra-stride patterns of activation and deactivation suggests that the human cortex is actively engaged during steady-speed locomotion. Given that corticospinal excitability is modulated during the human gait cycle (Capaday et al., 1999; Petersen et al., 2001; Schubert et al., 1997) it is likely that direct corticospinal pathways contribute to locomotor execution. However, tonic descending inputs to spinal networks from the mesencephalic locomotor region of the brainstem can also generate rhythmic muscle activation (Rossignol et al., 2006). A limitation of Chapter 3 of this dissertation is that it does not indicate whether human cortex is actively involved in controlling locomotion via direct pathways or whether human cortex processes sensory afferents that are used to modulate a descending signal to spinal generators via the mesencephalic locomotor region. Studying walking under challenging conditions, with either increased or decreased sensory demands or availability, may provide a means of further assessing the relative contribution of direct and indirect pathways to locomotor execution. Studies in the Human Neuromechanics Laboratory have already begun to address these questions. Using the technique of Chapter 3 these studies are examining the brain dynamics associated with walking on a narrow balance-beam and on uneven ground.

Interest in the use of EEG during walking extends well beyond the Human Neuromechanics Laboratory. Several research groups have already published studies utilizing EEG during walking based on the results presented in Chapter 3 of this

dissertation. Researchers from the University of Copenhagen demonstrated a causal relationship between contralateral sensorimotor cortex electrocortical source signals and tibialis anterior electromyography (Hvass Petersen et al., 2012). Researchers from the University of Maryland decoded lower limb kinematics from low frequency (theta-range) EEG signals during walking (Presacco et al., 2011). In a recent review article, a research group from Belgium confirmed the results from Chapter 3 of this dissertation and demonstrated that electrocortical spectral fluctuations combined with a dynamic recurrent neural network could be used to predict lower limb kinematics during treadmill walking. These are the first of what will likely be many studies inspired by the demonstration that it is possible to record intra-stride electrocortical dynamics using EEG.

Chapters 2 and 3 were groundbreaking studies because they demonstrated that EEG and ICA can be used to image the brain during locomotion. They have already been the subject of an invited review (Gramann et al., 2011b). These studies used high-density 256-channel EEG sensor arrays, which are likely too time-consuming to setup in a clinical or field setting (and too expensive for many research laboratories). Therefore, the goal of Chapter 4 was to evaluate how reducing the number of EEG channel signals affects the electrocortical source signals that can be parsed from EEG recorded during ambulatory activities. I demonstrated that an EEG montage with as few as 35 channels may be sufficient to record the more dominate electrocortical sources. This finding is task specific but should provide a guideline (and encouragement) for researchers

interested in implementing EEG and ICA in mobile environments without using costly high-density electrode arrays.

In the last two chapters, the same imaging techniques were used to study healthy subjects performing seated isometric and isotonic, knee and ankle exercises. I studied these simple tasks to better understand the relationship between electrocortical dynamics and lower limb muscle activity. Locomotion is a complex task requiring coordinated action of many muscles. Therefore, it was difficult to gain insight into aspects of lower limb neuro-motor control from the studies of human locomotion. Chapters 5 and 6 provided more direct insight. Specifically, I found that isometric and isotonic contractions elicit different patterns of sensorimotor electrocortical activity. Isometric contractions elicited an event related desynchronization (ERD) in the α-band (8-12 Hz) and β-band (12-30 Hz) at joint torque onset and offset, while isotonic contractions elicited a sustained α- and β-band ERD throughout the trial. Furthermore, I examined the causal relationship between contralateral sensorimotor electrocortical signals and lower-limb EMG. I found significant coherence in the beta- and gamma-range for all exercise types. Gamma-range coherence was significantly greater for isotonic exercises than for isometric exercises.

The results of these studies demonstrated that ICA of high-density EEG can be used to monitor a broad distribution of electrocortical sources that contribute to lower limb muscle actions. It remains to be seen how these task specific electrocortical dynamics (or those associated with locomotion presented in Chapter 3) are affected by neurological injuries, such as stroke or spinal cord injury, or how they change in

response to motor rehabilitation. Alternative imaging techniques suggest that functional recovery will rely on plasticity in multiple cortical regions and that the relative contribution of different regions will change throughout the course of rehabilitation (Eliassen et al., 2008; Enzinger et al., 2009; Kokotilo et al., 2009a; Kokotilo et al., 2009b; Miyai et al., 2006; Nishimura and Isa, In Press). The techniques used in this study may provide a means to better understand the cortical physiology underlying neurological rehabilitation and recovery.

Another important result of Chapter 5 was that task specific changes in electrocortical spectral power were consistent enough to decode the type of muscle action from the recorded EEG on a trial-by-trial basis. Perhaps more interestingly, the inclusion of a broad distribution of electrocortical signals improved the classification accuracy. Classifiers based on contralateral sensorimotor cortex sources achieved a 4-way classification accuracy (isometric versus isotonic and high versus low effort) of 69% while classifiers based on electrocortical sources in multiple brain regions achieved a 4-way classification accuracy of 87%. This finding is consistent with the emerging consensus that a broad distribution of electrocortical signals and a better understanding of underlying cortical physiology will improve brain computer interface information transfer rates (Leuthardt et al., 2009). In addition, incorporating spatial, spectral, and temporal features of electrocortical signals, across multiple cortical areas, can improve the fidelity of classification algorithms (Besserve et al., 2011; Muller-Gerking et al., 1999; Qin et al., 2004; Ramoser et al., 2000; Wentrup et al., 2005; Zhang et al., 2007). To make use of ICA in realtime it will be necessary to formulate a mechanism for periodically

updating the subject specific IC weight matrix (the matrix that transforms EEG channel signals into independent electrocortical processes). This is feasible but has not yet been attempted, to my knowledge.

In addition to the previously mentioned limitations related to individual chapters, there are several limitations that apply to this dissertation in its entirety. First, my subject population was predominantly male. This is because long haired research participants are problematic for studies using EEG. Future work should evaluate potential gender difference in the electrocortical dynamics presented throughout this dissertation because there are gender differences in cortical recruitment during both simple and complex motor tasks (Lissek et al., 2007). Second, the electrocortical source localization algorithms used throughout this dissertation were based on a standardized boundary element head model. The use of subject specific head models could greatly improve the localization accuracy. In future studies the use of the Neuroelectromagnetic Forward Head Modeling Toolbox (Acar and Makeig, In Press) and subject specific magnetic resonance based head models should be considered. Third, it is important to note that the terms *mobile* and *noninvasive,* which are used throughout this dissertation to describe the imaging techniques, are open to interpretation. Mobile refers to an imaging technique that allows subject to move relatively freely within a laboratory space. Future work should examine the use of wireless arrays of high-density active electrodes that are currently available (Biosemi, Amsterdam, The Netherlands). Noninvasive, in the context of recording electrocortical signals, refers to the use of EEG sensors that are placed on the scalp as opposed to more invasive techniques that use

sensors mounted directly on top of, or into, the cortex. Future work should examine ways to reduce the burden of donning and doffing the electrode caps including the use of cap mounted arrays of dry wireless electrodes (Chi et al., 2010).

In summary, this dissertation has expanded our understanding of cortical involvement in voluntary lower limb movement (including locomotion) and will contribute to the development of novel technologies for clinical neuro-monitoring, neuro-assessment, and neuro-rehabilitation. The findings from this dissertation may inform future uses of noninvasive electrical neuroimaging in clinical settings. To get the most clinical benefit from functional neuroimaging during neurological rehabilitation it is necessary to establish relationships between electrocortical dynamics and muscle activity in neurologically intact humans during a variety of lower limb motor tasks including individual muscle contractions, coordinated stepping, and locomotion. The techniques that I implemented can be used throughout the rehabilitation process to study both discrete lower limb muscle activations and more dynamic tasks, such as coordinated non-weight-bearing stepping or normal locomotion. Therefore, the results of this dissertation have implications for neurorehabilitation of gait, including monitoring cortical plasticity and providing real-time control of robotic lower limb exoskeletons.

References

Acar, Z.A., Makeig, S., In Press. Neuroelectromagnetic Forward Modeling Toolbox. Journal of Neuroscience Methods.

Alexander, L.D., Black, S.E., Patterson, K.K., Gao, F.Q., Danells, C.J., McIlroy, W.E., 2009. Association Between Gait Asymmetry and Brain Lesion Location in Stroke Patients. Stroke 40, 537-544.

Allen, D.P., MacKinnon, C.D., 2010. Time-frequency analysis of movement-related spectral power in EEG during repetitive movements: a comparison of methods. Journal of Neuroscience Methods 186, 107-115.

Allen, P.J., Josephs, O., Turner, R., 2000. A method for removing imaging artifact from continuous EEG recorded during functional MRI. Neuroimage 12, 230-239.

Andujar, J.E., Lajoie, K., Drew, T., 2010. A Contribution of Area 5 of the Posterior Parietal Cortex to the Planning of Visually Guided Locomotion: Limb-Specific and Limb-Independent Effects. Journal of Neurophysiology 103, 986-1006.

Armstrong, D.M., MarpleHorvat, D.E., 1996. Role of the cerebellum and motor cortex in the regulation of visually controlled locomotion. Canadian Journal of Physiology and Pharmacology 74, 443-455.

Barthelemy, D., Nielsen, J.B., 2010. Corticospinal contribution to arm muscle activity during human walking. Journal of Physiology, London 588, 967-979.

Bell, A.J., Sejnowski, T.J., 1995. An information-maximization approach to blind separation and blind deconvolution. Neural Computation 7, 1129-1159.

Beloozerova, I.N., Sirota, M.G., 2003. Integration of motor and visual information in the parietal area 5 during locomotion. Journal of Neurophysiology 90, 961-971.

Benar, C., Aghakhani, Y., Wang, Y., Izenberg, A., Al-Asmi, A., Dubeau, F., Gotman, J., 2003. Quality of EEG in simultaneous EEG-fMRI for epilepsy. Clinical Neurophysiology 114, 569-580.

Besserve, M., Martinerie, J., Garnero, L., 2011. Improving quantification of functional networks with EEG inverse problem: evidence from a decoding point of view. Neuroimage 55, 1536-1547.

Borghi, A.M., Cimatti, F., 2010. Embodied cognition and beyond: acting and sensing the body. Neuropsychologia 48, 763-773.

Boyd, L.A., Vidoni, E.D., Daly, J.J., 2007. Answering the call: The influence of neuroimaging and electrophysiological evidence on rehabilitation. Physical Therapy 87, 684-703.

Buechler, R.D., Rodriguez, A.J., Lahr, B.D., So, E.L., 2008. Ictal scalp EEG recording during sleep and wakefulness: Diagnostic implications for seizure localization and lateralization. Epilepsia 49, 340-342.

Bush, G., Luu, P., Posner, M.I., 2000. Cognitive and emotional influences in anterior cingulate cortex. Trends in Cognitive Sciences 4, 215-222.

Calhoun, V.D., Kiehl, K.A., Pearlson, G.D., 2008. Modulation of temporally coherent brain networks estimated using ICA at rest and during cognitive tasks. Human Brain Mapping 29, 828-838.

Capaday, C., Lavoie, B.A., Barbeau, H., Schneider, C., Bonnard, M., 1999. Studies on the corticospinal control of human walking. I. Responses to focal transcranial magnetic stimulation of the motor cortex. Journal of Neurophysiology 81, 129-139.

Chainay, H., Krainik, A., Tanguy, M.L., Gerardin, E., Le Bihan, D., Lehericy, S., 2004. Foot, face and hand representation in the human supplementary motor area. Neuroreport 15, 765-769.

Chakarov, V., Naranjo, J.R., Schulte-Monting, J., Omlor, W., Huethe, F., Kristeva, R., 2009. Beta-range EEG-EMG coherence with isometric compensation for increasing modulated low-level forces. Journal of Neurophysiology 102, 1115-1120.

Chao, Z.C., Nagasaka, Y., Fujii, N., 2010. Long-term asynchronous decoding of arm motion using electrocorticographic signals in monkeys. Front Neuroengineering 3.

Chi, Y.M., Jung, T.P., Cauwenberghs, G., 2010. Dry-contact and noncontact biopotential electrodes: methodological review. IEEE Rev Biomed Eng 3, 106-119.

Chiel, H.J., Beer, R.D., 1997. The brain has a body: adaptive behavior emerges from interactions of nervous system, body and environment. Trends in Neurosciences 20, 553-557.

Christensen, L.O.D., Andersen, J.B., Sinkjaeer, T., Nielsen, J., 2001. Transcranial magnetic stimulation and stretch reflexes in the tibialis anterior muscle during human walking. Journal of Physiology, London 531, 545-557.

Christensen, L.O.D., Johannsen, P., Sinkjaer, T., Petersen, N., Pyndt, H.S., Nielsen, J.B., 2000. Cerebral activation during bicycle movements in man. Experimental Brain Research 135, 66-72.

Collins, S.H., Adamczyk, P.G., Ferris, D.P., Kuo, A.D., 2009. A simple method for calibrating force plates and force treadmills using an instrumented pole. Gait and Posture 29, 59-64.

Cromwell, R.L., Aadland-Monahan, T.K., Nelson, A.T., Stern-Sylvestre, S.M., Seder, B., 2001. Sagittal plane analysis of head, neck, and trunk kinematics and electromyographic activity during locomotion. Journal of Orthopaedic and Sports Physical Therapy 31, 255-262.

Daly, J.J., Wolpaw, J.R., 2008. Brain-computer interfaces in neurological rehabilitation. Lancet Neurology 7, 1032-1043.

Damoiseaux, J.S., Beckmann, C.F., Arigita, E.J.S., Barkhof, F., Scheltens, P., Stam, C.J., Smith, S.M., Rombouts, S.A.R.B., 2008. Reduced resting-state brain activity in the “default network” in normal aging. Cerebral Cortex 18, 1856-1864.

De Raedt, R., Franck, E., Fannes, K., Verstraeten, E., 2008. Is the relationship between frontal EEG alpha asymmetry and depression mediated by implicit or explicit self-esteem. Biological Psychology 77, 89-92.

Debener, S., Strobel, A., Sorger, B., Peters, J., Kranczioch, C., Engel, A.K., Goebel, R., 2007. Improved quality of auditory event-related potentials recorded simultaneously with 3-T fMRI: removal of the ballistocardiogram artefact. Neuroimage 34, 587-597.

Debener, S., Ullsperger, M., Siegel, M., Fiehler, K., von Cramon, D.Y., Engel, A.K., 2005. Trial-by-trial coupling of concurrent electroencephalogram and functional magnetic resonance imaging identifies the dynamics of performance monitoring. Journal of Neuroscience 25, 11730-11737.

Delorme, A., Makeig, S., 2004. EEGLAB: an open source toolbox for analysis of single-trial EEG dynamics including independent component analysis. Journal of Neuroscience Methods 134, 9-21.

Delorme, A., Palmer, J., Onton, J., Oostenveld, R., Makeig, S., 2012. Independent EEG sources are dipolar. PLoS ONE 7, e30135.

Delorme, A., Sejnowski, T., Makeig, S., 2007. Enhanced detection of artifacts in EEG data using higher-order statistics and independent component analysis. Neuroimage 34, 1443-1449.

Dietz, V., 2003. Spinal cord pattern generators for locomotion. Clinical Neurophysiology 114, 1379-1389.

Dietz, V., Colombo, G., Jensen, L., Baumgartner, L., 1995. Locomotor capacity of spinal cord in paraplegic patients. Annals of Neurology 37, 574-582.

Dietz, V., Duysens, J., 2000. Significance of load receptor input during locomotion: a review. Gait and Posture 11, 102-110.

Dimitrijevic, M.R., Gerasimenko, Y., Pinter, M.M., 1998. Evidence for a spinal central pattern generator in humans. Annals of the New York Academy of Sciences 860, 360-376.

Dobkin, B.H., Firestine, A., West, M., Saremi, K., Woods, R., 2004. Ankle dorsiflexion as an fMRI paradigm to assay motor control for walking during rehabilitation. Neuroimage 23, 370-381.

Drew, T., 1993. Motor Cortical Activity during Voluntary Gait Modifications in the Cat .1. Cells Related to the Forelimbs. Journal of Neurophysiology 70, 179-199.

Drew, T., Jiang, W., Widajewicz, W., 2002. Contributions of the motor cortex to the control of the hindlimbs during locomotion in the cat. Brain Research Reviews 40, 178-191.

Drew, T., Prentice, S., Schepens, B., 2004. Cortical and brainstem control of locomotion. Progress in Brain Research 143, 251-261.

Eichele, T., Specht, K., Moosmann, M., Jongsma, M.L., Quiroga, R.Q., Nordby, H., Hugdahl, K., 2005. Assessing the spatiotemporal evolution of neuronal activation with single-trial event-related potentials and functional MRI. Proceedings of the National Academy of Sciences of the United States of America 102, 17798-17803.

Eliassen, J.C., Boespflug, E.L., Lamy, M., Allendorfer, J., Chu, W.J., Szaflarski, J.P., 2008. Brain-mapping techniques for evaluating poststroke recovery and rehabilitation: a review. Top Stroke Rehabil 15, 427-450.

Enzinger, C., Dawes, H., Johansen-Berg, H., Wade, D., Bogdanovic, M., Collett, J., Guy, C., Kischka, U., Ropele, S., Fazekas, F., Matthews, P.M., 2009. Brain activity changes associated with treadmill training after stroke. Stroke 40, 2460-2467.

Fang, Y., Siemionow, V., Sahgal, V., Xiong, F., Yue, G.H., 2001. Greater movement-related cortical potential during human eccentric versus concentric muscle contractions. Journal of Neurophysiology 86, 1764-1772.

Ferris, D.P., Gordon, K.E., Beres-Jones, J.A., Harkema, S.J., 2004. Muscle activation during unilateral stepping occurs in the nonstepping limb of humans with clinically complete spinal cord injury. Spinal Cord 42, 14-23.

Filimon, F., Nelson, J.D., Huang, R.S., Sereno, M.I., 2009. Multiple parietal reach regions in humans: cortical representations for visual and proprioceptive feedback during on-line reaching. Journal of Neuroscience 29, 2961-2971.

Fitzsimmons, N.A., Lebedev, M.A., Peikon, I.D., Nicolelis, M.A., 2009. Extracting kinematic parameters for monkey bipedal walking from cortical neuronal ensemble activity. Frontiers in Integrative Neuroscience 3.

Foffani, G., Bianchi, A.M., Cincotti, F., Babiloni, C., Carducci, F., Babiloni, F., Rossini, P.M., Cerutti, S., 2004. Independent component analysis compared to laplacian filtering as "Deblurring" techniques for event related desynchronization/synchronization. Methods of Information in Medicine 43, 74-78.

Fong, A.J., Roy, R.R., Ichiyama, R.M., Lavrov, I., Courtine, G., Gerasimenko, Y., Tai, Y.C., Burdick, J., Edgerton, V.R., 2009. Recovery of control of posture and locomotion after a spinal cord injury: solutions staring us in the face. Progress in Brain Research 175, 393-418.

Fukunaga, T., Kawakami, Y., Kubo, K., Kanehisa, H., 2002. Muscle and tendon interaction during human movements. Exercise and Sport Sciences Reviews 30, 106-110.

Gard, S.A., Miff, S.C., Kuo, A.D., 2004. Comparison of kinematic and kinetic methods for computing the vertical motion of the body center of mass during walking. Human Movement Science 22, 597-610.

Garreffa, G., Bianciardi, M., Hagberg, G.E., Macaluso, E., Marciani, M.G., Maraviglia, B., Abbafati, M., Carni, M., Bruni, I., Bianchi, L., 2004. Simultaneous EEG-fMRI acquisition: how far is it from being a standardized technique? Magnetic Resonance Imaging 22, 1445-1455.

Georgopoulos, A.P., Langheim, F.J., Leuthold, A.C., Merkle, A.N., 2005. Magnetoencephalographic signals predict movement trajectory in space. Experimental Brain Research 167, 132-135.

Godlove, D.C., 2010. Eye Movement Artifact May Account for Putative Frontal Feedback-Related Potentials in Nonhuman Primates. The Journal of Neuroscience 30, 4187-4189.

Gorassini, M.A., Norton, J.A., Nevett-Duchcherer, J., Roy, F.D., Yang, J.F., 2009. Changes in Locomotor Muscle Activity After Treadmill Training in Subjects With Incomplete Spinal Cord Injury. Journal of Neurophysiology 101, 969-979.

Gramann, K., Gwin, J.T., Bigdely-Shamlo, N., Ferris, D.P., Makeig, S., 2011a. Visual evoked responses during standing and walking. Frontiers in Human Neuroscience 4, 202.

Gramann, K., Gwin, J.T., Ferris, D.P., Oie, K., Jung, T.P., Lin, C.T., Liao, L.D., Makeig, S., 2011b. Cognition in action: imaging brain/body dynamics in mobile humans. Reviews in the Neurosciences 22, 593-608.

Gramann, K., Onton, J., Riccobon, D., Mueller, H.J., Bardins, S., Makeig, S., 2009. Human Brain Dynamics Accompanying Use of Egocentric and Allocentric Reference Frames during Navigation. Journal of Cognitive Neuroscience 22, 2836-2849.

Grillner, S., 1985. Neurobiological bases of rhythmic motor acts in vertebrates. Science 228, 143-149.

Grillner, S., Wallen, P., Saitoh, K., Kozlov, A., Robertson, B., 2008. Neural bases of goal-directed locomotion in vertebrates - An overview. Brain Research Reviews 57, 2-12.

Gross, J., Tass, P.A., Salenius, S., Hari, R., Freund, H.J., Schnitzler, A., 2000. Cortico-muscular synchronization during isometric muscle contraction in humans as revealed by magnetoencephalography. Journal of Physiology 527 Pt 3, 623-631.

Gwin, J.T., Ferris, D., 2011. High-density EEG and independent component analysis mixture models distinguish knee contractions from ankle contractions. Conference Proceedings of the 33rd Annual International Conference of the IEEE Engineering in Medicine and Biology Society 2011, 4195-4198.

Gwin, J.T., Ferris, D.P., [In Press]. An EEG-based study of discrete isometric and isotonic human lower limb muscle contractions. Journal of Neuroengineering and Rehabilitation.

Gwin, J.T., Gramann, K., Makeig, S., Ferris, D.P., 2010a. Electrocortical activity is coupled to gait cycle phase during treadmill walking. Neuroimage 54, 1289-1296.

Gwin, J.T., Gramann, K., Makeig, S., Ferris, D.P., 2010b. Removal of movement artifact from high-density EEG recorded during walking and running. Journal of Neurophysiology 103, 3526-3534.

Halliday, D.M., Conway, B.A., Farmer, S.F., Rosenberg, J.R., 1998. Using electroencephalography to study functional coupling between cortical activity and electromyograms during voluntary contractions in humans. Neuroscience Letters 241, 5-8.

Halliday, D.M., Rosenberg, J.R., Amjad, A.M., Breeze, P., Conway, B.A., Farmer, S.F., 1995. A framework for the analysis of mixed time series/point process data--theory and application to the study of physiological tremor, single motor unit discharges and electromyograms. Progress in Biophysics and Molecular Biology 64, 237-278.

Hammon, P.S., Makeig, S., Poizner, H., Todorov, E., de Sa, V.R., 2008. Predicting reaching targets from human EEG. IEEE Signal Processing Magazine 25, 69-77.

Hansen, N.L., Nielsen, J.B., 2004. The effect of transcranial magnetic stimulation and peripheral nerve stimulation on corticomuscular coherence in humans. Journal of Physiology, London 561, 295-306.

Hansen, S., Hansen, N.L., Christensen, L.O., Petersen, N.T., Nielsen, J.B., 2002. Coupling of antagonistic ankle muscles during co-contraction in humans. Experimental Brain Research 146, 282-292.

Harada, T., Miyai, I., Suzuki, M., Kubota, K., 2009. Gait capacity affects cortical activation patterns related to speed control in the elderly. Experimental Brain Research 193, 445-454.

Hatsopoulos, N.G., Donoghue, J.P., 2009. The science of neural interface systems. Annual Review of Neuroscience 32, 249-266.

Hausdorff, J.M., Peng, C.K., Ladin, Z., Wei, J.Y., Goldberger, A.L., 1995. Is walking a random walk? Evidence for long-range correlations in stride interval of human gait. Journal of Applied Physiology 78, 349-358.

Hausdorff, J.M., Purdon, P.L., Peng, C.K., Ladin, Z., Wei, J.Y., Goldberger, A.L., 1996. Fractal dynamics of human gait: stability of long-range correlations in stride interval fluctuations. Journal of Applied Physiology 80, 1448-1457.

Heuninckx, S., Wenderoth, N., Debaere, F., Peeters, R., Swinnen, S.P., 2005. Neural basis of aging: The penetration of cognition into action control. Journal of Neuroscience 25, 6787-6796.

Heuninckx, S., Wenderoth, N., Swinnen, S.P., 2008. Systems neuroplasticity in the aging brain: Recruiting additional neural resources for successful motor performance in elderly persons. Journal of Neuroscience 28, 91-99.

Hvass Petersen, T., Willerslev-Olsen, M., Conway, B.A., Bo Nielsen, J., 2012. The motor cortex drives the muscles during walking in human subjects. Journal of Physiology.

Irani, F., Platek, S.M., Bunce, S., Ruocco, A.C., Chute, D., 2007. Functional near infrared spectroscopy (fNIRS): an emerging neuroimaging technology with important applications for the study of brain disorders. Clin Neuropsychol 21, 9-37.

Jerbi, K., Vidal, J.R., Mattout, J., Maby, E., Lecaignard, F., Ossandon, T., Hamamé, C.M., Dalal, S.S., Bouet, R., Lachaux, J.P., Leahy, R.M., Baillet, S., Garnero, L., Delpuech, C., Bertrand, O., 2011. Inferring hand movement kinematics from MEG, EEG and intracranial EEG: From brain-machine interfaces to motor rehabilitation. IRBM 32, 8-18.

Jordan, K., Challis, J.H., Newell, K.M., 2006. Long range correlations in the stride interval of running. Gait and Posture 24, 120-125.

Jordan, K., Challis, J.H., Newell, K.M., 2007. Walking speed influences on gait cycle variability. Gait and Posture 26, 128-134.

Jung, T.P., Makeig, S., Humphries, C., Lee, T.W., McKeown, M.J., Iragui, V., Sejnowski, T.J., 2000a. Removing electroencephalographic artifacts by blind source separation. Psychophysiology 37, 163-178.

Jung, T.P., Makeig, S., Westerfield, M., Townsend, J., Courchesne, E., Sejnowski, T.J., 2000b. Removal of eye activity artifacts from visual event-related potentials in normal and clinical subjects. Clinical Neurophysiology 111, 1745-1758.

Jung, T.P., Makeig, S., Westerfield, M., Townsend, J., Courchesne, E., Sejnowski, T.J., 2001. Analysis and visualization of single-trial event-related potentials. Human Brain Mapping 14, 166-185.

Kachenoura, A., Albera, L., Senhadji, L., Comon, P., 2008. ICA: A potential tool for BCI systems. IEEE Signal Processing Magazine 25, 57-68.

Kandel, E.R., Schwartz, J.H., Jessell, T.M., 2000. Principles of neural science, 4th ed. McGraw-Hill, Health Professions Division, New York.

Kim, H.K., Park, S., Srinivasan, M.A., 2009. Developments in brain-machine interfaces from the perspective of robotics. Human Movement Science 28, 191-203.

Klimesch, W., 1999. EEG alpha and theta oscillations reflect cognitive and memory performance: a review and analysis. Brain Research Reviews 29, 169-195.

Kokotilo, K.J., Eng, J.J., Boyd, L.A., 2009a. Reorganization of brain function during force production after stroke: a systematic review of the literature. Journal of Neurologic Physical Therapy 33, 45-54.

Kokotilo, K.J., Eng, J.J., Curt, A., 2009b. Reorganization and preservation of motor control of the brain in spinal cord injury: a systematic review. Journal of Neurotrauma 26, 2113-2126.

Krakauer, J., Ghez, C., 2000. Voluntary Movement. In: Kandel, E.R., Schwartz, J.H., Jessell, T.M. (Eds.), Principles Of Neural Science. McGraw-Hill, New York, pp. 756-781.

Kristeva-Feige, R., Fritsch, C., Timmer, J., Lucking, C.H., 2002. Effects of attention and precision of exerted force on beta range EEG-EMG synchronization during a maintained motor contraction task. Clinical Neurophysiology 113, 124-131.

Kristeva, R., Patino, L., Omlor, W., 2007. Beta-range cortical motor spectral power and corticomuscular coherence as a mechanism for effective corticospinal interaction during steady-state motor output. Neuroimage 36, 785-792.

Kuo, A.D., Donelan, J.M., Ruina, A., 2005. Energetic consequences of walking like an inverted pendulum: Step-to-step transitions. Exercise and Sport Sciences Reviews 33, 88-97.

la Fougere, C., Zwergal, A., Rominger, A., Forster, S., Fesl, G., Dieterich, M., Brandt, T., Strupp, M., Bartenstein, P., Jahn, K., 2010. Real versus imagined locomotion: a [18F]-FDG PET-fMRI comparison. Neuroimage 50, 1589-1598.

Lajoie, K., Andujar, J.E., Pearson, K., Drew, T., 2010. Neurons in Area 5 of the Posterior Parietal Cortex in the Cat Contribute to Interlimb Coordination During Visually Guided Locomotion: A Role in Working Memory. Journal of Neurophysiology 103, 2234-2254.

Lancaster, J.L., Woldorff, M.G., Parsons, L.M., Liotti, M., Freitas, C.S., Rainey, L., Kochunov, P.V., Nickerson, D., Mikiten, S.A., Fox, P.T., 2000. Automated Talairach atlas labels for functional brain mapping. Human Brain Mapping 10, 120-131.

Le Ray, D., Juvin, L., Boutin, T., Auclair, F., Dubuc, R., 2010. A neuronal substrate for a state-dependent modulation of sensory inputs in the brainstem. European Journal of Neuroscience 32, 53-59.

Leach, J.B., Achyuta, A.K., Murthy, S.K., 2010. Bridging the Divide between Neuroprosthetic Design, Tissue Engineering and Neurobiology. Frontiers in Neuroengineering 2, 1-19.

Lee, T.W., Girolami, M., Sejnowski, T.J., 1999a. Independent component analysis using an extended infomax algorithm for mixed subgaussian and supergaussian sources. Neural Computation 11, 417-441.

Lee, T.W., Lewicki, M.S., Girolami, M., Sejnowski, T.J., 1999b. Blind source separation of more sources than mixtures using overcomplete representations. IEEE Signal Processing Letters 6, 87-90.

Leuthardt, E.C., Schalk, G., Roland, J., Rouse, A., Moran, D.W., 2009. Evolution of brain-computer interfaces: going beyond classic motor physiology. Neurosurgical Focus 27, E4.

Lewicki, M.S., Sejnowski, T.J., 2000. Learning overcomplete representations. Neural Computation 12, 337-365.

Lissek, S., Hausmann, M., Knossalla, F., Peters, S., Nicolas, V., Gunturkun, O., Tegenthoff, M., 2007. Sex differences in cortical and subcortical recruitment during simple and complex motor control: an fMRI study. Neuroimage 37, 912-926.

Liu, J.Z., Yao, B., Siemionow, V., Sahgal, V., Wang, X., Sun, J., Yue, G.H., 2005. Fatigue induces greater brain signal reduction during sustained than preparation phase of maximal voluntary contraction. Brain Research 1057, 113-126.

Londei, A., D'Ausilio, A., Basso, D., Sestieri, C., Del Gratta, C., Romani, G.L., Olivetti Belardinelli, M., 2007. Brain network for passive word listening as evaluated with ICA and Granger causality. Brain Research Bulletin 72, 284-292.

Luft, A.R., Smith, G.V., Forrester, L., Whitall, J., Macko, R.F., Hauser, T.K., Goldberg, A.P., Hanley, D.F., 2002. Comparing brain activation associated with isolated upper and lower limb movement across corresponding joints. Human Brain Mapping 17, 131-140.

MacKay, W.A., 2005. Wheels of Motion: Oscillatory Potentials in the Motor Cortex. In: Riehle, A., Vaadia, E. (Eds.), Motor Cortex in Voluntary Movements: A Distributed System for Distributed Functions. CRC Press, Boca Raton, FL, pp. 181-211.

Maegele, M., Muller, S., Wernig, A., Edgerton, V.R., Harkema, S.J., 2002. Recruitment of spinal motor pools during voluntary movements versus stepping after human spinal cord injury. Journal of Neurotrauma 19, 1217-1229.

Makeig, S., 1993. Auditory event-related dynamics of the EEG spectrum and effects of exposure to tones. Electroencephalography and Clinical Neurophysiology 86, 283-293.

Makeig, S., Bell, A.J., Jung, T.P., Sejnowski, T.J., 1996. Independent component analysis of electroencephalographic data. Advances in Neural Information Processing Systems 8, 145-151.

Makeig, S., Delorme, A., Westerfield, M., Jung, T.P., Townsend, J., Courchesne, E., Sejnowski, T.J., 2004. Electroencephalographic brain dynamics following manually responded visual targets. PLoS Biology 2, 747-762.

Makeig, S., Gramann, K., Jung, T.P., Sejnowski, T.J., Poizner, H., 2009. Linking brain, mind and behavior. International Journal of Psychophysiology 73, 95-100.

Makeig, S., Onton, J., Sejnowski, T., Poizner, H., 2007. Prospects for mobile, high-definition brain imaging: Spectral modulations during 3-D reaching. Neuroimage 36.

Marsden, J.F., Werhahn, K.J., Ashby, P., Rothwell, J., Noachtar, S., Brown, P., 2000. Organization of cortical activities related to movement in humans. Journal of Neuroscience 20, 2307-2314.

McLean, S.G., Beaulieu, M.L., 2010. Complex integrative morphological and mechanical contributions to ACL injury risk. Exercise and Sport Sciences Reviews 38, 192-200.

Michel, C.M., T., K., Brandeis, D., Gianotti, L.R.R., Wackermann, J. (Eds.), 2009. Electrical neuroimaging. Cambridge University Press, New York.

Mielke, R., Szelies, B., 2003. Neuronal plasticity in poststroke aphasia: insights by quantitative electroencephalography. Expert Reviews in Neurotherapeutics 3, 373-380.

Millan, J.D., Ferrez, P.W., Galan, F., Lew, E., Chavarriaga, R., 2008. Non-invasive brain-machine interaction. International Journal of Pattern Recognition and Artificial Intelligence 22, 959-972.

Mima, T., Hallett, M., 1999. Corticomuscular coherence: a review. Journal of Clinical Neurophysiology 16, 501-511.

Mima, T., Steger, J., Schulman, A.E., Gerloff, C., Hallett, M., 2000. Electroencephalographic measurement of motor cortex control of muscle activity in humans. Clinical Neurophysiology 111, 326-337.

Miyai, I., Suzuki, M., Hatakenaka, M., Kubota, K., 2006. Effect of body weight support on cortical activation during gait in patients with stroke. Experimental Brain Research 169, 85-91.

Miyai, I., Tanabe, H.C., Sase, I., Eda, H., Oda, I., Konishi, I., Tsunazawa, Y., Suzuki, T., Yanagida, T., Kubota, K., 2001. Cortical mapping of gait in humans: a near-infrared spectroscopic topography study. Neuroimage 14, 1186-1192.

Muller-Gerking, J., Pfurtscheller, G., Flyvbjerg, H., 1999. Designing optimal spatial filters for single-trial EEG classification in a movement task. Clinical Neurophysiology 110, 787-798.

Muller-Putz, G.R., Zimmermann, D., Graimann, B., Nestinger, K., Korisek, G., Pfurtscheller, G., 2007. Event-related beta EEG-changes during passive and attempted foot movements in paraplegic patients. Brain Research 1137, 84-91.

Müller, K.-R., Tangermann, M., Dornhege, G., Krauledat, M., Curio, G., Blankertz, B., 2008. Machine learning for real-time single-trial EEG-analysis: From brain-computer interfacing to mental state monitoring. Journal of Neuroscience Methods 167, 82-90.

Nam, H., Yim, T.-G., Han, Seung K., Oh, J.-B., Lee, Sang K., 2002. Independent Component Analysis of Ictal EEG in Medial Temporal Lobe Epilepsy. Epilepsia 43, 160-164.

Negro, F., Farina, D., 2011. Linear transmission of cortical oscillations to the neural drive to muscles is mediated by common projections to populations of motoneurons in humans. Journal of Physiology 589, 629-637.

Neuper, C., Wortz, M., Pfurtscheller, G., 2006. ERD/ERS patterns reflecting sensorimotor activation and deactivation. Progress in Brain Research 159, 211-222.

Niazy, R.K., Beckmann, C.F., Iannetti, G.D., Brady, J.M., Smith, S.M., 2005. Removal of FMRI environment artifacts from EEG data using optimal basis sets. Neuroimage 28, 720-737.

Nielsen, J.B., 2003. How we walk: Central control of muscle activity during human walking. The Neuroscientist 9, 195-204.

Nishimura, Y., Isa, T., In Press. Cortical and subcortical compensatory mechanisms after spinal cord injury in monkeys. Experimental Neurology.

Norton, J.A., Gorassini, M.A., 2006. Changes in cortically related intermuscular coherence accompanying improvements in locomotor skills in incomplete spinal cord injury. Journal of Neurophysiology 95, 2580-2589.

O'Connell, R.G., Dockree, P.M., Bellgrove, M.A., Kelly, S.P., Hester, R., Garavan, H., Robertson, I.H., Foxe, J.J., 2007. The role of cingulate cortex in the detection of errors with and without awareness: a high-density electrical mapping study. European Journal of Neuroscience 25, 2571-2579.

Omlor, W., Patino, L., Hepp-Reymond, M.C., Kristeva, R., 2007. Gamma-range corticomuscular coherence during dynamic force output. Neuroimage 34, 1191-1198.

Onton, J., Makeig, S., 2009. High-frequency Broadband Modulations of Electroencephalographic Spectra. Frontiers in Human Neuroscience 3, 61.

Onton, J., Westerfield, M., Townsend, J., Makeig, S., 2006. Imaging human EEG dynamics using independent component analysis. Neuroscience and Biobehavioral Reviews 30, 808-822.

Oostenveld, R., Oostendorp, T.F., 2002. Validating the boundary element method for forward and inverse EEG computations in the presence of a hole in the skull. Human Brain Mapping 17, 179-192.

Palmer, J.A., Kreutz-Delgado, K., Makeig, S., 2006. Super-Gaussian Mixture Source Model for ICA. In: Rosca, J., Erdogmus, D., Principe, J.C., Haykin, S. (Eds.), Lecture Notes in Computer Science. Springer, Berlin, pp. 854-861.

Palmer, J.A., Makeig, S., Kreutz-Delgado, K., Rao, B.D., 2008. Newton Method for the ICA Mixture Model. 33rd IEEE International Conferance on Acoustics and Signal Processing, Las Vegas, Nevada, pp. 1805-1808.

Patil, P.G., Turner, D.A., 2008. The Development of Brain-Machine Interface Neuroprosthetic Devices. Neurotherapeutics 5, 137-146.

Petersen, N.T., Butler, J.E., Marchand-Pauvert, V., Fisher, R., Ledebt, A., Pyndt, H.S., Hansen, N.L., Nielsen, J.B., 2001. Suppression of EMG activity by transcranial magnetic stimulation in human subjects during walking. Journal of Physiology 537, 651-656.

Pfurtscheller, G., Lopes da Silva, F.H., 1999. Event-related EEG/MEG synchronization and desynchronization: basic principles. Clinical Neurophysiology 110, 1842-1857.

Pfurtscheller, G., Neuper, C., Andrew, C., Edlinger, G., 1997. Foot and hand area mu rhythms. International Journal of Psychophysiology 26, 121-135.

Pfurtscheller, G., Stancak, A., Jr., Neuper, C., 1996. Event-related synchronization (ERS) in the alpha band--an electrophysiological correlate of cortical idling: a review. International Journal of Psychophysiology 24, 39-46.

Presacco, A., Goodman, R., Forrester, L., Contreras-Vidal, J.L., 2011. Neural decoding of treadmill walking from noninvasive electroencephalographic signals. Journal of Neurophysiology 106, 1875-1887.

Qin, L., Ding, L., He, B., 2004. Motor imagery classification by means of source analysis for brain-computer interface applications. Journal of Neural Engineering 1, 135-141.

Rabbi, A.F., Ivanca, K., Putnam, A.V., Musa, A., Thaden, C.B., Fazel-Rezai, R., 2009. Human performance evaluation based on EEG signal analysis: A prospective review. Engineering in Medicine and Biology Society, 2009. EMBC 2009. Annual International Conference of the IEEE, pp. 1879-1882.

Raethjen, J., Govindan, R.B., Binder, S., Zeuner, K.E., Deuschl, G., Stolze, H., 2008. Cortical representation of rhythmic foot movements. Brain Research 1236, 79-84.

Ramoser, H., Muller-Gerking, J., Pfurtscheller, G., 2000. Optimal spatial filtering of single trial EEG during imagined hand movement. IEEE Transactions on Rehabilitation Engineering 8, 441-446.

Ray, S., Niebur, E., Hsiao, S.S., Sinai, A., Crone, N.E., 2008. High-frequency gamma activity (80-150Hz) is increased in human cortex during selective attention. Clinical Neurophysiology 119, 116-133.

Rosenberg, J.R., Amjad, A.M., Breeze, P., Brillinger, D.R., Halliday, D.M., 1989. The Fourier approach to the identification of functional coupling between neuronal spike trains. Progress in Biophysics and Molecular Biology 53, 1-31.

Rossignol, S., 2000. Locomotion and its recovery after spinal injury. Current Opinion in Neurobiology 10, 708-716.

Rossignol, S., Dubuc, R.J., Gossard, J.P., 2006. Dynamic sensorimotor interactions in locomotion. Physiological Reviews 86, 89-154.

Rudzinski, L.A., Meador, K.J., 2011. Epilepsy. Neurology 76, S20-S25.

Sahyoun, C., Floyer-Lea, A., Johansen-Berg, H., Matthews, P.M., 2004. Towards an understanding of gait control: brain activation during the anticipation, preparation and execution of foot movements. Neuroimage 21, 568-575.

Santesso, D.L., Segalowitz, S.J., Ashbaugh, A.R., Antony, M.M., McCabe, R.E., Schmidt, L.A., 2008. Frontal EEG asymmetry and sensation seeking in young adults. Biological Psychology 78, 164-172.

Scherberger, H., 2009. Neural control of motor prostheses. Current Opinion in Neurobiology 19, 629-633.

Schroeder, C.E., Lakatos, P., 2009. Low-frequency neuronal oscillations as instruments of sensory selection. Trends in Neurosciences 32, 9-18.

Schubert, M., Curt, A., Colombo, G., Berger, W., Dietz, V., 1999. Voluntary control of human gait: conditioning of magnetically evoked motor responses in a precision stepping task. Experimental Brain Research 126, 583-588.

Schubert, M., Curt, A., Jensen, L., Dietz, V., 1997. Corticospinal input in human gait: Modulation of magnetically evoked motor responses. Experimental Brain Research 115, 234-246.

Schwartz, A.B., 2004. Cortical neural prosthetics. Annual Review of Neuroscience 27, 487-507.

Seidler, R.D., Bernard, J.A., Burutolu, T.B., Fling, B.W., Gordon, M.T., Gwin, J.T., Kwak, Y., Lipps, D.B., 2010. Motor control and aging: links to age-related brain structural, functional, and biochemical effects. Neuroscience and Biobehavioral Reviews 34, 721-733.

Serrien, D.J., Ivry, R.B., Swinnen, S.P., 2006. Dynamics of hemispheric specialization and integration in the context of motor control. Nature Reviews. Neuroscience 7, 160-166.

Shik, M.L., Orlovsky, G.N., 1976. Neurophysiology of locomotor automatism. Physiological Reviews 56, 465-501.

Siemionow, V., Yue, G.H., Ranganathan, V.K., Liu, J.Z., Sahgal, V., 2000. Relationship between motor activity-related cortical potential and voluntary muscle activation. Experimental Brain Research 133, 303-311.

Stanhope, S.J., Kepple, T.M., McGuire, D.A., Roman, N.L., 1990. Kinematic-based technique for event time determination during gait. Medical and Biological Engineering and Computing 28, 355-360.

Sullivan, T.J., Deiss, S.R., Tzyy-Ping, J., Cauwenberghs, G., 2008. A brain-machine interface using dry-contact, low-noise EEG sensors. Circuits and Systems, 2008. ISCAS 2008. IEEE International Symposium on, pp. 1986-1989.

Suzuki, M., Miyai, I., Ono, T., Kubota, K., 2008. Activities in the frontal cortex and gait performance are modulated by preparation. An fNIRS study. Neuroimage 39, 600-607.

Suzuki, M., Miyai, I., Ono, T., Oda, I., Konishi, I., Kochiyama, T., Kubota, K., 2004. Prefrontal and premotor cortices are involved in adapting walking and running speed on the treadmill: an optical imaging study. Neuroimage 23, 1020-1026.

Ting, L.H., McKay, J.L., 2007. Neuromechanics of muscle synergies for posture and movement. Current Opinion in Neurobiology 17, 622-628.

Urrestarazu, E., Iriarte, J., Alegre, M., Valencia, M., Viteri, C., Artieda, J., 2004. Independent Component Analysis Removing Artifacts in Ictal Recordings. Epilepsia 45, 1071-1078.

Vecchio, F., Del Percio, C., Marzano, N., Fiore, A., Toran, G., Aschieri, P., Gallamini, M., Cabras, J., Rossini, P.M., Babiloni, C., Eusebi, F., 2008. Functional cortico-muscular coupling during upright standing in athletes and nonathletes: a coherence electroencephalographic-electromyographic study. Behavioral Neuroscience 122, 917-927.

Villringer, A., Chance, B., 1997. Non-invasive optical spectroscopy and imaging of human brain function. Trends in Neurosciences 20, 435-442.

Walton, M.E., Croxson, P.L., Behrens, T.E.J., Kennerley, S.W., Rushworth, M.F.S., 2007. Adaptive decision making and value in the anterior cingulate cortex. Neuroimage 36, T142-T154.

Wang, W., Collinger, J.L., Perez, M.A., Tyler-Kabara, E.C., Cohen, L.G., Birbaumer, N., Brose, S.W., Schwartz, A.B., Boninger, M.L., Weber, D.J., 2010. Neural interface technology for rehabilitation: exploiting and promoting neuroplasticity. Physical Medicine and Rehabilitation Clinics of North America 21, 157-178.

Weiller, C., 1998. Imaging recovery from stroke. Experimental Brain Research 123, 13-17.

Weiskopf, N., Mathiak, K., Bock, S.W., Scharnowski, F., Veit, R., Grodd, W., Goebel, R., Birbaumer, N., 2004. Principles of a brain-computer interface (BCI) based on real-time functional magnetic resonance imaging (fMRI). IEEE Transactions on Biomedical Engineering 51, 966-970.

Wenderoth, N., Debaere, F., Sunaert, S., Swinnen, S.P., 2005. The role of anterior cingulate cortex and precuneus in the coordination of motor behaviour. European Journal of Neuroscience 22, 235-246.

Wentrup, M.G., Gramann, K., Wascher, E., Buss, M., 2005. EEG Source Localization for Brain Computer Interfaces. 2nd International IEEE EMBS Conference on Neural Engineering, Arlington, Virginia.

Whitmer, D., Worrell, G., Stead, M., Lee, I.K., Makeig, S., Utility of independent component analysis for interpretation of intracranial EEG. Frontiers in Human Neuroscience 4, 184.

Widajewicz, W., Kably, B., Drew, T., 1994. Motor Cortical Activity during Voluntary Gait Modifications in the Cat .2. Cells Related to the Hindlimbs. Journal of Neurophysiology 72, 2070-2089.

Wieser, M., Haefeli, J., Butler, L., Jancke, L., Riener, R., Koeneke, S., 2010. Temporal and spatial patterns of cortical activation during assisted lower limb movement. Experimental Brain Research 203, 181-191.

Wilson, M., 2002. Six views of embodied cognition. Psychonomic Bulletin and Review 9, 625-636.

Wirz, M., Colombo, G., Dietz, V., 2001. Long term effects of locomotor training in spinal humans. Journal of Neurology, Neurosurgery and Psychiatry 71, 93-96.

Woollacott, M., Shumway-Cook, A., 2002. Attention and the control of posture and gait: a review of an emerging area of research. Gait and Posture 16, 1-14.

Yang, J.F., Gorassini, M., 2006. Spinal and brain control of human walking: Implications for retraining of walking. The Neuroscientist 12, 379-389.

Yang, Q., Fang, Y., Sun, C.K., Siemionow, V., Ranganathan, V.K., Khoshknabi, D., Davis, M.P., Walsh, D., Sahgal, V., Yue, G.H., 2009. Weakening of functional corticomuscular coupling during muscle fatigue. Brain Research 1250, 101-112.

Zhang, H., Wang, C., Guan, C., 2007. Time-varient spatial filtering for motor imagery classification. 29th Conference of the IEEE EMBS, pp. 3124-3127.